

Deforming the Double-Scaled SYK & Reaching the Stretched Horizon From Finite Cutoff Holography

Sergio E. Aguilar-Gutierrez^{ib}^a

^a*Qubits and Spacetime Unit, Okinawa Institute of Science and Technology Graduate University, Onna, Okinawa 904 0495, Japan*

E-mail: sergio.ernesto.aguilar@gmail.com

ABSTRACT: We study the properties of the double-scaled SYK (DSSYK) model under chord Hamiltonian deformations based on finite cutoff holography for general dilaton gravity theories with Dirichlet boundaries. The formalism immediately incorporates a lower-dimensional analog of $T\bar{T}(+\Lambda_2)$ deformations, denoted $T^2(+\Lambda_1)$, as special cases. In general, the deformation mixes the chord basis of the Hilbert space in the seed theory, which we order through the Lanczos algorithm. The resulting Krylov complexity for the Hartle-Hawking state represents a wormhole length at a finite cutoff in the bulk. We study the thermodynamic properties of the deformed theory; the growth of Krylov complexity; the evolution of n -point correlation functions with matter chords; and the entanglement entropy between the double-scaled algebras of the DSSYK model for a given chord state. The latter, in the triple-scaling limit, manifests as the minimal codimension-two area in the bulk following the Ryu-Takayanagi formula. By performing a sequence of T^2 and $T^2 + \Lambda_1$ deformations in the upper tail of the energy spectrum in the deformed DSSYK, we concretely realize the cosmological stretched horizon proposal in de Sitter holography by Susskind [1]. We discuss other extensions with sine dilaton gravity, end-of-the-world branes, and the Almheiri-Goel-Hu model.

Contents

1	Introduction	1
2	Dilaton Gravity at Finite Cutoff and its Boundary Dual	7
2.1	Hamiltonian Deformations from Finite Cutoff Holography	7
2.2	Solutions to the Flow Equation	10
2.3	Thermodynamics	12
3	Deforming the DSSYK Model: Chord Basis, Bulk Length & Complexity	17
3.1	Review of the DSSYK model	17
3.2	Krylov Spread Complexity	21
4	Correlation Functions	26
4.1	n-Point Correlation Functions	28
4.2	Semiclassical Evaluation	29
4.3	Triple-Scaling Limit of Crossed Four-Point Functions	35
5	Holographic Entanglement Entropy from the Double-Scaled Algebra	36
5.1	Double-Scaled Algebras & Entanglement Entropy	36
5.2	Boundary Perspective: Entropy From the Chord Number State	38
5.3	Bulk Perspective: Ryu-Takayanagi Formula	40
6	Stretched Horizon Holography From the Deformed DSSYK Model	41
6.1	UV Limit of the DSSYK Model vs dS Space at Finite Cutoff	42
6.2	Hyperfast Krylov Spread Complexity Growth	44
6.3	Hyperfast Scrambling From OTOCs	46
6.4	Holographic Entanglement Entropy and dS Space	47
7	Discussion	49
7.1	Outlook	50
A	Notation	57
B	Matching Time/Space-like Geodesics with (3.53)	59
C	Sine Dilaton Gravity at Finite Cutoff	61
D	An Alternative Chord Number Basis	65
D.1	Path Integral Formulation	67
D.2	IR/UV Triple-Scaling Limits and $T^2(+\Lambda_1)$ Deformations	69
D.3	Algebraic Entanglement Entropy	71

E	Deformations with End-Of-The-World Branes and Wormholes	74
E.1	Matter Chords as ETW Branes from Deformed DSSYK Model	75
E.2	Deformed ETW Brane theory	77
E.3	Euclidean Wormholes from the DSSYK Model	78
F	Almheiri-Goel-Hu Model	81
G	First Law of Thermodynamics at Finite Cutoff	88

1 Introduction

$T\bar{T}$ Deformations and Their Bulk Interpretation Explicit examples of holography outside the anti-de Sitter (AdS)/ conformal field theory (CFT) correspondence [2] remains, arguably, not well understood and perplexing in comparison with those in conventional AdS/CFT. However, there are different approaches to bridge the gap. Some of the best examples studied have been developed through a class of tractable irrelevant deformations in the boundary theory for CFT_2 introduced in $T\bar{T}$ deformations in [3–5] with several attractive properties [6–16] (reviewed in [17–19]). Single-trace $T\bar{T}$ -deformations (e.g. [20, 21]) and its extensions [22] modify the bulk’s background metric, while double-trace $T\bar{T}$ -deformations break the conformal symmetry in the dual quantum field theory (QFT). Depending on the sign of the deformation, the latter case can be interpreted in the bulk as a finite cutoff in AdS [23]; or gluing an auxiliary AdS path connected to the original asymptotic boundary [24, 25]; or introducing mixed boundary conditions in the asymptotic boundary [26]; among others. Given that the deformation parameter introduces a length scale, it serves to regularize the deformed theory. This has motivated studying higher [11, 27–31] and lower dimensional analogs/extensions [32–42]; we collectively refer to them as T^2 deformations¹. Other multi-trace deformations [43–49], which modify boundary conditions in the bulk dual, are under active scrutiny. T^2 deformations have several exciting features, and they deserve further development in an explicitly solvable ultraviolet (UV)-finite setting, which is our aim in this work.

The DSSYK Model and its Holograms Another prominent approach, lower dimensional quantum gravity offers the possibility of developing non-AdS holography from first principles in an analytically tractable manner.

In particular, the Sachdev-Ye-Kitaev (SYK) model [50–53] in the double-scaling limit [54, 55], called the DSSYK model [56, 57], is a remarkable testing ground to develop concepts and techniques to study lower-dimensional quantum gravity from a concrete and solvable (through chord diagram methods [56, 57]) boundary theory relevant for holography beyond

¹Also referred to as 1D $T\bar{T}$ deformations in the lower-dimensional case in [32, 33].

AdS/CFT, which might carry some relevant lessons in higher dimensional holography. Key insights to understand the DSSYK model and its bulk dual include the double-scaled [58–60] and chord [61] von Neumann algebras; the quantum group structure [62–67]; Krylov complexity [59, 68–85] for operators [86] and states [87] (see recent reviews in [88–90]);² algebraic entanglement entropy [98, 99].³ However, there has been active debate about the specific bulk dual to the DSSYK model. The most-discussed bulk dual proposals include sine dilaton gravity [66, 92, 94, 109–114], and de Sitter (dS) space through different approaches, including Schwarzschild-dS₃ space [81, 95, 96, 112, 115–117], and dS₂ space as a s-wave reduction of dS₃ space, where the DSSYK model is conjectured to live in the **stretched cosmological horizon** (illustrated in Fig. 1 (d)) which is defined as a timelike codimension-one surface with Dirichlet boundary conditions somewhere in the static patch very close to the cosmological horizon, possibly a few Planck’s lengths away [1, 117–127]. Other interesting approaches can be found in e.g. [99, 116, 128–133].

At a first glance, it might seem the diversity of bulk dual proposals for the same boundary theory means that at least some of them might be incorrect. However, they are not necessarily incompatible with one another [39, 74, 99, 112]. For instance, concrete connections between dS₃ space holography with sine dilaton gravity as its world-sheet theory and complex Liouville string [134–139] and the SYK model as a collective field theory was recently investigated in [112]. To fully understand the DSSYK model, the relationship between these different proposals needs to be closely studied.

Addressing Susskind’s Conjectures A prominent member in this family of proposals, initiated by the work of Susskind [1], seemingly has very different features from the others [122]. Whether it fits with sine dilaton gravity and other dS₃ proposals, or if it is incompatible with the other proposals is not well-understood. According to [1], there are specific properties expected in dS holography that are realized by the DSSYK model at infinite (Boltzmann) temperature. Namely, [1] postulates the following conjectures:

- (i) There is a RT formula in dS space that takes the same form as in AdS space when the asymptotic boundary is replaced by the stretched horizon.
- (ii) The scrambling time in the boundary theory dual to dS space, as measured by the operator size of fundamental operators in the theory [140], which is linearly related to the out-of-time-ordered correlators (OTOCs) of the same operators [140], is of the order of the dS length scale.
- (iii) There is a similar (hyper)fast growth of (some notion of) complexity associated to the exponential growth of the dS scale factor.
- (iv) The SYK model at infinite (Boltzmann) temperature and with a scaling $p \sim N^\alpha$, where p is the number of all-to-all interactions, N the total number of fermions, and $0 < \alpha < 1$,

²Krylov complexity in the semiclassical limit reproduces to bulk geodesic lengths [42, 58, 61, 91–96] in the bulk dual of the DSSYK model, which corresponds to an explicit realization of the volume=complexity (CV) conjecture [97].

³Holographically, the entanglement entropy between the double-scaled algebras manifests in terms of a Ryu-Takayanagi (RT) [100, 101] formula (see e.g. [102–105] for reviews, and [106–108] for extensions).

satisfies the above properties.

The motivation for the hyperfast properties and the infinite temperature limit comes from the fact that a surface at a finite radial distance in a gravitational spacetime experiences a Tolman temperature [15, 141–143] with a redshift factor which diverges when the surface is close to the horizon. The temperature scale controls the rate of growth or decay of correlation functions, which would therefore lead to the hyperfast scrambling of OTOCs. This suggests that a boundary theory dual located at the cosmological stretched horizon should not be of the k -local type defined in [1], where k is an order one parameter in the $N \gg 1$ limit, and it represents the power of fundamental operators appearing in the Hamiltonian of the system. Indeed, if k is fixed in the large N limit, the scrambling time scales with $\log N$ [144], and circuit complexity grows linearly in time [97], while the CV proposal in dS space [145] suggests it should grow faster than linear and it should end at a given static patch time with respect to the stretched horizon [1]. In the SYK proposal of [1], we need to allow p (which is the analog of k) to scale with N . In particular, when $p = N^{\alpha=1/2}$ the above conjecture suggests that the DSSYK model may be a specific example of boundary theory in stretched horizon holography [1].

The stretched horizon conjectures are seemingly *in tension* with the DSSYK model being located at the asymptotic boundaries of an effective AdS₂ black hole in sine dilaton gravity [92] (as well as some entropic considerations [122]). Nevertheless, there is a specific regime in sine dilaton gravity where the theory reduces Jackiw-Teitelboim (JT) [146, 147] gravity and to dS JT gravity [82, 109]. This limit in the bulk corresponds to zooming in the UV regime in the energy spectrum of the DSSYK model. However, the boundary theory would be located at \mathcal{I}^\pm when taking the appropriate limit [82, 109]. In contrast, the boundary theory would be located at the stretched horizon in Susskind’s proposal. The tension between them is closely related to dS₂/CFT₁ and static patch holography in dS₂ space.

To move the asymptotic boundary from \mathcal{I}^\pm to inside the static patch, we cannot restrict ourselves to T^2 deformations, since they lead to a complex energy spectrum once the theory reaches a Killing horizon [23]. However, it was recently realized by [148] that by applying a two-step process the boundaries can pass behind the horizon of asymptotically AdS₃ black holes through a combination of $T\bar{T}$ and $T\bar{T} + \Lambda_2$ deformations (which have been recently updated to $T^2 + \Lambda_3$ deformations [149]). In this process, the corresponding boundaries move from the asymptotic region to the black hole horizon through a $T\bar{T}$ deformation, and then from the horizon towards the singularity through a $T\bar{T} + \Lambda_2$ deformation. This procedure was recently applied in dS₃ holography by [150]; albeit without a concrete boundary theory in dS₃/CFT₂.

Thus, a natural way to resolve this tension is based on finite cutoff holography, by T^2 deforming the DSSYK model in the UV limit of its energy spectrum and implementing a lower dimensional version of $T\bar{T} + \Lambda_2$ deformations [151–155] to place the boundary theory near the cosmological horizon of dS₂ space.⁴

⁴Note that dS₃ space with Dirichlet boundaries is thermodynamically unstable, and thus also its s-wave

Results in This Work In summary, we study chord Hamiltonian deformations in the DSSYK model.⁵ We focus on the boundary description with guidance from finite cutoff holography for general dilaton gravity theories; and including the infrared (IR) and UV triple-scaling limits in the DSSYK model, which are associated to JT and dS JT gravity respectively. This allows us to investigate the thermodynamic properties and dynamical observables, particularly correlation functions, in the deformed chord theory associated to a finite cutoff in the bulk dual of the DSSYK model, while allowing general counterterms in the bulk to study their role in the holographic dictionary. We deduce the Krylov basis in the deformed theory, Krylov complexity and the corresponding representation of the chord operators under a Hamiltonian deformation, as well as the entanglement entropy between the double-scaled algebras in the deformed theory. At last, these steps allow us to realize Susskind’s stretched horizon proposal from the UV triple-scaling limit [99].⁶

To elaborate on the summary, we first present a more complete derivation of the flow equation for the energy spectrum of the deformed boundary theory following up our companion work [39] based on finite cutoff holography for dilaton gravity theories in [32–34]. For that, we consider the Hamilton-Jacobi (HJ) equation in a generic dilaton-gravity theory and we derive the flow equation encoding the energy spectrum of the dual. In contrast to the previous literature [32–34, 37, 42], we allow the counterterm in the bulk action to be modified when the boundary radial cutoff is finite. This results in more general Hamiltonian deformations in the boundary dual, including as special cases one-dimensional T^2 deformations and a lower dimensional analog of $T\bar{T} + \Lambda_2$, which we refer to as $T^2 + \Lambda_1$ deformations. This construction extends the holographic dictionary between the DSSYK model and a generic dilaton-gravity theory dual at finite cutoff.⁷ We analyze the thermodynamic properties of the deformed model from its partition function (including the density of states, microcanonical temperature, and heat capacity). A summary of the thermodynamics of the deformed model is shown in Fig. 2. Since the chord Hamiltonian is deformed, the chord number basis used to tridiagonalize the seed Hamiltonian does not do the same in the deformed theory. We will also derive the chord basis that is associated to the length of an Einstein-Rosen bridge in the dual AdS_2 black hole (which we refer to as a “wormhole length”) at a finite cutoff, which is the Krylov basis [87], and we study the representation of operators in the chord

sector; while in the $\text{dS}_{d+1 \geq 4}$ case, it does not lead to a well-posed initial value problem [156].

⁵In the lower-dimensional context, this seems to be a natural choice given that the ensemble-averaged description of the SYK model is the one with a clearer bulk theory dual at the disk topology level. One could first perform the T^2 deformation in the physical SYK model, work out its double-scaling limit and take ensemble averaging at the end, to study the differences with respect to our approach. However, this procedure might not have a chord Hamiltonian description, or it would be non-trivially modified. This might also lead to a different holographic dual, if any. We discuss more details about this in the outlook, Sec. 7.1.

⁶See [68, 78, 80, 81, 145, 157–166], and [1, 167–171] for studies on quantum complexity and entanglement entropy (through bilayer vs monolayer proposals [169–171]) in connection to the dS stretched horizon conjecture in [1].

⁷The evaluations in this work are at the non-perturbative level in the deformation parameter, unless explicitly stated.

algebra. We use these results to evaluate Krylov spread complexity [87] in the HH state of the deformed theory, which reproduces the wormhole length in the bulk at finite cutoff. We proceed evaluating n -point correlation functions. We find that in the semiclassical limit, they have the same functional dependence as the seed theory, but the parameters involving the “fake” temperature [92] (also called “temperature” [1], which is associated to the decay rate of correlation functions) contain a redshift factor, associated to the Tolman temperature at a finite distance in the bulk [23, 172]. Lastly, we evaluate the von Neumann entropy with respect to a density matrix associated to the chord number of the DSSYK model. The algebraic entanglement entropy is holographic, it matches the dilaton in JT gravity and dS JT gravity at a finite cutoff when we restrict to the IR and UV triple-scaling limits in the chord theory.

In particular, when applying our results in the UV limit of the DSSYK model, we realize Susskind’s proposal for stretched horizon holography [1], by implementing the T^2 and $T^2 + \Lambda_1$ deformations, and taking a limit in deformation parameter such that the boundary is placed inside the static and close to the cosmological horizon. The thermodynamic properties of the model match those in dS₂ JT gravity at a finite cutoff. Due to the fake temperature being infinite, the rate of growth of OTOCs and Krylov spread complexity are enhanced; the scrambling time is order one in units of the dS length scale, instead of order $\log N$ expected for a fast scrambler [1] (which would diverge in the DSSYK model). The Krylov spread complexity also reproduces the minimal length between the finite Dirichlet boundaries in dS₂, and in the case of the $T^2 + \Lambda_1$ deformed theory, it reaches a maximum value at a time of order of the dS length scale expected for hyperfast complexity growth [145]. Meanwhile, the algebraic entanglement entropy for the chord number state agrees with the RT formula for dS₂ JT gravity if the boundaries are in the Milne patch of dS₂ (Fig. 1 (c)). The cosmological horizon limit reproduces the Gibbons-Hawking (GH) entropy of dS₃ space. However, if the boundaries are located in the static patch the RT formula in dS₂ does not apply, the dilaton at the minimal extremal surface becomes trivial (see Sec. 6.4). However, in higher dimensions there are more possible entangling surfaces where Susskind’s conjecture might apply. Our study takes the dS₂ geometric perspective instead of a dS₃ embedding, whose precise connection with the DSSYK model is actively debated [112, 115, 122].

A summary comparing our results and the conjectures in [1] is displayed in Tab. 1.

In addition, we study other generalizations and additional technical details in the appendices. In particular, we study the consequences of interpreting the results in terms of sine dilaton gravity in finite cutoff holography. The energy spectrum generically becomes complex-valued since the bulk metric and dilaton at the cutoff location are complex-valued. In those cases, there is no Lorentzian evolution, rather than the deformed theory being non-unitary, so the DSSYK Hamiltonian is not isometrically dual to a canonically quantized Arnowitt–Deser–Misner [173–179] (ADM) Hamiltonian in the bulk, which is the generator of time translations. We adopt a similar prescription as in Cauchy slice holography [180–183], where the stress tensor is allowed to be complex-valued. In contrast to previous literature, the T^2 deformation parameter is generically a complex number, and it can take both positive

Conjecture	Confirmation in Deformed DSSYK	Details
Hyperfast complexity growth (iii+iv)	✓	Sec. 6.2
Hyperfast scrambling (ii+iv)	✓	Sec. 6.3
Validity of RT formula using the stretched horizon (i+iv)	✗	Sec. 6.4

Table 1. Comparison between the (i-iv) conjectures in [1], which were explained above, and the explicit realization of the cosmological stretched horizon from the $T^2 + \Lambda_1$ deformation of the UV limit of the DSSYK model, corresponding to the assumption (iv). Two out of the three remaining conjectures are satisfied in this model. Further details can be found in the respective sections.

and negative values (without an auxiliary geometric extension [24, 25]). Later, we T^2 deform the Almheiri-Goel-Hu (AGH) model [184], which is a simplification of the DSSYK model in the $q \rightarrow 1$ described by the Heisenberg-Weyl algebra. This integrable analog of the DSSYK model allows for analytic evaluations of correlation functions beyond the semiclassical limit.

Outline The paper is organized as follows. In Sec. 2, we introduce Hamiltonian deformations in holographic quantum mechanics based on moving the HJ equation of the dual dilaton graviton theory with Dirichlet boundary conditions, and we study its thermodynamic properties. In Sec. 3, we specialize the results in the DSSYK model to deduce a chord basis associated with a bulk geodesic in finite cutoff holography, and the representation of the chord operators after the deformation. We also evaluate the Krylov spread complexity of the HH state. In Sec. 4 we evaluate correlation functions, including its semiclassical and its triple-scaling limits. In Sec. 5, we investigate the entanglement entropy between the double-scaled algebras in the deformed DSSYK model, and their holographic interpretation. In Sec. 6 we apply our previous results to realize the stretched horizon proposal of Susskind. We then conclude in Sec. 7 with a summary of our findings, and some relevant future directions.

In addition, App. A contains a summary of the notation used in the manuscript. In App. B we provide more details about the derivation of spacelike and timelike extremal geodesic lengths connecting the asymptotic boundaries of an effective AdS_2 black hole. App. C discusses reality conditions in sine dilaton gravity at a finite cutoff. In App. D we investigate an additional chord number basis, different from the Krylov basis, which has an interpretation in finite cutoff holography. In App. E we explore chord Hamiltonian deformations in the presence of ETW branes and Euclidean wormholes in the bulk. In App. F we T^2 -deform the AGH model to study its thermodynamics and correlation functions. At last, in App. G we discuss the first law of thermodynamics in the deformed DSSYK.

2 Dilaton Gravity at Finite Cutoff and its Boundary Dual

Before specializing in the DSSYK model, we generalize previous studies of T^2 deformations for holographic (0+1)-dimensional models [32, 33, 185] assuming a dual dilaton gravity model with Dirichlet boundary conditions. In this section, we are particularly interested in deriving the energy flow equation in holographic quantum mechanics with a Hamiltonian deformation, and to study its semiclassical thermodynamics. In particular, one recovers a lower-dimensional analog of $T\bar{T}$ and $T\bar{T} + \Lambda_2$ deformations as special cases.

Outline In Sec. 2.1, we study HJ equation in dilaton gravity theories and the associated flow equation. In Sec. 2.2 we study its solutions, including one-dimensional T^2 deformations and we propose a “ $T^2 + \Lambda_1$ ” deformation in the DSSYK model, which can be interpreted as pushing the finite cutoff inside the black hole horizon/ outside the cosmological horizon. In Sec. 2.3 we study the thermodynamic properties of the deformed theories, specializing to the DSSYK model for concreteness. In addition, the reader is referred to App. C for details on the reality conditions to implement the chord Hamiltonian deformations from sine dilaton gravity at a finite cutoff.

2.1 Hamiltonian Deformations from Finite Cutoff Holography

Our first goal is to derive the flow equation controlling the evolution of the energy spectrum of a (0+1)-dimensional system dual to a generic dilaton gravity theory of the form

$$I_E \equiv -\frac{\Phi_0}{16\pi G_N} \left(\int_{\mathcal{M}} d^2x \sqrt{g} \mathcal{R} + 2 \int_{\partial\mathcal{M}} dx \sqrt{h} K \right) - \frac{1}{16\pi G_N} \left(\int_{\mathcal{M}} d^2x \sqrt{g} (\Phi \mathcal{R} + U(\Phi)) + 2 \int_{\partial\mathcal{M}} dx \sqrt{h} \left(\Phi_B K - \sqrt{G(\Phi_B)} \right) \right), \quad (2.1)$$

where the first line is a topological term, $U(\Phi)$ and $G(\Phi_B)$ are generic C^∞ functions; G_N in being the two-dimensional Newton’s constant; \mathcal{M} is the spacetime manifold, $\partial\mathcal{M}$ is the location of the radial cutoff boundary where we impose Dirichlet boundary conditions on the dilaton and the induced metric,

$$\partial\mathcal{M} : \quad \Phi = \Phi_B, \quad h_{\mu\nu} \text{ fixed}. \quad (2.2)$$

This allows us to generalize the flow equation in [32] for dilaton-gravity theories without AdS boundary conditions, which is motivated by the proposed duality between sine dilaton gravity and the DSSYK model [66]. One should note that a canonical choice of the counterterm is

$$G(\Phi_B)^{(\text{others})} = \int^{\Phi_B} d\Phi U(\Phi), \quad (2.3)$$

which guarantees the on-shell action is finite when $\Phi_B \gg 1$; however, we will not make this restriction in deriving the flow equation below, since we investigate cases where Φ_B is a finite

cutoff, instead of a radial regulator of the asymptotic boundary.⁸ Also, note that in the following one may allow $g_{\mu\nu}$ and $\Phi \in \mathbb{C}$; which is the case of interest for sine dilaton gravity at finite cutoff. We will discuss this case in detail in App. C.

The strategy proposed in [27] is to recover the T^2 flow equation from the HJ equation controlling radial evolution along the flow.⁹ For this reason, we will consider the dilaton-gravity theory as the input for defining the deformed DSSYK model.¹⁰ Note that while we implement a similar strategy as [27, 32] to define the Hamiltonian deformations in the boundary theory, the crucial difference with previous approaches in the derivation of the flow equation from finite cutoff holography is that we do not require AdS asymptotics in the bulk, which is the reason for allowing the general counterterm $G(\Phi)$ in (2.1), leading to a larger class of deformations than the T^2 case.

We begin considering the general variation of an action of the form (2.1), given by

$$\delta I_E = -\frac{1}{16\pi G_N} \int_{\mathcal{M}} d^2x \sqrt{g} [\mathcal{E}^{\mu\nu} \delta g_{\mu\nu} + \mathcal{E}_\Phi \delta \Phi] + \int_{\partial\mathcal{M}} d\tau \sqrt{h} \left[\frac{1}{2} \tilde{T}^{ab} \delta h_{ab} + \mathcal{O}_{\Phi_B} \delta \Phi_B \right], \quad (2.5)$$

where

$$\mathcal{E}_{\mu\nu} \equiv \nabla_\mu \nabla_\nu \Phi - g_{\mu\nu} \nabla^2 \Phi + \frac{1}{2} g_{\mu\nu} U(\Phi), \quad (2.6)$$

$$\mathcal{E}_\Phi \equiv \mathcal{R} + \partial_\Phi U(\Phi). \quad (2.7)$$

Here we have introduced the Brown-York (BY) [188] stress tensor and the scalar operator conjugate to Φ , which we denote respectively as:

$$\tilde{T}^{ab} \equiv \frac{2}{\sqrt{h}} \frac{\delta I_E}{\delta h_{ab}} = \frac{2}{\sqrt{h}} \left(\pi^{ab} + \frac{\sqrt{h}}{16\pi G_N} \sqrt{G(\Phi_B)} h^{ab} \right), \quad (2.8a)$$

$$\mathcal{O}_{\Phi_B} \equiv \frac{1}{\sqrt{h}} \frac{\delta I_E}{\delta \Phi_B} = \frac{1}{\sqrt{h}} \left(\pi_{\Phi_B} + \frac{\sqrt{h} G'(\Phi_B)}{16\pi G_N \sqrt{G(\Phi_B)}} \right), \quad (2.8b)$$

where $G'(\Phi_B) \equiv \frac{dG(\Phi_B)}{d\Phi_B}$; and π_{Φ_B} and π_{ab} are the canonical momenta of h_{ab} and Φ_B , defined as

$$\pi^{ab} \equiv -\frac{\sqrt{h}}{16\pi G_N} h^{ab} n^c \nabla_c \Phi_B, \quad \pi_{\Phi_B} \equiv -\frac{\sqrt{h}}{8\pi G_N} K. \quad (2.9)$$

⁸If one were to follow (2.3), the Φ_B variation of the boundary action leads to the on-shell mean-curvature at the radial boundary

$$K = \frac{U(\Phi_B)}{2\sqrt{G(\Phi_B)}}. \quad (2.4)$$

⁹A different but related approach is taken in [34], who instead study the radial quantization of the Wheeler-DeWitt (WDW) [186, 187] equation (at the reduced phase space level), and the path integral dilaton gravity of the form (2.1); without a counterterm, (see e.g. (2.20) [34]). After properly introducing the corresponding counter term, one can then recover a relation equivalent to [32], which agrees with results (see (2.16)) after rescaling.

¹⁰An alternative way to define it would be to keep the asymptotic boundary in the same location but modify the boundary conditions instead of using Dirichlet [26]. This type of procedure was considered by [32] in JT gravity. We reserve future directions to study if such modifications can be adapted to this context (see more comments in Sec. 7.1).

We can now study the HJ equation controlling the radial equation of the on-shell solutions. Using the general variation (2.5) evaluated on-shell (i.e. $\mathcal{E}_{\mu\nu} = 0$, $\mathcal{E}_\Phi = 0$), in the strict large $N \gg 1$ limit in the boundary theory, $G_N \rightarrow 0$ in the bulk, we recover

$$\partial_{\Phi_B} I_E^{(\text{on})} = \int_{\partial\mathcal{M}} d\tau \sqrt{h} \left[\frac{1}{2} \tilde{T}^{ab} \partial_{\Phi_B} h_{ab} + \mathcal{O}_{\Phi_B} \right], \quad (2.10)$$

and we have to implement the ADM Hamiltonian constraint \mathcal{H} for general dilaton gravity theories (2.1), which we evaluate at the cutoff location, and it is given by [189]

$$\mathcal{H} \equiv 16\pi G_N \pi_{\Phi_B} \pi^{\tau\tau} - \frac{U(\Phi_B)}{16\pi G_N} = 0. \quad (2.11)$$

This constraint leads to the following relation for the dilaton source in (2.8b):

$$\mathcal{O}_{\Phi_B} = \frac{U(\Phi_B) + \left(\frac{8\pi G_N}{G(\Phi_B)} \tilde{T}_\tau^\tau - 1 \right) G'(\Phi_B)}{16\pi G_N \sqrt{G(\Phi_B)} \left(\frac{8\pi G_N}{G(\Phi_B)^2} \tilde{T}_\tau^\tau - 1 \right)}. \quad (2.12)$$

Following the procedure of [33], we need to identify the scaling of the different terms in (2.10) with respect to r_B . Similar to [27, 32], we recognize that at the finite boundary, Φ_B , we should have the following scaling for the metric and the stress tensor given the counterterm (2.1),

$$\sqrt{h} = \sqrt{G(\Phi_B)} \sqrt{\gamma}, \quad \tilde{T}_{\tau\tau} = \sqrt{G(\Phi_B)} T_{\tau\tau}, \quad (2.13)$$

which is a choice of normalization to match the boundary metric in the bulk to the metric of the boundary theory.¹¹ (2.13) corresponds to a natural general generalization of the AdS₂ boundary conditions (with the corresponding $G(\Phi_B) = \Phi_B^2$). Our proposal for extending the holographic dictionary at finite cutoff beyond AdS (2.13) agrees with [42] using a different method that results in the same flow equation from general dilaton gravity theories at finite cutoff, which appeared after our results in [39].

Next, we use that in 1D we can express the following relation [32],

$$I_E = \int d\tau \sqrt{\gamma} T_\tau^\tau = \int d\tau \sqrt{\gamma} E_y, \quad (2.14)$$

where γ_{ij} is the background metric of the 1D quantum mechanical theory, and T_{ij} the corresponding boundary stress tensor, and in the last equality we use the fact that in (0+1)-dimensions, $T_\tau^\tau \equiv E_y$ which denotes the energy spectrum of the deformed theory, y denotes a deformation parameter, which we define below. This allows us to express the HJ equation (2.11) as

$$\partial_{\Phi_B} \int_{\partial\mathcal{M}} d\tau \sqrt{\gamma} T_\tau^\tau = \int_{\partial\mathcal{M}} d\tau \sqrt{\gamma} \frac{G'(\Phi_B) \left(\left(\frac{8\pi G_N}{G(\Phi_B)} T_\tau^\tau \right)^2 - 1 \right) + U(\Phi_B)}{2 \left(\frac{8\pi G_N}{G(\Phi_B)^2} T_\tau^\tau - 1 \right)}. \quad (2.15)$$

¹¹I thank Simon Lin for comments about this.

Using the relation (2.14), we identify that (2.15) can then be expressed as a flow equation for the spectrum of the boundary theory

$$\boxed{\partial_y E_y = \frac{(E_y)^2 + (\eta - 1)/y^2}{2(1 - yE_y)}}, \quad (2.16)$$

where we have defined the parameters

$$y \equiv 8\pi G_N/G(\Phi_B), \quad \eta \equiv U(\Phi_B)/G'(\Phi_B). \quad (2.17)$$

Note that while E_y depends on both y and η , where the latter is not completely determined by y . The functional dependence on the parameter η will be implicit in all expressions involving y to lighten the notation.

The above relation can be interpreted as a flow equation (2.16) for the energy spectrum of the boundary dual to the dilaton gravity theory at finite cutoff. Indeed, (2.16) takes the same form as other places in the literature (see e.g. [33, 34]) which are restricted to $\eta = U(\Phi_B)/G'(\Phi_B) = 1$. The latter choice of counterterm $G'(\Phi_B) = U(\Phi_B)$ leads to a finite on-shell action in general dilaton-gravity theories with asymptotic Dirichlet boundaries [189]. Meanwhile, the case $\eta = -1$ can be used when the cutoff surface is located at some finite r_B , so there is no issue with the renormalization of the on-shell action, while keeping the same holographic identification for the deformation parameter (2.17). We remark that the deformation parameter (2.17) and the flow equation (2.16) generalize the results in [33] which are a special case of this formulation, corresponding to a class of asymptotically AdS dilaton gravity theories.

Deformed Boundary Hamiltonian We promote (2.16) to an operator relation in the quantum theory as

$$\partial_y \hat{H}_y = \hat{\Theta}(\hat{H}_y, y), \quad \hat{\Theta} = \frac{1}{2}(\hat{H}_y^2 + y^{-2}(\eta - 1))(1 - y\hat{H}_y)^{-1} \quad (2.18)$$

where $\hat{\Theta}(\hat{H}_y, y)$ is the T $\bar{\text{T}}$ deformation operator [190], and \hat{H}_y is the Hamiltonian deformation of the boundary theory.

2.2 Solutions to the Flow Equation

First, notice from (2.17) that $\eta = \eta(y)$ generically. As mentioned in the introductions, when we deformed the boundary theory starting at the asymptotic boundary in the bulk, we need to set $G(\Phi_B)$ as in (2.3). However, once we reach a finite cutoff value Φ_B , we can allow $G(\Phi_B)$ to be more arbitrary, which defines a set of possible deformed theories. Below we specialize in one of them due to its applications for studying the stretched horizon conjecture of Susskind [1].

We will be interested in the case $\eta = \pm 1$, as this allows us to introduce an analogous type of deformation as T $\bar{\text{T}}(+\Lambda_2)$ [149, 151, 153, 155] deformations, which we define below as

$$T^2(+\Lambda_1) \text{ deformations: } U(\Phi) \text{ fixed, } G(\Phi_B) \rightarrow \pm G(\Phi_B), \quad (2.19)$$

resulting in $\eta = \pm 1$ in (2.16). We note that the solutions to the flow equation when η is a fixed parameter are

$$E_y = \frac{1}{y} \left(1 \pm \sqrt{\eta - 2yf(E)} \right). \quad (2.20)$$

where $f(E)$ is a function determined by initial conditions.

T^2 deformation The best studied case from the lower dimensional perspective corresponds to $\eta = +1$. The deformed energy spectrum in terms of the seed theory takes the form

$$E_y^{\eta=+1}(\theta) = \frac{1}{y} \left(1 \pm \sqrt{1 - 2yE} \right). \quad (2.21)$$

The solution with a relative $-$ sign represents the energy spectrum at a finite cutoff in the holographic dual (see e.g. [23, 27]), as seen from the on-shell action (2.32), which is smoothly connected to the seed theory in the limit $y \rightarrow 0$. Meanwhile, the solution with the relative $+$ sign represents the complementary spacetime region with respect to the finite cutoff. Both are represented in Fig. 1.

$T\bar{T} + \Lambda_1$ deformations When $\eta = -1$, this corresponds to a s-wave reduction of $T\bar{T} + \Lambda_2$ deformations [46, 148, 151, 154, 155], which we refer to as $T^2 + \Lambda_1$ deformations. In this case $\eta = -1$ means that at some point along the flow, we modify the boundary counterterm in the action (2.1) with $G(\Phi_B) \rightarrow -G(\Phi_B)$,¹² while retaining the same dilaton potential $U(\Phi) \rightarrow U(\Phi)$.¹³

In particular, we consider a transition between the perturbative branch (2.21) in the $\eta = +1$ case to the $\eta = -1$ case when the square-root term in (2.21) vanishes, corresponding to

$$y = y_0 \equiv 1/(2E). \quad (2.22)$$

By demanding continuity in (2.20), the energy spectrum then takes the form

$$E_y^{\eta=-1} = \frac{1}{y} \left(1 \pm \sqrt{2yE - 1} \right). \quad (2.23)$$

As before, there are two relative signs; both of them are continuously connected to the T^2 deformation since the square root factor in either case vanishes for the transition point of the deformation parameter (2.22). We will specialize in the one with the relative $+$ sign for concreteness, and to probe the cosmological patch in the dS_2 space limit of the bulk. However,

¹²One may recover the same sign as the $T\bar{T} + \Lambda_2$ analogue in [148] by setting $U(\Phi) = 0$, however, we do not analyze this case.

¹³Previous literature has approached the bulk interpretation of the $T\bar{T} + \Lambda_2$ deformation in CFT_2 in different ways. [46, 151, 154, 155] gives evidence that this deformation corresponds to changing the bulk from an AdS black hole to dS_3 space. Meanwhile [148] shows that one can probe the black hole interior by changing timelike and spacelike boundaries in the $T\bar{T}$ and $T\bar{T} + \Lambda_2$ flow respectively. The latter interpretation corresponds to the case we explore; the former interpretation of $\eta = -1$ can also be studied in our set-up by modifying the dilaton potential $U(\Phi) \rightarrow -U(\Phi)$ while keeping $G(\Phi_B) \rightarrow G(\Phi_B)$ at the transition.

it is equally valid to adopt the $-$ sign;¹⁴ similar to the T^2 case, the different signs simply correspond to different bulk regions [148]. In particular, the relative $-$ sign in the $\eta = -1$ in the (2.23) spectrum corresponds to the bulk region connecting the asymptotic boundary to the finite cutoff inside the horizon, while the $+$ relative sign in (2.23) corresponds to the complement. The relative $+$ solution in the $\eta = -1$ case is illustrated in Figs. 1b and 1d.

Note that since there are no modifications in the dilaton potential in the $\eta = -1$ case, it describes the same bulk metric as its $\eta = +1$ analog, similar to [148, 150] (in contrast to other approaches [149, 151–153, 155] which can be realized by changing the dilaton potential).¹⁵ In fact, the BY stress tensor evaluated at the radial boundary Φ_B ($\hat{T}_\tau^\tau = G(\Phi_B)T_\tau^\tau$ (2.13)) changes sign during the transition between $\eta = +1$ and $\eta = -1$. This means that the normal vector to the constant r_B surface changes from spacelike to timelike as explained in [148]. Thus, the finite cutoff crosses the horizon once we turn on the $T^2 + \Lambda_1$ deformation. We illustrate the two-step bulk interpretation of the T^2 and $T^2 + \Lambda_1$ deformation in Fig. 1.¹⁶

2.3 Thermodynamics

In this subsection, we specialize the previous results to study the semiclassical thermodynamics of the deformed DSSYK model from its partition function to evaluate its energy spectrum, thermodynamic entropy, density of states, and heat capacity as a function of its temperature. This leads to conditions when the deformed theory is thermodynamically stable. We do not assume a specific dual dilaton gravity theory (2.1) to the DSSYK model in this section (see App. C for considerations in sine dilaton gravity).

Energy spectrum, entropy and temperature Consider the partition function of the deformed DSSYK model which we evaluate in the semiclassical limit as¹⁷

$$Z_y(\beta) \equiv \langle \Omega | e^{-\beta \hat{H}_y} | \Omega \rangle \underset{\lambda \rightarrow 0}{=} \int dE(\theta) e^{-\beta E_y(\theta)} \rho(\theta), \quad (2.24)$$

¹⁴If one requires the functional expression for the deformed energy spectrum $E_y(E(\theta))$ (2.16) for energies beyond a given seed theory spectrum $E(\theta)$, then there is a prescription in [148] for only studying the $-$ sign solution. Since we are only concerned with the flow of the seed theory spectrum, we do not follow the prescription in [148].

¹⁵The approaches in [148] and [153] differ in terms of the sign of the cosmological constant deformation term; however, they both give rise to the same spectrum of the deformed CFT. Our approach suggests that the overall sign of the corresponding deformation is not relevant, but how this term arises in the derivation of the flow equation, which in our case corresponds to either changing the dilaton potential, $U(\Phi) \rightarrow -U(\Phi)$, in the T^2 to $T^2 + \Lambda_1$ transition, or the sign of term $G(\Phi_B) \rightarrow -G(\Phi_B)$.

¹⁶Note that both asymptotic boundaries move at once in the $N \gg 1$ limit [23].

¹⁷There is a proposal for improvement in the partition function in finite cutoff holography in [42] where one includes the perturbative and non-perturbative branches of the one-dimensional T^2 deformation with an appropriate contour of integration with a cutoff in the energy integration to regularize the integral. The contour is subtle for periodic potentials such as in sine dilaton gravity. Moreover, this prescription is not necessary for the DSSYK model whose partition function is UV finite, so it will not be discussed.

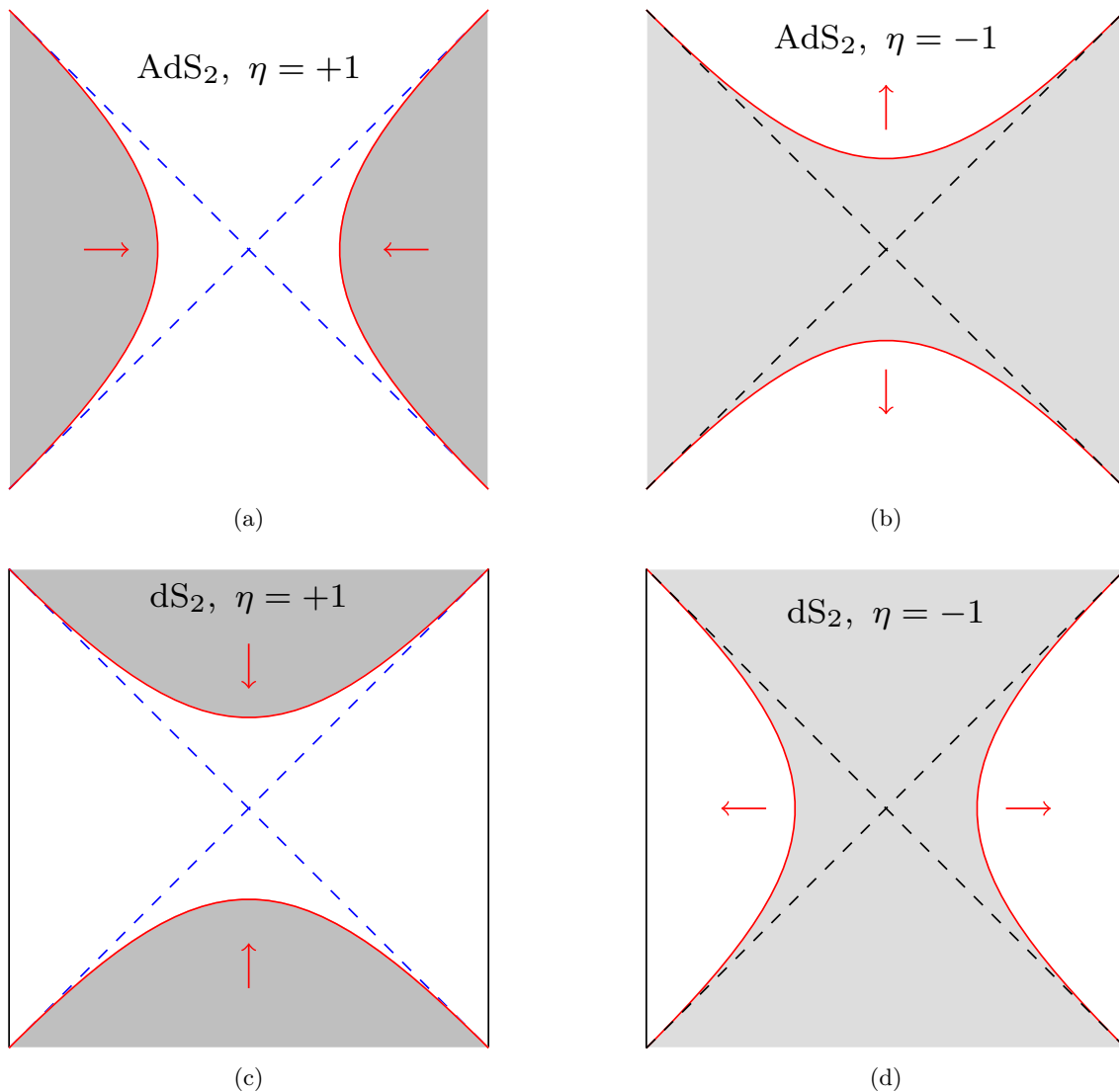


Figure 1. Bulk interpretation of the T^2 and $T^2 + \Lambda_1$ flow in the boundary theory describing (a,b) an AdS_2 black hole, and (c, d) dS_2 space based on the IR/UV triple-scaling limits of the deformed DSSYK in Sec. 3. The gray regions represent the parts of the bulk that are cut out. (a) By implementing the T^2 deformation, with spectrum (2.21), there is a finite boundary cutoff (red solid curve) in the Rindler- AdS_2 patch til it reaches the horizon. (b) We implement the $T^2 + \Lambda_1$ deformation (2.23) which moves the boundary inside the black hole horizon. A similar procedure applies for dS_2 space for (c) T^2 and (d) $T^2 + \Lambda_1$ deformations. In the latter, the cosmological stretched horizon [1] is realized when the Dirichlet boundaries are very close to the dS_2 horizon.

where $E(\theta)$ is the energy spectrum of the seed theory; $\rho(\theta) = e^{S(\theta)}$ is the semiclassical density of states, and $S(\theta)$ is the thermodynamic entropy, given by [191],¹⁸

$$E(\theta) \equiv -\frac{2J \cos(\theta)}{\sqrt{\lambda(1-q)}}, \quad S(\theta) \equiv S_0 + \frac{2\theta}{\lambda}(\pi - \theta), \quad \theta \in [0, \pi], \quad (2.25)$$

¹⁸Note that the entropy is proportional to $1/\lambda = N/(2p^2)$ at all temperature scales, where N is the number of degrees of freedom in the SYK and p the number of all-to-all interacting Majorana fermions. While it has

where J , $\lambda \equiv -\log q \geq 0$ are constant parameters of the theory, which will be specified in Sec. 3.1, and we have introduced S_0 , resulting from an overall normalization of the partition function. The microcanonical inverse temperature in this theory is given by¹⁹

$$\beta_y(\theta) \equiv \frac{dS}{dE_y} = \beta(\theta) \frac{dE}{dE_y}, \quad \beta(\theta) \equiv \frac{2\pi - 4\theta}{J \sin \theta}, \quad (2.26)$$

where there is a redshift factor is

$$\frac{dE}{dE_y} = \begin{cases} \sqrt{1 - 2yE(\theta)}, & \eta = +1, \\ \sqrt{2yE(\theta) - 1}, & \eta = -1. \end{cases} \quad (2.27)$$

Given that β_y is the periodicity of the thermal circle, the T^2 deformation effectively shrinks it. One can similarly recast (2.24) in the form:

$$Z_y(\beta) = \int dE_y(\theta) e^{-\beta E_y(\theta)} \rho_y(\theta), \quad (2.28a)$$

$$\rho_y(\theta) \equiv \rho(\theta) \frac{dE(\theta)}{dE_y(\theta)}, \quad (2.28b)$$

where ρ_y can be interpreted as the density of states in the deformed theory [32]. Note that since the redshift factor is $\mathcal{O}(1)$, it does not modify the thermodynamic entropy which is $\mathcal{O}(\lambda^{-1})$ in the limit where $\lambda \rightarrow 0$.

We include Fig. 2 to exemplify the resulting thermodynamic properties of the T^2 deformed DSSYK model for generic values of the deformation parameter y appearing in the flow equation (2.16) for $\eta = +1$.²⁰

First law of thermodynamics The previous results can be used to express variations of the energy spectrum with respect to the parameters of the model. We include details about the relevant calculations in App. G.

Heat capacity Next, we use the previous results to determine the thermal stability of the system, using the definition of the heat capacity

$$C_y(\theta) \equiv -\beta_y(\theta)^2 \frac{dE_y(\theta)}{d\beta_y(\theta)}. \quad (2.29)$$

been debated (see e.g. [123, 124]) if the DSSYK model at infinite temperature should behave like any other system of N qubits at infinite temperature, the entropy would instead scale as $S \propto N$. The double scaling introduces the $1/p^2$ factor (as seen explicitly in partition function in Sec. 2.3). I thank Takanori Anegawa and Jiuci Xu for useful discussions related to this point.

¹⁹This is a Boltzmann temperature, in contrast to the temperature scale in the correlation functions, which we discuss in Sec. 4.2.

²⁰One can repeat the same semiclassical thermodynamic analysis in sine-dilaton gravity at finite cutoff, which has the same density of states [66]; one needs to replace the deformed energy spectrum for the BY one.

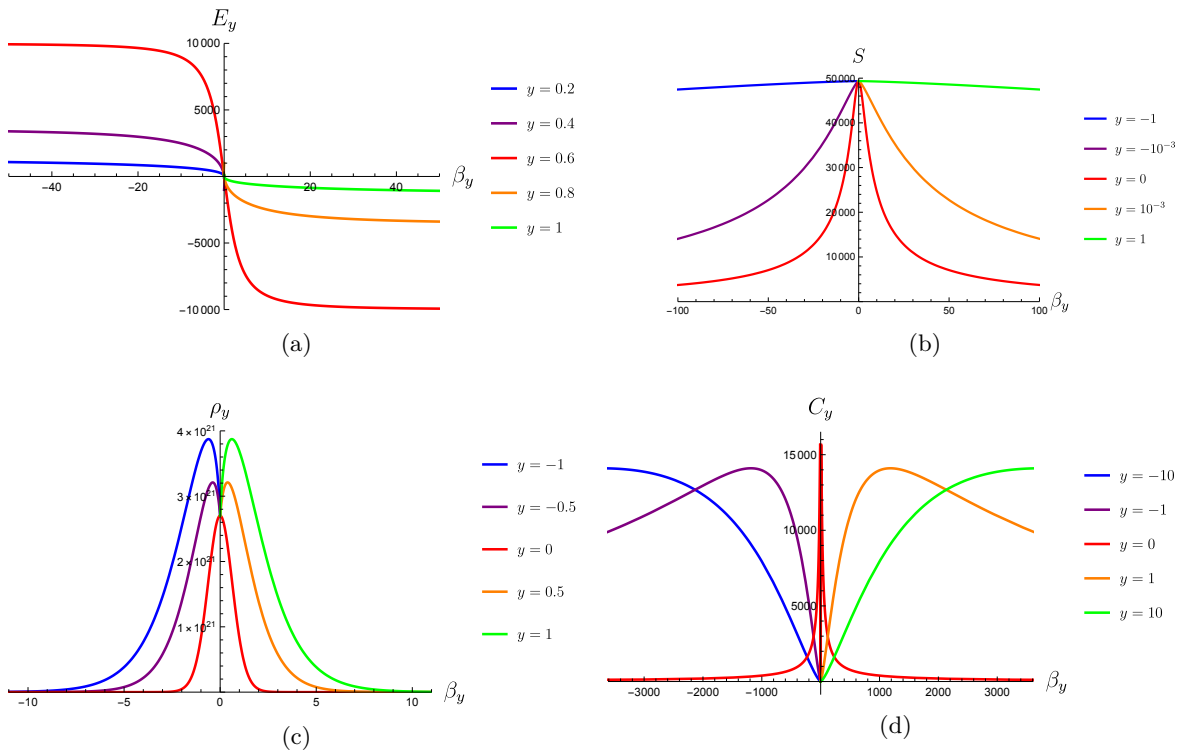


Figure 2. (a) The energy spectrum (3.14), (b) thermodynamic entropy (2.25), (c) density of states (2.28b), and (d) heat capacity (2.29) for generic values of the deformation parameter y (2.17) (shown in the legends) and fixing $\eta = +1$. We use $\lambda = 10^{-4}$ in all subfigures, except in (c) where $\lambda = 0.1$ for visualization purposes.

For concreteness, we consider the main cases of interest where $\eta = \pm 1$ so that E_y is given by (3.14) ($\eta = +1$) and (2.23) ($\eta = -1$) respectively, so that (2.29) becomes,²¹

$$C_y(\theta) = \frac{\eta(J \sin \theta \beta_y(\theta))^2}{2Jy \sin \theta(\pi - 2\theta) + 4Jy \cos \theta(2 + (\pi - 2\theta) \cot \theta) + 2(2 + (\pi - 2\theta) \cot \theta) \sqrt{\lambda(1 - q)}}. \quad (2.30)$$

The argument in the numerator is positive definite when $y \in \mathbb{R}$, $\lambda > 0$ and $\theta \in [0, \pi]$. Note that the case where $\eta = +1$ has a positive heat capacity while $\eta = -1$ a negative one assuming that E_y can be interpreted as the conserved energy spectrum of the deformed theory.

It is important to distinguish when $C_y(\theta)$ physically corresponds to heat capacity when performing the T^2 and $T^2 + \Lambda_1$ flow. For instance in dS_2 , one performs the T^2 deformation, associated with $E_y^{\eta=+1}$, using the Dirichlet boundaries in the Milne patch which are spacelike [150]; while during the $T^2 + \Lambda_1$ flow, associated to $E_y^{\eta=-1}$, the finite cutoff boundaries are located in the static patch of dS_2 and they are timelike, so that $E_y^{\eta=-1}$ can indeed be associated with a quasilocal BY energy [192]. Then, (2.30) is indeed physically a heat capacity and the

²¹Note we are using the $-$ relative sign solution in the T^2 deformed energy spectrum (2.21) and $+$ in the $T^2 + \Lambda_1$ case (2.23); the signs in the heat capacity reverses.

system can thus be thermodynamically unstable, as found in different parts of the literature, see e.g. Sec 6.1. As additional comparison, when $T\bar{T}$ deforming CFTs, one finds negative heat capacities at high energies for T^2 -deformed CFTs and quantum mechanical systems in [193]; while in this system, the energy spectrum is bounded. To make more contrast, opposite observations appear in the AdS_2 case, one performs the T^2 deformation when the boundaries are timelike, and thus the system is stable since (2.30) indeed corresponds to a positive heat capacity, and $T^2 + \Lambda_1$ when the boundaries are spacelike, similar to [148].

Finite cutoff Holographic Interpretation We now provide a bulk interpretation of (2.26) from finite cutoff holography. Let us consider the dilaton gravity theory (2.1), where the metric solution to the equations of motions without matter sources is

$$ds^2 = F(\Phi)d\tau + \frac{d\Phi}{F(\Phi)}, \quad F(x) = \int_{r_h}^x U(\Phi)d\Phi, \quad (2.31)$$

where r_h is the horizon radius. This can be used to evaluate the on-shell action from (2.1), resulting in

$$I_E^{(\text{on})} = -\frac{1}{16\pi G_N} \left(2\pi(\Phi_0 + r_h) + \beta \left(F(\Phi_B) - \sqrt{F(\Phi_B) G(\Phi_B)} \right) \right), \quad (2.32)$$

where we have used the fact that \mathcal{M} has a disk topology when $\Phi_0 \gg |\Phi|$ everywhere. From (2.32) we find:

$$\beta_T E_{\text{BY}} = \left(\beta \sqrt{\frac{F(\Phi_B)}{G(\Phi_B)}} \right) \left(\frac{G(\Phi_B)}{16\pi G_N} \left(1 - \sqrt{\frac{F(\Phi_B)}{G(\Phi_B)}} \right) \right), \quad (2.33)$$

where we identified the inverse the BY quasi-local energy and *Tolman temperature* (i.e. the respective energy and temperature that an observer in a bulk spacetime would associate with a given system at a finite distance Φ_B from it [188]) as

$$E_{\text{BY}} \equiv \frac{1}{16\pi G_N} \left(\sqrt{G(\Phi_B)} - \sqrt{F(\Phi_B)} \right), \quad \beta_T \equiv \beta \sqrt{F(\Phi_B)}. \quad (2.34)$$

Comparing (2.34) with the microcanonical temperature of the deformed theory in (2.26) due to (2.17), we identify the parameters:

$$E_y = \sqrt{G(\Phi_B)} E_{\text{BY}}, \quad \beta_y = \frac{\beta_T}{\sqrt{G(\Phi_B)}}. \quad (2.35)$$

For these relations to hold, we have that

$$\lambda = 8\pi G_N, \quad (2.36)$$

which is consistent with [112].²²

Thus, we find a holographic dictionary at the level of finite cutoff thermodynamics. In contrast with previous literature, we include a more general counterterm $G(\Phi_B)$ in the above expressions, which permits the analysis for non-trivial η in the flow equations (2.16).

²²See e.g. (2.32) [112] where $\pi \mathbf{b}^2 = 4G_N$ in our notation.

Moreover, it follows from (2.35) that the specific heat in the bulk at a fixed finite radial cutoff can be expressed as

$$C_{r_B} \equiv -\beta_T^2 \frac{dE_{BY}}{d\beta_T} = -(\beta_y)^2 \frac{dE_y}{d\beta_y} = C_y . \quad (2.37)$$

This means that there is a direct relation between the heat capacity in the boundary theory at a fixed deformation parameter y (as well as η) (2.29) with respect to the heat capacity in the bulk. Similar results were recovered in related settings by [38].

Hagedorn growth Before closing the section, we make contrast with other results in the literature, we analyze the semiclassical partition function with $\eta = -1$ (2.23)

$$\int_{-\frac{2J}{\lambda}}^{\frac{2J}{\lambda}} dE(\theta) e^{S(\theta) - \beta E_y^{\eta=-1}(\theta)} = \int_{-\frac{2J}{\lambda}}^{\frac{2J}{\lambda}} dE(\theta) e^{S(\theta) - \frac{\beta}{y} (1 + \sqrt{2yE(\theta)-1})} . \quad (2.38)$$

Notably, there no divergence associated to Hagedorn growth for the $T^2 + \Lambda_1$ deformed theory, in contrast to other studies [148]. The reason that there is no divergence even when $\beta \rightarrow 0$ is that the integration is performed over a finite energy range and the factor $e^{S(\theta)}$ is finite, thus the model remains UV finite. It was interpreted by [148], that one reaches a divergence once the boundary in the dual theory reaches a curvature singularity, which is not present in JT gravity, seen as a s-wave reduction of higher dimensional charged black hole, nor in sine dilaton gravity [66].

3 Deforming the DSSYK Model: Chord Basis, Bulk Length & Complexity

Following up the last subsection, we specialize in chord Hamiltonian deformations of the DSSYK model. We study the Krylov basis and Krylov spread complexity for the HH state in the deformed theory and show that in the semiclassical limit, it reproduces a wormhole length in finite cutoff holography.²³

Outline In Sec. 3.1 we briefly review the DSSYK model, including its Hilbert space extension with matter chords. Sec. 3.2 presents the evaluation of Krylov spread complexity for the HH state from a path integral formulation of the model. It reproduces a wormhole length in finite cutoff holography. We discuss the IR/UV triple-scaling limits of the deformed theory.

In addition, we construct a chord number basis related to finite cutoff holography in App. D, as an alternative to the Krylov basis in this section that leads to similar results.

3.1 Review of the DSSYK model

In this subsection, we briefly review the DSSYK model.

²³There is ongoing work by a different group following up [42], which has some overlap with the deformed DSSYK chord Hamiltonian in this section from a bulk perspective. I thank the authors for pointing it out.

The SYK model [50–53, 194] is a system with N Majorana fermions in $(0+1)$ -dimensions, and p -body all-to-all interactions. The theory is given by

$$\hat{H}_{\text{SYK}} = i^{p/2} \sum_I J_I \hat{\psi}_I , \quad (3.1)$$

where $I = i_1, \dots, i_p$ is a collective index, $1 \leq i_1 < \dots < i_p \leq N$; and similarly $\hat{\psi}_I \equiv \hat{\psi}_{i_1} \dots \hat{\psi}_{i_p}$ is a string of Majorana fermions, obeying the Clifford algebra

$$\{\hat{\psi}_i, \hat{\psi}_j\} = 2\delta_{ij}\mathbb{1} ; \quad (3.2)$$

and the coupling constants $J_I = J_{i_1 \dots i_p}$ follow a Gaussian distribution

$$J_I = 0 , \quad \langle J_I J_J \rangle = \binom{N}{p}^{-1} \frac{J^2 N}{2p^2} \delta_{IJ} , \quad (3.3)$$

with $J \in \mathbb{R}$ being a constant, and the expectation values denote annealed averaging over the couplings. We also introduce matter operators, which have the form:

$$\hat{\mathcal{O}}_\Delta \equiv i^{\frac{p'}{2}} \sum_{I'} K_{I'} \hat{\psi}_{I'} . \quad (3.4)$$

Here $I' = i_1, \dots, i_{p'}$; and $K_{I'}$ represents Gaussian random couplings that are independent of J_I . We also define $\Delta \equiv p'/p$, so that we can express

$$\langle K_I \rangle = 0 , \quad \langle K_I J_{I'} \rangle = 0 , \quad \langle (K_I)^2 \rangle = \frac{\mathcal{K}^2}{\Delta^2 \lambda} \binom{N}{p'}^{-1} , \quad (3.5)$$

where $\mathcal{K} \in \mathbb{R}$. In the following, we will set $\mathcal{K} = 1$, which can be restored back with dimensional analysis. Importantly for us, once we consider the double scaling regime, where:

$$N, p \rightarrow \infty , \quad q = e^{-\lambda} \equiv e^{-\frac{2p^2}{N}} \text{ fixed} . \quad (3.6)$$

The SYK model becomes analytically solvable even away from the low energy regime; its ensemble averaged Hamiltonian moments can be described with chord diagrams techniques [54–57],²⁴ whose auxiliary Hilbert space without matter is

$$\mathcal{H}_0 = \text{span}\{|n\rangle \mid n \in \mathbb{Z}_{\geq 0}\} = L^2(\theta \in [0, \pi], d\mu(\theta)) , \quad (3.7)$$

where n denotes the number of open chords at a given time slice in the chord diagram (see e.g. [199] for a review). From now on we will denote the zero-chord number state as

$$|n = 0\rangle \equiv |\Omega\rangle . \quad (3.8)$$

²⁴Other models in the same universality class as the DSSYK model can be solved using the same type of chord counting techniques [184, 195–198].

The auxiliary quantum mechanical theory, described by a chord Hamiltonian \hat{H} , contains the thermal information about the physical system, as captured by the Hamiltonian moments

$$\langle \text{tr}(\hat{H}_{\text{SYK}}^k) \rangle = \langle \Omega | \hat{H}^k | \Omega \rangle , \quad (3.9)$$

where the trace is taken over the Hilbert space states. By an appropriate orthogonal transformation, $\{|n\rangle\}$ can be orthonormalized (i.e. $\langle n|m\rangle = \delta_{nm}$), such that the Hamiltonian takes a symmetric form (see e.g. [56])

$$\hat{H} |n\rangle = -\frac{J}{\sqrt{\lambda}} \left(\sqrt{[n]_q} |n-1\rangle + \sqrt{[n+1]_q} |n+1\rangle \right) , \quad (3.10)$$

where $[n]_q \equiv \frac{1-q^n}{1-q}$. We can now define the chord number operator \hat{n} and its conjugate momentum, \hat{p} :

$$e^{\pm i\hat{p}} |n\rangle = |n \mp 1\rangle , \quad \hat{n} |n\rangle = n |n\rangle , \quad (3.11)$$

which obey the commutation relation:

$$[\hat{n}, e^{i\hat{p}}] = e^{i\hat{p}} , \quad [\hat{n}, e^{-i\hat{p}}] = -e^{-i\hat{p}} . \quad (3.12)$$

The Hamiltonian can be then expressed as

$$\hat{H} = -\frac{J}{\sqrt{\lambda}} \left(e^{i\hat{p}} \sqrt{[\hat{n}]_q} + \sqrt{[\hat{n}]_q} e^{-i\hat{p}} \right) . \quad (3.13)$$

One can also find the energy basis $|\theta\rangle$ of \hat{H} , whose eigenvalues are given as [56, 57]

$$\hat{H} |\theta\rangle = E(\theta) |\theta\rangle , \quad E(\theta) \equiv -\frac{2J \cos(\theta)}{\sqrt{\lambda(1-q)}} , \quad \theta \in [0, \pi] . \quad (3.14)$$

Solving the eigenvalue problem in (3.13) one can then find that the inner product between the energy basis $\{|\theta\rangle\}$ and the chord number $\{|n\rangle\}$ is given by

$$\langle \theta | n \rangle = \frac{H_n(\cos \theta | q)}{\sqrt{(q; q)_n}} , \quad (3.15)$$

with $(a; q)_n$ the q-Pochhammer symbol:

$$(a; q)_n \equiv \prod_{k=0}^{n-1} (1 - aq^k) , \quad (a_0, \dots, a_N; q)_n \equiv \prod_{i=1}^N (a_i; q) , \quad (3.16)$$

and $H_n(x|q)$ is the q-Hermite polynomial:

$$H_n(\cos \theta | q) \equiv \sum_{k=0}^n \begin{bmatrix} n \\ k \end{bmatrix}_q e^{i(n-2k)\theta} , \quad \begin{bmatrix} n \\ k \end{bmatrix}_q \equiv \frac{(q; q)_n}{(q; q)_{n-k} (q; q)_k} . \quad (3.17)$$

The $|\theta\rangle$ basis is normalized such that

$$\langle \theta | \theta_0 \rangle = \frac{1}{\mu(\theta)} \delta(\theta - \theta_0) , \quad \mathbb{1} = \int_0^\pi d\theta \mu(\theta) |\theta\rangle \langle \theta| = \sum_{n=0}^\infty |n\rangle \langle n| , \quad (3.18)$$

$$\mu(\theta) = \frac{(q, e^{\pm 2i\theta}; q)_\infty}{2\pi} \equiv \frac{1}{2\pi} (q, q)_\infty (e^{2i\theta}, q)_\infty (e^{-2i\theta}, q)_\infty . \quad (3.19)$$

For later convenience, we introduce a simple generalization when considering that the DSSYK model with matter insertions [58], which we denote as

$$\mathcal{H}_{\text{full}} \equiv \bigoplus_{m=0}^{\infty} \mathcal{H}_m , \quad \mathcal{H}_m \equiv \text{span} \left\{ \left| \tilde{\Delta}, n_0, n_1, \dots, n_m \right\rangle \right\} , \quad (3.20)$$

where $\tilde{\Delta} = \{\Delta_1, \dots, \Delta_m\}$ is a set of conformal dimensions, and Δ_i characterizes each matter chord operator $\hat{\mathcal{O}}_{\Delta_i}$ which is the ensemble averaged analog of the SYK operator (3.4).

It is also useful to define a total chord number operator

$$\hat{N} \left| \tilde{\Delta}, n_0, \dots, n_m \right\rangle = \sum_{i=0}^m n_i \left| \tilde{\Delta}, n_0, \dots, n_m \right\rangle , \quad (3.21)$$

which will be applied in later sections to evaluate correlation functions.

Next, we consider the two-sided chord Hamiltonian with m operator insertions:

$$\hat{H}_{L/R} = -\frac{J}{\sqrt{\lambda}} \left(\hat{a}_{L/R} + \hat{a}_{L/R}^\dagger \right) , \quad \text{where} \quad (3.22a)$$

$$\hat{a}_L^\dagger = \hat{a}_0^\dagger , \quad \hat{a}_L = \sum_{i=0}^m \hat{\alpha}_i [\hat{n}_i]_q q^{\hat{n}_i^<} , \quad \text{with} \quad \hat{n}_i^< = \sum_{j=0}^{i-1} (\hat{n}_j + \Delta_{j+1}) , \quad (3.22b)$$

$$\hat{a}_R^\dagger = \hat{a}_m^\dagger , \quad \hat{a}_R = \sum_{i=0}^m \hat{\alpha}_i [\hat{n}_i]_q q^{\hat{n}_i^>} , \quad \text{with} \quad \hat{n}_i^> = \sum_{j=i+1}^m (\hat{n}_j + \Delta_j) , \quad (3.22c)$$

where the creation and annihilation operators for the chord number sectors (3.22) in (3.20) act as,

$$\hat{a}_i^\dagger \left| \tilde{\Delta}; n_0, \dots, n_i, \dots, n_m \right\rangle = \left| \tilde{\Delta}; n_0, \dots, n_i + 1, \dots, n_m \right\rangle , \quad (3.23a)$$

$$\hat{\alpha}_i \left| \tilde{\Delta}; n_0, \dots, n_i, \dots, n_m \right\rangle = \left| \tilde{\Delta}; n_0, \dots, n_i - 1, \dots, n_m \right\rangle . \quad (3.23b)$$

For instance, in terms of the above basis, the one-particle chord Hamiltonian, corresponding to $m = 1$ in (3.22) becomes

$$\hat{H}_{L/R} = \frac{J}{\sqrt{\lambda(1-q)}} \left(e^{-i\hat{P}_{L/R}} + e^{i\hat{P}_{L/R}} \left(1 - e^{-\hat{\ell}_{L/R}} \right) + q^\Delta e^{i\hat{P}_{R/L}} e^{-\hat{\ell}_{L/R}} \left(1 - e^{-\hat{\ell}_{R/L}} \right) \right) , \quad (3.24)$$

where we expressed

$$\hat{a}_i^\dagger = \frac{e^{-i\hat{P}_i}}{\sqrt{1-q}} , \quad \hat{\alpha}_i = \sqrt{1-q} e^{i\hat{P}_i} , \quad q^{\hat{n}_i} = e^{-\hat{\ell}_i} , \quad i = L, R . \quad (3.25)$$

At last, there is an energy basis conjugate to the one-particle chord number basis, diagonalizing the two-sided Hamiltonians (3.22a), i.e.

$$\hat{H}_{L/R} \left| \Delta; \theta_L, \theta_R \right\rangle = E(\theta_{L/R}) \left| \Delta; \theta_L, \theta_R \right\rangle , \quad (3.26)$$

where $E(\theta)$ appears in (3.14).

For later convenience, when discussing the IR and UV triple-scaling limits of the DSSYK model [58, 99], we zoom in on the edges of the energy spectrum, i.e.

$$\text{IR} : \theta \sim \mathcal{O}(\lambda) , \quad \text{UV} : \pi - \theta \sim \mathcal{O}(\lambda) , \quad (3.27)$$

and we define the zero-point energy-subtracted and rescaled chord Hamiltonians in the seed theory,

$$\hat{H}_{\text{IR/UV}} \equiv \frac{\sqrt{\lambda(1-q)}}{2J} \left(\pm \hat{H} + \frac{2J}{\sqrt{\lambda(1-q)}} \right) \Big|_{\mathcal{O}(\lambda), \text{IR/UV}} , \quad (3.28a)$$

$$E_{\text{IR/UV}} \equiv \pm \frac{\sqrt{\lambda(1-q)}}{J} E(\theta) + 1 \Big|_{\mathcal{O}(1), \text{IR}} = \frac{\theta_{\text{IR/UV}}^2}{2} , \quad (3.28b)$$

where $\theta_{\text{IR/UV}} \sim \mathcal{O}(\lambda)$ in the corresponding triple-scaling limit; the relative $+$ sign corresponds to the IR, while $-$ for the UV.

We will apply the above definitions to evaluate different properties and observables of the theory under a Hamiltonian deformation in the remainder of the manuscript.

3.2 Krylov Spread Complexity

We now explore the structure of the chord Hilbert space after a generic Hamiltonian deformation

$$\hat{H} \rightarrow \hat{H}_y \equiv f_y(\hat{H}) |\Omega\rangle , \quad (3.29)$$

for some analytic function f_y .²⁵ While the deformed and seed theories have the same Hilbert space, the chord basis can take different forms, and the Hamiltonian (3.29) can have different representations depending on the basis that we choose. For instance, consider the chord number basis where the seed theory Hamiltonian takes the form (3.13). The deformed chord Hamiltonian (3.29) for $y \neq 0$ is in general not diagonal in the chord number basis (3.13). Since the Hamiltonian deformation scrambles the chord basis, we search for a meaningful ordering provided by the Krylov basis. This basis allows us to minimize a so-called ‘‘cost function’’ associated with a general quantum state, as we explain below based on the seminal work by [87], which defines Krylov spread complexity. Moreover, recent developments indicate that the Krylov spread complexity in the seed theory DSSYK model can be interpreted in terms of minimal geodesic lengths between asymptotic boundaries in the bulk dual [58, 68, 71]. We search for the corresponding interpretation of Krylov spread complexity in the finite cutoff holographic dictionary.

²⁵For instance, in the particular case of a T^2 deformation [32]

$$f_y(x) = \frac{1}{y} \left(1 - \sqrt{1 - 2yx} \right) . \quad (3.30)$$

Cost Function In general, following [87] and [200] we refer to the cost function of an ordered basis $\{|B_0\rangle, |B_1\rangle, \dots, |B_n\rangle, \dots\}$ with respect to a reference state $|\psi(\tau)\rangle$ as

$$\mathcal{C} \equiv \sum_{n=0}^{\infty} c_n \frac{|\langle B_n | \psi(\tau) \rangle|^2}{\langle \psi(\tau) | \psi(\tau) \rangle} , \quad (3.31)$$

where $\{c_n \in \mathbb{R}\}$ is a monotonically increasing sequence, and we allow that the reference state evolves in complex-valued time τ as [200]

$$|\psi(\tau)\rangle \equiv e^{-\tau \hat{\mathcal{L}}} |\psi(0)\rangle , \quad (3.32)$$

where $\tau \equiv \frac{\beta}{2} + it$, with β and $t \in \mathbb{R}$, leading to standard Schrödinger evolution when $\beta = 0$, and $\hat{\mathcal{L}}$ is the corresponding generator of evolution in terms of the parametrization τ . Spread complexity in [87] is defined by minimizing the cost function (3.31) over all possible basis sets, which occurs when $\{|B_n\rangle\}$ is the Krylov basis, defined below.

Krylov complexity We now specialize in Krylov spread complexity [87] in deformed DSSYK, so that $\hat{\mathcal{L}} = \hat{H}_y$ in (3.32). We seek to build a Krylov basis $\{|K_n\rangle\}$ with $|K_0\rangle = |\psi(\tau=0)\rangle$ as the initial state in the basis, which we may choose to be $|\Omega\rangle$. The other elements in the Krylov basis are obtained recursively through the Lanczos algorithm,

$$|K_n^{(y)}\rangle \equiv f_n(\hat{H}_y) |\Omega\rangle , \quad (3.33a)$$

$$x f_n(x) = b_{n+1}(y) f_{n+1}(x) + b_n(y) f_{n-1}(x) + a_n(y) f_n(x) , \quad (3.33b)$$

which is initialized by $b_0 = 0$, $f_0(x) = 1$; and $b_n(y)$ and $a_n(y)$ are the Lanczos coefficients. The deformed chord Hamiltonian in this basis then takes the form

$$\hat{H}_y = \hat{b}_n(y) e^{-i\hat{p}_y} + e^{-i\hat{p}_y} \hat{b}_n(y) + \hat{a}_n(y) , \quad (3.34)$$

where the action of the operators in the Krylov basis is defined as

$$e^{\mp i\hat{p}_y} |K_m^{(y)}\rangle = |K_{m\pm 1}^{(y)}\rangle , \quad \hat{a}_n(y) |K_m^{(y)}\rangle = a_m(y) |K_m^{(y)}\rangle , \quad \hat{b}_n(y) |K_m^{(y)}\rangle = b_m(y) |K_m^{(y)}\rangle . \quad (3.35)$$

One can then use the above algorithm to find the explicit coefficients in terms of Hamiltonian moments (see e.g. [201])

$$\begin{aligned} a_0(y) &= m_1 , \quad b_1(y) = m_2 - m_1^2 , \quad a_1(y) = \frac{m_3 + m_1^3 - 2m_1 m_2}{m_2 - m_1^2} , \\ b_2(y) &= \frac{m_2 m_4 - m_2^3 - m_3^2 - m_1^2 m_4 - 2m_1^2 m_2 m_4}{(m_2 - m_1^2)^2} \end{aligned} \quad (3.36)$$

where

$$m_n = (-1)^n \left. \frac{\partial^n \mathcal{Z}_y(\beta)}{\partial \beta^n} \right|_{\beta=0} , \quad \mathcal{Z}_y(\beta) \equiv \frac{\langle \psi(t=0) | e^{-\beta \hat{H}_y} | \psi(t=0) \rangle}{\langle \psi(t=0) | \psi(t=0) \rangle} . \quad (3.37)$$

Then, based on (3.31) with $\{B_n\} = \{|K_n^{(y)}\rangle\}$ and $c_n = n$, Krylov spread complexity is simply defined as

$$\mathcal{C}_S = \sum_{n=0}^{\infty} n \frac{|\langle K_n^{(y)} | \psi(t) \rangle|^2}{\langle \psi(t) | \psi(t) \rangle} , \quad |\psi(t)\rangle = e^{-(\frac{\beta}{2} + it)\hat{H}_y} |\Omega\rangle . \quad (3.38)$$

Semiclassical Approximation To derive the explicit form of the Krylov basis from the Lanczos coefficients (3.36), we search for simplifications in the semiclassical limit,

$$\ell_y \equiv \begin{cases} \lambda \mathcal{C}_S, & 0 \leq y \leq y_0 = \frac{1}{2E(\theta)}, \\ -i\lambda \mathcal{C}_S, & y \geq y_0, \end{cases} \quad \text{fixed as } \lambda \rightarrow 0, \quad (3.39)$$

which corresponds to $n \sim \mathcal{O}(1/\lambda)$, with n being the order in the Lanczos basis $|K_n\rangle$, as the dominant contribution in the evaluation of Krylov complexity, which will allow us to evaluate a_n and b_n for $n \gg 1$.

In this limit, the Hamiltonian on the Krylov basis becomes (3.33b)

$$H_y = 2b(\ell_y) \cos p_y + a(\ell_y), \quad (3.40)$$

where p_y is the conjugate momentum to ℓ_y in the $\lambda \rightarrow 0$ limit. This allows us to express the path integral of the theory as

$$\int [d\ell_y][dp_y] \exp \left[\int d\tau (ip_y \partial_\tau \ell_y - H_y) \right]. \quad (3.41)$$

This path integral prepares the HH state of the deformed theory $e^{-\tau \hat{H}_y} |\Omega\rangle$, with $\tau = \frac{\beta}{2} + it$, so that the Krylov basis is built with $|K_0\rangle = |\Omega\rangle$.

We require that the measure of time scales as $t \sim \mathcal{O}(1/\lambda)$ to perform the saddle point approximation since the energy spectrum of the Hamiltonian scales with $y \propto \lambda^{-1}$. Then in the $\lambda \rightarrow 0$ limit, one then finds the equations of motion

$$\frac{d\ell_y}{dt} = -2 \sin p_y b(\ell_y), \quad -\frac{dp_y}{dt} = 2 \cos p_y \frac{db}{d\ell_y} + \frac{da}{d\ell_y}, \quad (3.42a)$$

$$\frac{1}{2} \frac{d^2 \ell_y}{dt^2} = \frac{d}{d\ell_y} \left(b(\ell_y)^2 \right) + \frac{da}{d\ell_y} b(\ell_y) \cos p_y = \frac{d}{d\ell_y} \left(b(\ell_y)^2 \right) - \frac{1}{2} \frac{da}{d\ell_y} (E_y - a(\ell_y)), \quad (3.42b)$$

where we applied conservation of the deformed Hamiltonian H_y , with an energy spectrum

$$E_y \equiv \begin{cases} \frac{1}{y} (1 - \sqrt{1 - 2yE(\theta)}), & 0 \leq y \leq y_0 = \frac{1}{2E(\theta)}, \\ \frac{1}{y} (1 + \sqrt{2yE(\theta) - 1}), & y \geq y_0, \end{cases} \quad (3.43)$$

in the last relation. The equations of motion (3.42) are supplemented with initial conditions

$$\ell_y(t=0) = \ell_* , \quad \left. \frac{d\ell_y}{dt} \right|_{t=0} = 0, \quad (3.44)$$

where ℓ_* is a constant, and by considering that the expectation values of the chord number are taken with respect to the HH state of the deformed theory $e^{-\tau \hat{H}_y} |\Omega\rangle$, the second condition

follows from the commutation relation

$$\begin{aligned}
& \left. \frac{d}{dt} \langle \psi(\tau) | \hat{n}_y | \psi(\tau) \rangle \right|_{t=0} = \langle \Omega | e^{-\frac{\beta}{2} \hat{H}_y} [\hat{H}_y, \hat{n}_y] e^{-\frac{\beta}{2} \hat{H}_y} | \Omega \rangle \\
& = 2 \sum_{n=0}^{\infty} n \left(\langle \Omega | e^{-\beta \hat{H}_y} | K_n^{(y)} \rangle \langle K_n^{(y)} | \frac{d e^{-\beta \hat{H}_y}}{d\beta} | \Omega \rangle - \langle \Omega | \frac{d e^{-\frac{\beta}{2} \hat{H}_y}}{d\beta} | K_n^{(y)} \rangle \langle K_n^{(y)} | e^{-\frac{\beta}{2} \hat{H}_y} | \Omega \rangle \right) \\
& = 2 \sum_{n=0}^{\infty} n (\psi_n(\beta, y) \psi_n'(\beta, y) - \psi_n(\beta, y) \psi_n'(\beta, y)) = 0 .
\end{aligned} \tag{3.45}$$

Here, we expanded the chord number \hat{n}_y in the Krylov basis and defined

$$\psi_n(\beta, y) \equiv \langle \Omega | e^{-\frac{\beta}{2} \hat{H}_y} | K_n^{(y)} \rangle , \quad \psi_n'(\beta, y) = d\psi_n(\beta, y)/d\beta , \tag{3.46}$$

while assuming that \hat{H}_y is Hermitian. Thus, we recover the second initial condition in (3.44).

In particular, from the second initial condition in (3.44) we recover that $p_y(t=0) = 0$, and thus, by conservation of the energy spectrum of the deformed Hamiltonian represented in (3.40), we have

$$E_y = \frac{1}{y} \left(1 \pm \sqrt{\eta(1 - 2yE(\theta))} \right) = 2b(\ell_*) + a(\ell_*) . \tag{3.47}$$

where $\eta = \pm$ and the relative ± 1 signs in front of the square root indicate the perturbative, non-perturbative solutions in $T^2(+\Lambda_1)$ deformations. Then, to reproduce the conserved energy spectrum of the deformed theory we make an ansatz such that (3.42b) takes the form

$$\frac{d^2 \ell_y}{dt_y^2} = \frac{1}{y^2} \tanh\left(\frac{\ell_y}{2}\right) \operatorname{sech}^2\left(\frac{\ell_y}{2}\right) , \tag{3.48}$$

which means that in this ansatz

$$\frac{da}{d\ell_y} = 0 , \quad \frac{db(\ell_y)^2}{d\ell_y} = \frac{1}{2y^2} \frac{d}{d\ell_y} \left(\tanh^2(\ell_y/2) - 1 \right) , \tag{3.49}$$

where we implemented a rescaling in time parameter of (3.48) with $R(y)t \rightarrow 2yt$ such that the deformed Hamiltonian has the energy spectrum in (3.43).

Using the initial conditions (3.44), one finds that the solutions of (3.49) are

$$a(\ell_y) = \frac{1}{y} , \quad b(\ell_y) = \pm \frac{1}{2y} \tanh(\ell_y/2) , \tag{3.50}$$

where \pm corresponds to the perturbative and non-perturbative branches of the T^2 and $T^2 + \Lambda_1$ deformations, which were discussed in Sec. 2.2. Thus, specializing to $T^2(+\Lambda_1)$ deformations, we find that

$$\begin{aligned}
y \in [0, y_0] : \quad \sinh\left(\frac{\ell_*}{2}\right) &= \sqrt{\frac{1}{2yE(\theta)} - 1} , \\
y \in [y_0, \infty] : \quad \sin\left(\frac{i\ell_*}{2}\right) &= \sqrt{1 - \frac{1}{2yE(\theta)}} .
\end{aligned} \tag{3.51}$$

The deformed chord Hamiltonian in the continuum limit (3.40) then becomes

$$H_y = \begin{cases} \frac{1}{y} \left(1 - \tanh\left(\frac{\ell_y}{2}\right) \cos(p_y) \right), & 0 \leq y \leq y_0 = \frac{1}{2E(\theta)}, \\ \frac{1}{y} \left(1 + \tanh\left(\frac{\ell_y}{2}\right) \cos(p_y) \right), & y \geq y_0. \end{cases} \quad (3.52)$$

From (3.42b) and (3.44) we recover the Krylov spread complexity (3.38) of the HH state in the deformed theory as:

$$\mathcal{C}_S = \begin{cases} \frac{\ell_y}{\lambda} = \frac{2}{\lambda} \operatorname{arcsinh}\left(\sqrt{\frac{1}{2yE(\theta)} - 1} \cosh\left(\frac{\sin\theta}{2} \tilde{t}\right)\right), & 0 \leq y \leq y_0 = \frac{1}{2E(\theta)}, \\ \frac{\ell_y}{i\lambda} = \frac{2}{\lambda} \operatorname{arcsin}\left(\sqrt{1 - \frac{1}{2yE(\theta)}} \cosh\left(\frac{\sin\theta}{2} \tilde{t}\right)\right), & y \geq y_0, \end{cases} \quad (3.53a)$$

where $\tilde{t} \equiv \csc\theta \sqrt{2E(\theta)/y} t$. This rescaled time is convenient for comparison with the geodesic length between the asymptotic boundaries in the bulk (see App. B).

Interpretation From (3.34, 3.52) it follows that the chord Hamiltonian when $n \sim \mathcal{O}(1/\lambda)$ can be expressed in the Krylov basis as,

$$\hat{H}_y = \frac{1}{y} \left(1 \pm \frac{1}{2} \left(\tanh\left(\frac{\lambda \hat{n}_y}{2}\right) e^{-i\hat{p}_y} + e^{i\hat{p}_y} \tanh\left(\frac{\lambda \hat{n}_y}{2}\right) \right) \right), \quad (3.54a)$$

$$\hat{n}_y \equiv \sum_n n |K_n^{(y)}\rangle \langle K_n^{(y)}|, \quad (3.54b)$$

where the action of the above operators in the Krylov basis was specified in (3.35), and the \pm signs correspond to the cases in (3.52). Crucially, while we used an ansatz to solve the differential equation for the evolution of the chord number in the semiclassical limit, the specific form of the Hamiltonian is determined from the conserved energy spectrum in the deformed theory E_y such that the deformed Hamiltonian in (3.54a) is tridiagonal and symmetric. Thus, the resulting Hamiltonian is expressed in the (unique) Krylov basis with the corresponding Lanczos coefficients,²⁶

$$\lambda \rightarrow 0, \quad n \sim \mathcal{O}(\lambda^{-1}) : \left\{ |K_n^{(y)}\rangle \mid \langle K_m^{(y)} | K_n^{(y)} \rangle = \delta_{nm}, \quad |K_0^{(y)}\rangle = |\Omega\rangle \right\}, \quad (3.55)$$

$$a_n(y) = y^{-1}, \quad b_n(y) = \pm \frac{1}{2y} \tanh\left(\frac{\lambda n}{2}\right).$$

Therefore, the relation between Krylov spread complexity and the wormhole length (i.e. the extremal codimension-one volume) in the bulk [68, 71] still holds, corresponding to an explicit manifestation of the CV conjecture [97, 203, 204] in finite cutoff holography [205], as expected by [42].

²⁶Given that $a_n = \text{constant}$ at leading order when $\lambda \rightarrow 0$, it means that the weight $w(E_y - a_n)$ in the integration measure $d\mu(E_y) \equiv dE_y w(E_y)$ obeys the property $w(E_y - a_n) = w(-(E_y - a_n))$ [202] at leading order in a $\lambda \rightarrow 0$ expansion.

Triple-Scaling Limit In addition, we observe from the relative minus sign case in (3.52) that the deformed chord Hamiltonian takes the same form as the canonically quantized ADM Hamiltonian of JT gravity at a finite cutoff found by [37] (7.6) where the parameter r_b in the JT gravity case corresponds to y in the boundary theory (3.52). This implies that we can define the IR/UV triple-scaling limits to recover the generators of time and spatial translations along the finite cutoff boundaries in (dS) JT gravity by simply focusing on the energy spectrum of the seed theory (3.27):

$$\text{IR} : \theta \equiv \theta_{\text{IR}} \ll 1, \quad \text{UV} : \pi - \theta \equiv \theta_{\text{UV}} \ll 1. \quad (3.56)$$

Note that the triple-scaling limit in the deformed theory shows some sharp differences with respect to the one in the seed theory limit ($y = 0$), where one instead defines a regularized length operator $\lambda \hat{n} + 2 \log \lambda$ [58]. Meanwhile in (3.52) the finite cutoff in the bulk dual implies that the corresponding lengths in the bulk do not need additional regularization. In contrast, [42] mentions that the canonically quantized Hamiltonian in JT gravity (3.52) may be isometrically dual to the Hamiltonian in a matrix model. Thus, our work contains a different interpretation, where (dS) JT gravity at the disk level is holographically described by the IR/UV tails of DSSYK model. In particular, while the bulk length is spacelike or time-like depending on whether the cutoff boundaries are located outside or inside the black hole or the static patch, the Krylov spread complexity (3.53) with the corresponding substitution (3.56) for each limit remains real-valued. We display the growth of Krylov spread complexity in the IR limit and its bulk interpretation in Fig. 3.

Furthermore, in this limit one can simplify the critical value of the deformation parameter y (2.17) y_0 in (2.22) where the spectrum of the Hamiltonians corresponds to $\theta_{\text{IR/UV}}^2/2$. That is,

$$\text{IR} : y_0 = \theta_{\text{IR}}^{-2}, \quad \text{UV} : y_0 = \theta_{\text{UV}}^{-2}. \quad (3.57)$$

In particular, the UV case with the $T^2 + \Lambda_1$ deformation describes the static patch of dS₂, realizing the cosmological stretched horizon proposal by Susskind [1] (detailed in Sec. 6).

4 Correlation Functions

In this section, we study n -point correlation functions of the deformed DSSYK model. They are directly defined in the chord theory with Hamiltonian deformations. We evaluate them in the semiclassical limit. Consistent with the literature, the semiclassical results are modified only by a redshift factor associated with the Tolman temperature in the bulk.

Outline In Sec. 4.1 we define n -point correlation functions in the chord theory after the deformation. In Sec. 4.2 we perform the semiclassical evaluation of the correlation functions from a path integral argument, which leads to the expected redshift parameter. At last, in Sec. 4.3 we discuss the triple-scaling limits of the expressions.

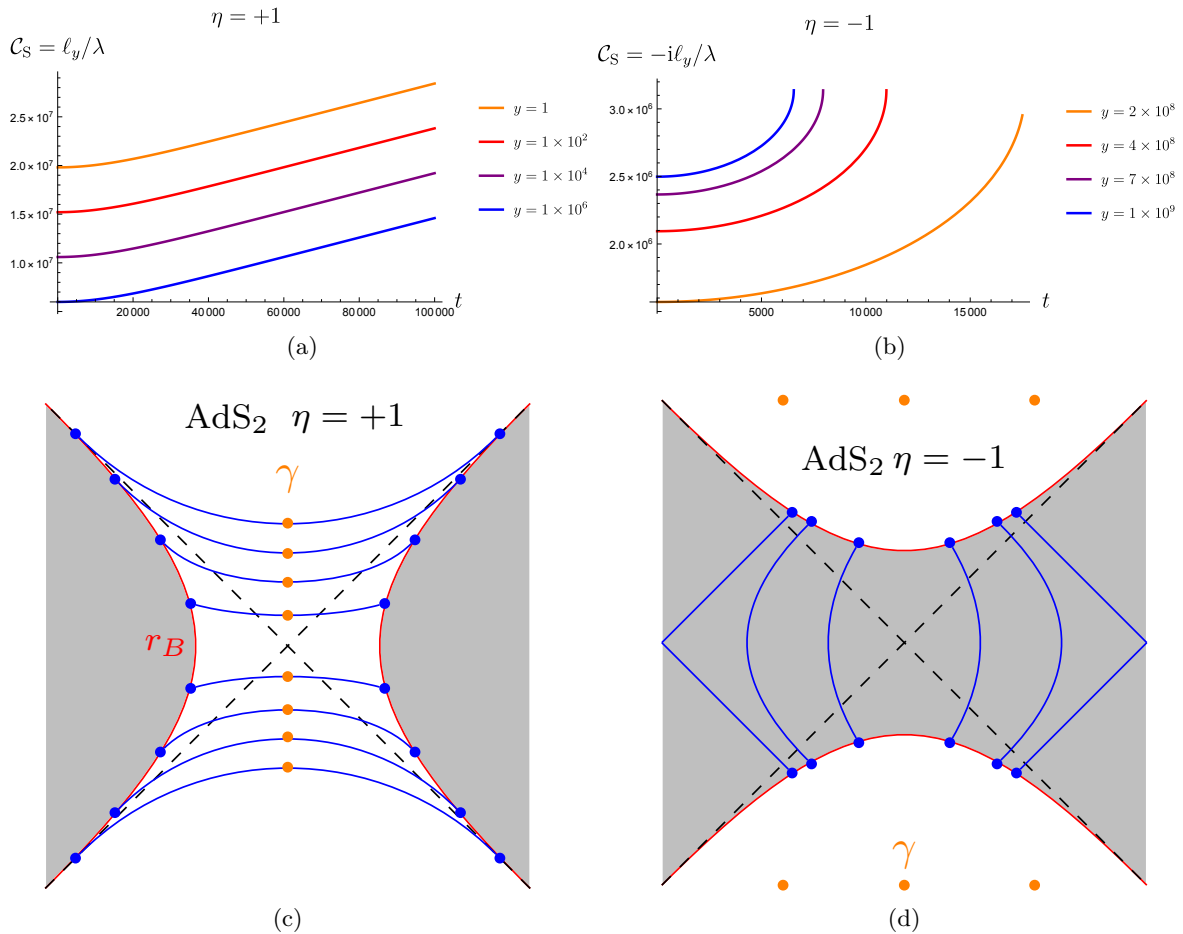


Figure 3. *Top:* Krylov spread complexity of the HH state in the IR limit (3.53) after (a) a T^2 ($\eta = +1$) and (b) $T^2 + \Lambda_1$ ($\eta = -1$) deformation, with $\theta_{\text{IR}} = 10^{-4}$. *Bottom:* Corresponding bulk interpretation in terms of (c) spacelike and (d) timelike extremal Einstein-Rosen bridges (blue solid curves) connecting the finite Dirichlet boundaries (red solid curve), located at a constant $r = r_B$ in the Rindler- AdS_2 coordinates (B.2). We marked the minimal extremal codimension-two area (measured by the dilaton) surfaces γ (orange dots) subject to the homology constraint to the entangling surface (blue dots at the Dirichlet boundaries). Increasing the deformation parameter y (2.17) enhances the rate of growth of the Krylov spread complexity for the $\eta = +1$ case. In finite cutoff holography, this moves the location of the boundaries towards the corresponding black hole horizon, which increases the Tolman temperature, resulting in an enhancement of the growth of the length with respect to the boundary time. Meanwhile, for the $\eta = -1$ case, increasing y moves the boundary cutoff away from the horizon in the bulk, leading to a decrease in the Tolman temperature. However, there is no eternal growth unlike the $\eta = +1$ case, since the timelike geodesic eventually reaches $r \rightarrow \infty$ in Rindler- AdS_2 space (B.3) as one increases the spacelike coordinate t .

4.1 n-Point Correlation Functions

In the following, we generalize the original flow equation (2.16) for the chord Hamiltonian with matter (3.22a),

$$\partial_y \hat{H}_{L/R,y} = \frac{\hat{H}_{L/R,y}^2 + (\eta - 1)/y^2}{2(1 - y\hat{H}_{L/R,y})} . \quad (4.1)$$

The holographic dictionary entry relating the deformation parameter y with a finite Dirichlet cutoff in the bulk, such as in (2.17), may be modified since we need to account for matter in the dilaton gravity action (2.1). In this case, finite cutoff holography is less understood in general [27]; and one in principle may use a different holographic interpretation of (4.1) related to mixed boundary conditions [26]. Regardless of the bulk interpretation, we will study the solutions of (4.1) as a deformed chord theory by itself.

While correlation functions are originally defined by taking the double-scaling limit of operators in the physical SYK model, we work directly in chord space since we are interested in evaluating correlation functions in the ensemble averaged theory. For a simple illustration, we define a (normalized) two-point function by simply deforming the chord Hamiltonian, while keeping the matter operators unchanged

$$G^\Delta \equiv Z_y(\beta)^{-1} \langle \Omega | \hat{\mathcal{O}}_\Delta e^{-\tau^* \hat{H}_{L,y}} e^{-\tau \hat{H}_{L,y}} \hat{\mathcal{O}}_\Delta | \Omega \rangle , \quad (4.2)$$

where $\hat{\mathcal{O}}_\Delta$ represents the chord matter operator $\hat{\mathcal{O}}_\Delta^L$ (3.20), and $\tau \equiv \frac{\beta}{2} + it$.

Note that the above definition has the same structure as the two-point function of the seed theory [56], where we simply replace the corresponding Hamiltonians as $\hat{H}_{L/R} \rightarrow \hat{H}_{L/R,y}$.

To evaluate the correlation function in the one-particle space (4.2) we can use the resolution of the identity

$$\mathbb{1} = \int d\theta_L d\theta_R \mu(\theta_L) \mu(\theta_R) \hat{\mathcal{F}}_\Delta^\dagger (|\theta_L\rangle \otimes |\theta_R\rangle) (\langle \theta_L | \otimes \langle \theta_R |) \hat{\mathcal{F}}_\Delta , \quad (4.3)$$

where we introduce a chord intertwiner [67, 73]:

$$\hat{\mathcal{F}}_\Delta |\Delta; \theta_L, \theta_R\rangle = \sqrt{\langle \theta_L | q^{\Delta \hat{n}} | \theta_R \rangle} |\theta_L\rangle \otimes |\theta_R\rangle . \quad (4.4)$$

Then, (4.2) becomes

$$\begin{aligned} G^\Delta &= Z_y(\beta)^{-1} \prod_{i=1}^2 \int d\theta_i \mu(\theta_i) e^{-\tau^* E_y(\theta_1) - \tau E_y(\theta_2)} \langle \theta_1 | q^{\Delta \hat{n}} | \theta_2 \rangle \\ &= Z_y(\beta)^{-1} \langle \Omega | e^{-\tau^* \hat{H}_y} q^{\Delta \hat{n}} e^{-\tau \hat{H}_y} | \Omega \rangle . \end{aligned} \quad (4.5)$$

Therefore, since the chord number in the original chord basis without deformation $\hat{n} = \sum_{n=0}^{\infty} n |n\rangle \langle n|$ appears in the above expressions, we can perform the evaluation of the correlation functions with path integral methods using the representation of the Hamiltonian in the original basis. This implies that correlation functions in the deformed theory defined above might not capture the behavior of geodesic lengths in finite cutoff holography. As we

will see, this is consistent with the commonly employed definitions of correlation function in the literature on T^2 deformations and its extensions.²⁷

Next, applying (4.5), it follows that higher-point functions can be expressed [58, 61]

$$\begin{aligned} & \langle \Omega | e^{-\tau_m^* \hat{H}_{L,y}} \dots \hat{\mathcal{O}}_\Delta e^{-\tau_2^* \hat{H}_{L,y}} \hat{\mathcal{O}}_\Delta e^{-\tau_1^* \hat{H}_{L,y} - \tau_1 \hat{H}_{R,y}} \hat{\mathcal{O}}_\Delta e^{-\tau_2 \hat{H}_{L,y}} \hat{\mathcal{O}}_\Delta \dots e^{-\tau_m \hat{H}_{L,y}} | \Omega \rangle \\ & = \langle \Omega | e^{-\tau_m^* \hat{H}_{L,y}} \dots \hat{\mathcal{O}}_\Delta e^{-(\tau_1 + \tau_2)^* \hat{H}_{L,y}} q^{\Delta \hat{N}} e^{-(\tau_1 + \tau_2) \hat{H}_{L,y}} \hat{\mathcal{O}}_\Delta \dots e^{-\tau_m \hat{H}_{L,y}} | \Omega \rangle \end{aligned} \quad (4.6)$$

where

$$\tau_i = \frac{\beta_i}{2m} + it_i, \quad t_i \in \mathbb{R}, \quad 2 \sum_{i=1}^m \beta_i = \beta, \quad (4.7)$$

with β being the periodicity of the thermal circle, and \hat{N} is the total chord number operator (3.21).

4.2 Semiclassical Evaluation

Having found that correlation functions in the deformed theory can be treated in terms of the chord number in the Krylov basis, we will now proceed to evaluate them in the semiclassical limit [58], i.e. λn fixed as $\lambda \rightarrow 0$.

Based on (4.6) the $(2m+2)$ -correlation function of interest is,²⁸

$$G_{\tilde{\Delta}}^{\Delta_0} = \frac{\langle \Psi_{\tilde{\Delta}}^y(\tau_0, \tau_1, \dots, \tau_m) | q^{\Delta_0 \hat{N}} | \Psi_{\tilde{\Delta}}^y(\tau_0, \tau_1, \dots, \tau_m) \rangle}{\langle \Psi_{\tilde{\Delta}}^y(\tau_0, \tau_1, \dots, \tau_m) | \Psi_{\tilde{\Delta}}^y(\tau_0, \tau_1, \dots, \tau_m) \rangle}, \quad (4.9a)$$

$$| \Psi_{\tilde{\Delta}}^y(\tau_0, \tau_1, \dots, \tau_m) \rangle \equiv e^{-\tau_m \hat{H}_{L,y}} \hat{\mathcal{O}}_{\Delta_m} \dots e^{-\tau_1 \hat{H}_{L,y}} \hat{\mathcal{O}}_{\Delta_1} e^{-\tau_0 \hat{H}_{L,y}} | \Omega \rangle, \quad (4.9b)$$

with $\tilde{\Delta}$ in (3.21), $\tau_i \in \mathbb{C}$ and $\sum_{i=0}^m \tau_i = \beta$, and $\tilde{\Delta} = \{\Delta_1, \dots, \Delta_m\}$. Meanwhile, $\hat{\mathcal{O}}_{\Delta_1}, \dots, \hat{\mathcal{O}}_{\Delta_m}$ are general matter chord operators, which may be light (i.e. $\Delta_i \mathcal{O}(1)$ as $\lambda \rightarrow 0$) or heavy (i.e. $\lambda \Delta_{1 \leq i \leq m} \sim \mathcal{O}(1)$ as $\lambda \rightarrow 0$). We display the representation of the correlation function (4.9a) in Fig. 4 (based on [73]),

To evaluate the general correlation function (4.9a), we are interested in the semiclassical regime where

$$\langle f(\hat{N}) \rangle_{\lambda \rightarrow 0} \equiv f(\langle \hat{N} \rangle) = f\left(\frac{\ell}{\lambda}\right), \quad \ell \equiv \sum_{i=0}^m \ell_i. \quad (4.10)$$

²⁷It might be interesting to use alternative definitions for the correlation functions, for instance, by promoting the chord number \hat{n} in (4.5) to \hat{n}_y (3.54b).

²⁸In the bulk, this correlation function is associated with a bulk propagator being that of a probe massive scalar coupled in the effective geometry as [92, 111],²⁹

$$I_{\text{matter}} = \int d^2x \sqrt{g_{\text{eff}}} (g_{\text{eff}}^{\mu\nu} \partial_\mu \tilde{\phi} \partial_\nu \tilde{\phi} + m^2 \tilde{\phi}^2), \quad (4.8)$$

$\beta_y(\theta = \pi) \rightarrow \infty$. It would be interesting to do an explicit matching between the finite cutoff sine dilaton gravity with the $\text{T}\bar{\text{T}}$ deformed DSSYK model; or more general multitrace deformations for the DSSYK model corresponding to other modifications in the boundary conditions in the bulk.

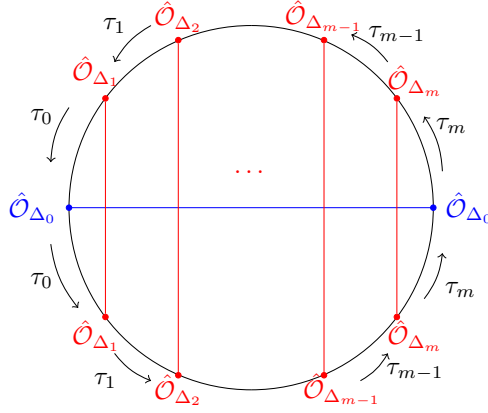


Figure 4. $(2m+2)$ -correlation function in (4.9a) with \hat{O}_{Δ_0} (blue) being light operators and $\hat{O}_{\Delta_{1 \leq i \leq m}}$ (red) at different locations, $\tau_{1 \leq i \leq m}$, within the thermal circle.

Here, we denote f as a generic function; the expectation value is taken in a generic state (which in our case of interest corresponds to (4.9a)); and at last we defined

$$\ell_{0 \leq i \leq m} \equiv \lambda \langle \hat{n}_i \rangle, \quad (4.11)$$

as expectation values of the rescaled chord number for each chord subsector, defined in (3.21); and note that the quantum fluctuations for the parameter \hat{N} are suppressed in the $\lambda \rightarrow 0$ limit.³⁰

We now evaluate the expectation value of the length from the path integral of the DSSYK model with matter as

$$\int \prod_{i=0}^m [d\ell_i][dP_i] \exp \left[\int d\tau_L d\tau_R \left(\frac{i}{\lambda} \sum_{i=0}^m (P_i (\partial_{\tau_L} + \partial_{\tau_R}) \ell_i) + H_{L,y} + H_{R,y} \right) \right], \quad (4.14)$$

where $H_{L/R,y}$ are the deformed chord Hamiltonians with one particle insertion (3.24) $m=1$

$$H_{L/R,y} \equiv f_y(H_{L/R}), \quad (4.15a)$$

$$H_{L/R} = \frac{J}{\sqrt{\lambda(1-q)}} \left(e^{-iP_{L/R}} + e^{iP_{L/R}} \left(1 - e^{-\ell_{L/R}} \right) + q^\Delta e^{iP_{R/L}} e^{-\ell_{L/R}} \left(1 - e^{-\ell_{R/L}} \right) \right). \quad (4.15b)$$

³⁰This argument can also be used to evaluate a generalized notion of Krylov complexity [87]

$$\tilde{C} \equiv \frac{\langle \psi(t) | f(\hat{n}) | \psi(t) \rangle}{\langle \psi(t) | \psi(t) \rangle} = \sum_n f(n) \frac{|\langle n | \psi(t) \rangle|^2}{\langle \psi(t) | \psi(t) \rangle}. \quad (4.12)$$

where $f(n) = c_n$ in the notation of the cost function (3.31); \hat{n} the Krylov complexity operator, which can be extended with operator insertions [69, 70, 72, 73]. In the semiclassical limit, quantum fluctuations are suppressed (4.10) and (4.12) becomes

$$\tilde{C} = f(\ell/\lambda). \quad (4.13)$$

Holographically (4.13) corresponds to a general function of the wormhole length.

In the $\lambda \rightarrow 0$ limit, we evaluate the path integral through saddle points that split into the left/right chord sectors

$$\frac{1}{\lambda} \frac{\partial \ell}{\partial t_{L/R}} = \sum_{i=0}^m \frac{\partial H_{L/R, y}}{\partial P_i}, \quad \frac{1}{\lambda} \frac{\partial P_i}{\partial t_{L/R}} = -\frac{\partial H_{L/R, y}}{\partial \ell_i}, \quad (4.16)$$

given that $\hat{H}_{L/R, y}$ are the translation generators in $t_{L/R}$.

Using (4.15a) it follows that (4.16) can be expressed as

$$\frac{1}{\lambda} \frac{\partial \ell}{\partial t_{L/R}} = f'_y(\hat{H}_{L/R}) \sum_{i=0}^m \frac{\partial H_{L/R}}{\partial P_i}, \quad \frac{1}{\lambda} \frac{\partial P_i}{\partial t_{L/R}} = -f'_y(\hat{H}_{L/R}) \frac{\partial H_{L/R}}{\partial \ell_i}, \quad (4.17)$$

It is clear from this derivation of the saddle points of the path integral (4.14) that $f'_y(\hat{H}_{L/R})$ are just overall constant factors since the two-sided Hamiltonian $H_{L/R}$ is conserved (3.14). This means that the correlation function (4.9a) for the deformed theory is the same the seed correlation function after rescaling the $t_{L/R} \rightarrow f'_y(E_{L/R})t_{L/R}$. Given that the temperature is the only energy scale in the correlation functions, the effect of the deformation is equivalent to rescaling the temperature by an appropriate redshift factor. This means

$$\frac{t}{\beta} \rightarrow \frac{t}{\beta_y}, \quad \text{when } t \rightarrow f'_y(E)t, \quad (4.18)$$

where $\beta_y = f'_y(E)\beta$ (2.26) as we defined in the semiclassical thermodynamic analysis in Sec. 2.3. This means that the rate of growth is modified by the Hamiltonian deformation. A similar finding was reported in TT deformations to study OTOCs in the shockwave BTZ black hole geometry [148, 207]. We should note that (4.18) is consistent with finite cutoff holography [23], given that the factor $\beta \rightarrow \beta_y$ corresponds to a change in the Tolman temperature in the bulk, as we discussed at the end of Sec. 2.3.

Using the above results we can immediately evaluate all the correlation functions of the type (4.14) in the deformed theory based on those in the seed theory. This follows from solving ℓ based on the specific equations of motion in (4.17) with appropriate boundary conditions and then applying (4.10) to evaluate correlation functions, as we specify below.

Two-Point Functions Consider (4.9a) for $m = 1$ with an analytic continuation in the parameter

$$\tau = \frac{\beta(\theta)}{2} + it, \quad (4.19)$$

where $\beta(\theta)$ is the semiclassical temperature (2.26) to compute Lorentzian correlators in the microcanonical ensemble. Based on our results from the saddle point analysis above, and using the semiclassical seed theory two-point correlation function at finite temperature in [191], the corresponding correlation function in the deformed theory is given by

$$\begin{aligned} G_2(t, \theta) &\equiv G^{\Delta_0}(\tau) \Big|_{\tau = \frac{\beta(\theta)}{2} + it} = \frac{\langle \Omega | e^{-\tau \hat{H}_y} q^{\Delta_0 \hat{n}} e^{-\tau \hat{H}_y} | \Omega \rangle}{\langle \Omega | e^{-\beta(\theta) \hat{H}_y} | \Omega \rangle} \Big|_{\tau = \frac{\beta(\theta)}{2} + it} \\ &\stackrel{\lambda \rightarrow 0}{=} \frac{\exp(-\Delta_0 \ell)}{\langle \Omega | e^{-\beta(\theta) \hat{H}_y} | \Omega \rangle} = \left(\sin \theta \operatorname{sech} \frac{\pi t}{\beta_y(\theta)} \right)^{2\Delta_0}, \end{aligned} \quad (4.20)$$

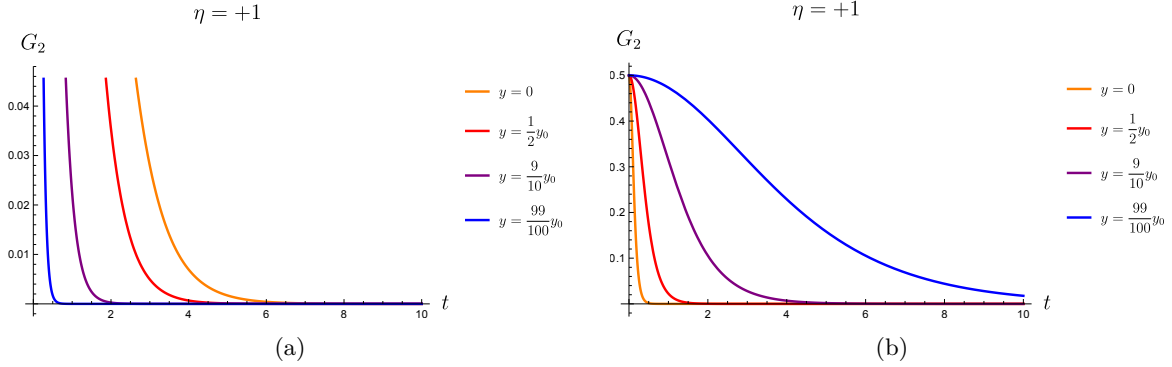


Figure 5. Evolution of the two-point correlation function (4.20) for (a) T^2 , and (b) $T^2 + \Lambda_1$ deformations. As the deformation parameter reaches the critical value y_0 (3.57) the fake temperature (4.21) increases resulting in faster decay of the correlation function. The parameters in this evaluation are: $\lambda = 10^{-4}$, $J = 1$, $\Delta = 1$ and $\theta = 3\pi/4$.

where $\tilde{\beta}_{y=0}$ above is termed as fake temperature [92], which in our case contains a redshift factor

$$\tilde{\beta}_y(\theta) \equiv \frac{2\pi}{J \sin \theta} \frac{dE}{dE_y} = \begin{cases} \frac{2\pi}{J \sin \theta} \sqrt{1 - 2yE(\theta)} & \eta = +1, \\ \frac{2\pi}{J \sin \theta} \sqrt{2yE(\theta) - 1} & \eta = -1. \end{cases}, \quad (4.21)$$

and $\ell \equiv \lambda \langle \Omega | e^{-\tau^* \hat{H}_y} \hat{n} e^{-\tau \hat{H}_y} | \Omega \rangle$ as in (4.10); while the last step comes from solving the equations of motion for ℓ in (4.17) (in the case $m = 0$), which follows analogously to [72] with the fake temperature in (4.21).

We illustrate the behavior of the above expressions in Fig. 5. The fake temperature, which corresponds to the inverse rate of decay of two-point functions, is argued to represent the black hole temperature in the bulk so that the system is only maximally chaotic with respect to $\tilde{\beta}_y$ [92]. In particular, Fig. 5 indicates that as the deformation parameter reaches its critical value y_0 (3.57) the boundary cutoff in the bulk approaches the location of a black hole horizon, which has infinite Tolman temperature (2.34) in accordance with finite cutoff holography. In contrast, the system is submaximally chaotic with respect to the physical temperature as defined from the partition function β_y (2.26), as we find below.

Crossed Four-Point Functions Similarly, we can evaluate explicitly (4.9a) for $m = 2$ to recover a Lorentzian crossed four-point function using the analytic continuation (4.19) when $\lambda \rightarrow 0$ based on the seed theory result for the crossed four-point function of matter chord operators in [72] and the time rescaling in (4.18). Including the fake temperature (4.21), the

previous procedure gives:

$$G_4(t_L, t_R; \theta_L, \theta_R) \equiv G_{\Delta_1}^{\Delta_0}(\tau_L, \tau_R) \Big|_{\tau_{L/R} = \frac{\beta(\theta_{L/R})}{2} + it_{L/R}} \Bigg|_{\lambda \rightarrow 0}^{\equiv} \left(\frac{e^{-\ell_*(q^{\Delta_1}, \theta_L, \theta_R)/2}}{\cosh\left(\frac{\pi t_L}{\tilde{\beta}_{L,y}}\right) \cosh\left(\frac{\pi t_R}{\tilde{\beta}_{R,y}}\right) + \frac{e^{-\ell_*(q^{\Delta_1}, \theta_L, \theta_R)} q^{\Delta_1}}{\sin \theta_L \sin \theta_R} \sinh\left(\frac{\pi t_L}{\tilde{\beta}_{L,y}}\right) \sinh\left(\frac{\pi t_R}{\tilde{\beta}_{R,y}}\right)} \right)^{2\Delta_0}, \quad (4.22)$$

where $\tilde{\beta}_{L/R,y} \equiv \tilde{\beta}_y(\theta_{L/R})$ which appears in (4.21), while

$$e^{-\ell_*(q^{\Delta_1}, \theta_L, \theta_R)} = \frac{q^{-2\Delta_1}}{2} \left(1 + q^{2\Delta_1} - 2q^{\Delta_1} \cos \theta_L \cos \theta_R - \sqrt{1 + q^{4\Delta_1} + 2q^{2\Delta_1} (1 + \cos(2\theta_L) + \cos(2\theta_R)) - 4q^{\Delta_1} (1 + q^{2\Delta_1}) \cos \theta_L \cos \theta_R} \right). \quad (4.23)$$

In particular, when $t_L = -t_R := t$ and $\beta_L = -\beta_R = \beta(\theta)/2$ then (4.22) takes the form

$$G_4(-t, t; \theta, \pi - \theta) \Big|_{\lambda \rightarrow 0}^{\equiv} \left(\frac{e^{-\ell_0}}{\cosh^2\left(\frac{\pi t}{\tilde{\beta}_y}\right) - \frac{q^{\Delta_1} e^{-\ell_0}}{\sin^2 \theta} \sinh^2\left(\frac{\pi t}{\tilde{\beta}_y}\right)} \right)^{2\Delta_0}, \quad (4.24)$$

where we denote $e^{-\ell_0} \equiv e^{-\ell_*(q^{\Delta_1}, \theta, \pi - \theta)}$.³¹

The expression (4.24) can then be approximated as

$$G_4(-t, t; \theta, \theta) \simeq \begin{cases} e^{-2\Delta_0 \ell_0} \left(1 - 2\Delta_0 \left(1 - \frac{q^{\Delta_1} e^{-\ell_0}}{\sin^2 \theta} \right) \left(\frac{\pi t}{\tilde{\beta}_y} \right)^2 \right), & t \ll \frac{\tilde{\beta}_y}{2\pi}, \\ \left(\frac{2 \sin^2 \theta e^{-\ell_0}}{\sin^2 \theta + q^{\Delta_1} e^{-\ell_0}} \right)^{2\Delta_0} \left(1 - \Delta_0 \frac{\sin^2 \theta - q^{\Delta_1} e^{-\ell_0}}{\sin^2 \theta + q^{\Delta_1} e^{-\ell_0}} e^{\frac{2\pi t}{\tilde{\beta}_y}} \right), & \frac{\tilde{\beta}_y}{2\pi} \ll t \ll t_{\text{sc}}, \\ \left(\frac{e^{-\ell_0}}{\sin^2 \theta - q^{\Delta_1} e^{-\ell_0}} \right)^{2\Delta_0} e^{-\frac{4\pi \Delta_0 t}{\tilde{\beta}_y}}, & t \gg t_{\text{sc}}, \end{cases} \quad (4.26)$$

where in the second line we approximated

$$\sinh^2 \frac{\pi}{\tilde{\beta}_y} \simeq \frac{1}{4} e^{\frac{2\pi t}{\tilde{\beta}_y}} - \frac{1}{2}, \quad e^{\frac{2\pi t}{\tilde{\beta}_y}} \gg 1, \quad (4.27)$$

up to the scrambling time,

$$t_{\text{sc}} \equiv \frac{\tilde{\beta}_y}{2\pi} \log \frac{2(\sin^2 \theta + q^{\Delta_1} e^{-\ell_0})}{\sin^2 \theta - q^{\Delta_1} e^{-\ell_0}}, \quad (4.28)$$

³¹Note that (4.24) in the $y \rightarrow 0$ limit corresponds to a crossed four-point correlation function in the physical SYK model [56]

$$G_4 = \left\langle \text{Tr} \left[\hat{\mathcal{O}}_{\Delta_1}(t) e^{-\frac{\beta(\theta)}{4}} \hat{\mathcal{O}}_{\Delta_0}(0) e^{-\frac{\beta(\theta)}{4}} \hat{\mathcal{O}}_{\Delta_1}(t) e^{-\frac{\beta(\theta)}{4}} \hat{\mathcal{O}}_{\Delta_0}(0) e^{-\frac{\beta(\theta)}{4}} \right] \right\rangle, \quad (4.25a)$$

$$\hat{\mathcal{O}}_{\Delta_0}(t) \equiv e^{it\hat{H}_{\text{SYK}}} \hat{\mathcal{O}}_{\Delta} e^{-it\hat{H}_{\text{SYK}}}, \quad (4.25b)$$

which is evaluated in the double-scaling limit and with annealed ensemble averaging in [56].

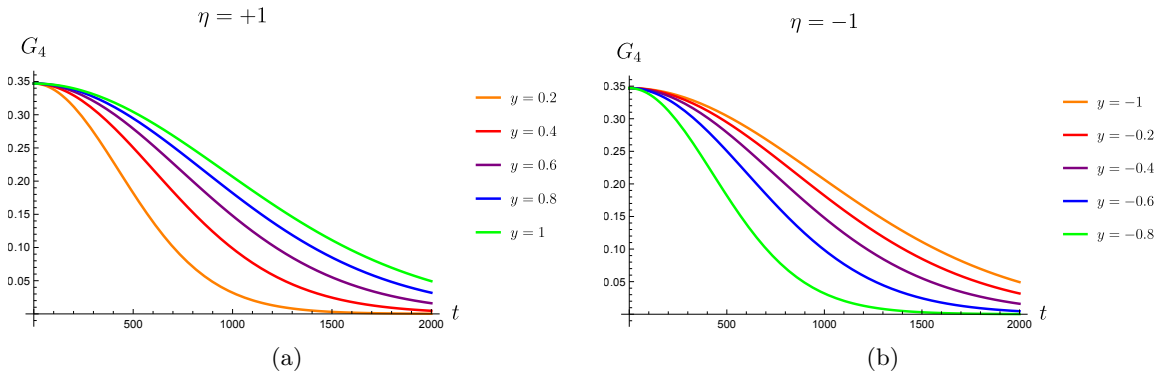


Figure 6. Evolution of the OTOC (4.24) based on the energy spectrum of the deformed theory E_y for (a) $\eta = +1$ (2.21), and (b) $\eta = -1$ (2.23). The parameters applied in the plot are $\theta = \pi/4$, $\lambda = 10^{-6}$, $J = 1$, $\Delta_0 = 1$, $\lambda\Delta_1 = 1$. We observe that the rate of decay is slower as the deformation parameter increases.

which is the time scale of validity for the Taylor expansion used to derive the exponential growth in (4.26).

Note that the chaos bound [144] in the deformed theory is satisfied in terms of the fake temperature $\tilde{\beta}_y$ since the OTOC decays by a rate $2\pi/\tilde{\beta}_y$ fixed by the Tolman temperature in the bulk dual theory (as we have discussed in Sec. 2.3). In contrast, if we compare the rate of growth with respect to the physical temperature of the deformed DSSYK model, given by $1/\beta_y$, then the system is submaximally chaotic given that $\tilde{\beta}_y(\theta) \geq \beta_y(\theta)$, as seen from (4.21, (2.26)), when $\theta \in [0, \pi]$. This result has been observed in the seed theory [73].

To exemplify the results, we display the growth of the OTOCs using the energy spectrum of the deformed theory E_y in (2.23) ($\eta = -1$) and (2.21) ($\eta = +1$) in Fig. 6. Note that we recover the expected behavior as the solution smoothly connected to the $y = 0$ solution when $y \geq 0$ for $\eta = +1$ and $y \leq 0$ for $\eta = -1$. The reason for this is that the redshift factor dE_y/dE (determined from (2.21) ($\eta = +1$) and (2.23) ($\eta = -1$)) can become imaginary when $y \leq 0$ for $\eta = +1$ and $y \geq 0$ for $\eta = -1$, which modifies the evolution (as exponential functions become trigonometric ones). When the redshift factor is complex-valued, the assumptions that $\hat{H}_{L/R, y}$ has a conserved energy spectrum are not valid, so that one has to modify the analysis.

As we elaborate further in App. C, when $y \geq 0$ and $\eta = +1$ (2.17) one describes timelike boundaries in the bulk at finite cutoff, as well as for $y \geq 0$ and $\eta = -1$, when $\hat{H}_{L/R, y}$ can be interpreted as a generator of time translations. Furthermore, we note from the results that the decay rate decreases as the magnitude of the deformation parameter y increases in both cases.

Similarly, for higher point functions in (4.9a) one can perform the evaluation using the time rescaling by the redshift factor in (4.18) and the semiclassical correlation functions for the seed theory in [73]. However, since this is not necessary for the subsequent analysis.

4.3 Triple-Scaling Limit of Crossed Four-Point Functions

For later convenience, we analyze an extension of the UV and IR triple-scaling limits (3.56) in the canonical variables of the one-particle Hamiltonian (3.24)

$$\text{IV} : e^{i\hat{P}_{L/R}} \rightarrow e^{i\lambda\hat{P}_{\text{IR}}^{(L/R)}}, \quad q^{\hat{n}_{L/R}} \rightarrow \lambda e^{-\hat{L}_{\text{IR}}^{(L/R)}}, \quad (4.29a)$$

$$\text{UV} : e^{i\hat{P}_{L/R}} \rightarrow e^{-\hat{P}_{\text{UV}}^{(L/R)}}, \quad q^{\hat{n}_{L/R}} \rightarrow \lambda e^{i\hat{L}_{\text{UV}}^{(L/R)}} \quad (4.29b)$$

where the eigenvalues of the operators $\hat{L}_{\text{IR}}^{(L/R)}$, $\hat{L}_{\text{UV}}^{(L/R)}$, $\hat{P}_{\text{IR}}^{(L/R)}$, $\hat{P}_{\text{UV}}^{(L/R)}$, and the conformal dimension of matter chord Δ_1 , are $\mathcal{O}(1)$ as $\lambda \rightarrow 0$. This means that the one-particle chord Hamiltonian (3.24) can be expressed similarly to (3.28) as

$$\hat{H}_{\text{IR}}^{(L/R)} \equiv \frac{\sqrt{\lambda(1-q)}}{2J} \left(\hat{H}_{L/R} + \frac{2J}{\sqrt{\lambda(1-q)}} \mathbb{1} \right), \quad (4.30a)$$

$$\hat{H}_{\text{UV}}^{(L/R)} \equiv \frac{\sqrt{\lambda(1-q)}}{2J} \left(-\hat{H}_{L/R} + \frac{2J}{\sqrt{\lambda(1-q)}} \mathbb{1} \right), \quad (4.30b)$$

The corresponding correlation functions in the IR/UV triple-scaling limit can be solved based on the same procedure leading to (4.22) for the crossed four-point function, and, for instance, for the IR case one finds

$$G_4(t_L, t_R; \theta_L, \theta_R) \xrightarrow{\text{IR}} \left(\frac{e^{-\ell_0/2}}{\cosh\left(\frac{\pi t_L}{\beta_{\text{IR},y}^L}\right) \cosh\left(\frac{\pi t_R}{\beta_{\text{IR},y}^R}\right) + \frac{2e^{-\ell_0}}{\tilde{\theta}_{\text{IR}}^{(L)} \tilde{\theta}_{\text{IR}}^{(R)}} \sinh\left(\frac{\pi t_L}{\beta_{\text{IR},y}^L}\right) \sinh\left(\frac{\pi t_R}{\beta_{\text{IR},y}^R}\right)} \right)^{2\Delta_0}, \quad (4.31)$$

where $\tilde{\theta}_{\text{IR}}^{(L/R)} \equiv \theta_{L/R}/\lambda$ is a fixed constant in the triple-scaling limit; while the fake temperature (4.21) in the IR limit takes the form

$$\tilde{\beta}_{\text{IR},y}^{L/R} \xrightarrow{\text{IR}} \frac{2\pi}{J\tilde{\theta}_{\text{IR}}^{(L/R)}} \begin{cases} \sqrt{1-y(\tilde{\theta}_{\text{IR}}^{(L/R)})^2}, & \eta = +1, \\ \sqrt{y(\tilde{\theta}_{\text{IR}}^{(L/R)})^2 - 1}, & \eta = -1. \end{cases} \quad (4.32)$$

with the deformation parameter y (2.17) (with $16\pi G_N = 1$ from (4.30)) being related to the radial cutoff in JT gravity by $y = r_B^{-2}$. Meanwhile, the constant ℓ_0 is determined from energy conservation in the corresponding triple-scaled Hamiltonian (4.30). To recover real solutions in the triple-scaling limit, we implement a homogeneous energy condition after the operator insertion (such as that used in shockwave geometries [208]) $\tilde{\theta}_{\text{IR}}^L = \tilde{\theta}_{\text{IR}}^R \equiv \tilde{\theta}_{\text{IR}}$, which leads to

$$e^{-\ell_0} = \frac{1}{2} \left(\tilde{\theta}_{\text{IR}}^2 + \Delta_1^2 - \Delta_1 \sqrt{2\tilde{\theta}_{\text{IR}}^2 + \Delta_1^2} \right). \quad (4.33)$$

The $y \rightarrow 0$ limit of the above results has appeared previously in [85]. Similar outcomes are recovered in the UV limit, which we discuss in Sec. 6.3 in the context of the stretched horizon, i.e. when $y \rightarrow y_0$ (3.57). This leads to an infinite temperature limit (already noticed in [23]) enhancing the rate of growth of the OTOC (4.31).

Summary Our findings show that all the correlation functions at the semiclassical level experience the same evolution as the correlation functions in the seed theory; where the temperature is affected by a redshift factor, in agreement with the existing literature on finite cutoff holography. The results also highlight the analytic control on the DSSYK model. In $\text{CFT}_{d \geq 2}$ real-time correlation functions at finite temperature are known only in terms of perturbative expansions in the deformation parameter [19]. In contrast, in this specific system we evaluate the correlation functions at a non-perturbative order in the deformation parameter y .

Additionally, we discuss how to apply the results in this section to evaluate ETW brane partition functions and correlation functions, including trumpet geometries, in App. E.

5 Holographic Entanglement Entropy from the Double-Scaled Algebra

In this section, we study the entanglement entropy between the double-scaled algebras of the DSSYK [58, 59], defined below, given a chord state and we analyze its finite cutoff holographic interpretation. The analysis is based on recent developments in von Neumann algebras and generalized entropies in quantum gravity [209–213]; see [214–217] for modern reviews. Note that while a $\overline{\text{T}\overline{\text{T}}}$ deformation generates spatial non-locality in higher-dimensional theories, we consider a theory without spatial dimensions, which remains local, at least from the boundary theory perspective. This might be a reason that there is a precise match between the boundary and bulk evaluations; even non-perturbatively in terms of the deformation parameter.

Outline In Sec. 5.1 we discuss the double-scaled algebra of the (deformed) DSSYK model and define entanglement entropy between the algebras given a pure global state. We illustrate the definitions considering the HH state. In Sec. 5.2 we then evaluate entanglement entropy using the chord number state in the basis that reproduces a wormhole length with finite cutoff, particularly its IR triple-scaling limit. In Sec. 5.3 we show that the expressions have a bulk interpretation.

5.1 Double-Scaled Algebras & Entanglement Entropy

As argued in the previous sections, in general the chord operators in the deformed theory belong to the operator algebra of the seed theory since we study chord Hamiltonian deformations encoded in the flow equation (2.18). This means the double-scaled algebras [58, 59] can be expressed in terms of the (un)deformed Hamiltonian

$$\mathcal{A}_{L/R} = \left\{ \hat{H}_{L/R, y}, \hat{\mathcal{O}}_{\Delta}^{(L/R)} \right\}, \quad (5.1)$$

where $\hat{\mathcal{O}}_{\Delta}^{(L/R)}$ are matter chord operators. Moreover, we know that $\mathcal{A}_{L/R}$ is a type II_1 algebra [59], where the $|\Omega\rangle$ is the cyclic separating state in both the deformed and seed theories. This allows us to define traces

$$\text{Tr}(\hat{w}_{L/R}) = \langle \Omega | \hat{w}_{L/R} | \Omega \rangle, \quad \forall \hat{w}_{L/R} \in \mathcal{A}_{L/R}. \quad (5.2)$$

We may then define the density matrix in $\hat{\rho}_{L/R} \in \mathcal{A}_{L/R}$ associated to a state $|\Psi\rangle \in \mathcal{H}_{\text{chord}}$ as [209]

$$\text{Tr}\left(\hat{\rho}_{L/R} \hat{w}_{L/R}\right) = \langle \Psi | \hat{w}_{L/R} | \Psi \rangle, \quad \forall \hat{w}_{L/R} \in \mathcal{A}_{L/R}, \quad (5.3)$$

Next, from the Gelfand–Naimark–Segal construction [218, 219], we can express any state in the chord Hilbert space by applying a string of the operators in the double-scaled algebras to the cyclic separating state,

$$|\psi\rangle = f\left(\hat{H}_{L/R,y}, \hat{\mathcal{O}}_{\Delta}^{(L/R)}\right) |\Omega\rangle \in \mathcal{H}_{\text{chord}}, \quad (5.4)$$

where f is a generic function, then combining (5.3) and (5.4) we identify

$$\hat{\rho}_{L/R} = f\left(\hat{H}_{L/R,y}, \hat{\mathcal{O}}_{\Delta}^{(L/R)}\right) f\left(\hat{H}_{L/R,y}, \hat{\mathcal{O}}_{\Delta}^{(L/R)}\right)^{\dagger}, \quad (5.5)$$

where we applied cyclicity of the trace (5.2).

Given that $|\Omega\rangle$ is the tracial state in the double-scaled algebra, the von Neumann entropy of (5.5) can be defined as

$$S \equiv \log \langle \Omega | \hat{\rho} | \Omega \rangle - \frac{\langle \Omega | \hat{\rho} \log \hat{\rho} | \Omega \rangle}{\langle \Omega | \hat{\rho} | \Omega \rangle}, \quad (5.6)$$

where we have suppressed the L/R index since both density matrices lead to the same result. For this reason, we associate (5.6) as a notion of algebraic entanglement entropy [220].

Note that while we can evaluate entanglement entropy between the double-scaled algebras in the seed and deformed theory in the same way, the main difference is the physical interpretation of the entropies which depend on the form that $\hat{\rho}$ takes, given that it can either involved the (un)deformed chord Hamiltonian.

Thermodynamic Entropy For instance, there is a thermodynamic entropy that can be computed from the partition function of the deformed theory

$$S = (1 - \beta \partial_{\beta}) \log Z_y(\beta) \quad Z_y(\beta) = \langle \Omega | e^{-\beta \hat{H}_y} | \Omega \rangle \quad (5.7)$$

where $e^{-\frac{\beta}{2} \hat{H}_y} |\Omega\rangle$ is the HH state in the zero-particle chord space.

The above result can also be interpreted as entanglement entropy between the double-scaled algebra using the definition of the density matrix:

$$Z_y(\beta) = \text{Tr}(\hat{\rho}_{\text{HH}}), \quad \hat{\rho}_{\text{HH}} = e^{-\beta \hat{H}_y}. \quad (5.8)$$

Note that the density matrix is not normalized. The von Neumann entropy in the corresponding state (5.6) is thus the thermal entropy in the deformed theory (5.7). Holographically, since the effect of a T^2 deformation represents a finite cutoff in the bulk [23], the above expressions would have a natural geometric interpretation in terms of a finite cutoff AdS₂ black hole effective geometry, similar to the partition functions computed in finite cutoff holography for JT gravity [34, 42].³²

³²Additionally, there are simple extensions to evaluate the algebraic entanglement entropy (5.6) using particle insertions in the HH state, which follow similarly to our discussion, and which were connected to the partially-entangled thermal state [191, 221] in the DSSYK model in [99].

5.2 Boundary Perspective: Entropy From the Chord Number State

In this subsection, we will investigate the holographic nature of the algebraic entropy (5.6) by considering the chord number state in the Krylov basis and its corresponding density matrix (5.5) in the double-scaled algebra (5.1).

We begin with the state

$$|\Psi\rangle = |K_n^{(y)}\rangle = \tilde{f}_n(\hat{H}_y) |\Omega\rangle, \quad \hat{\rho} = \tilde{f}_n(\hat{H}_y)^2, \quad (5.9)$$

The algebraic entanglement entropy (5.6) for the $|\Psi\rangle$ state is then

$$S \equiv - \int_0^\pi d\theta \mu(\theta) \tilde{f}_n(E_y(\theta))^2 \log \tilde{f}_n(E_y(\theta))^2, \quad (5.10)$$

with $\mu(\theta)$ in (3.18), and $E_y(\theta) \equiv f_y(E(\theta))$ (3.29). Next, we compute the integral (5.10) using the Wentzel-Kramers-Brillouin (WKB) approximation [222–224] approximation. We introduce a change of variables adapted for the (IR) triple-scaling limit (3.27), $\theta \equiv \lambda k$, so that

$$S \xrightarrow{IR} -2\lambda \int_0^\infty dk p(k, \ell_y) \log \frac{p(k, \ell_y)}{\mu(\lambda k)}, \quad (5.11)$$

where we defined

$$p(k, \ell_y \equiv \lambda n) \equiv \tilde{N} \mu(\lambda k) \tilde{f}_n(\lambda k)^2 \Big|_{IR}, \quad (5.12)$$

where \tilde{N} is a normalization such that $p(k, \ell_y)$ represents a probability distribution in terms of the parameter k ,

$$\int_0^\infty dk p(k, \ell_y) = 1. \quad (5.13)$$

(5.11) then transforms in

$$S \xrightarrow{IR} 2\lambda \int_0^\infty dk p(k, \ell_y) \log \mu(\lambda k) + \mathcal{O}(\lambda). \quad (5.14)$$

where we use the fact that $p(k, \ell_y) \sim \mathcal{O}(1)$ as $\lambda \rightarrow 0$ while [191]

$$\lambda \log \mu(\lambda k) = -\frac{\pi^2}{2} + \mathcal{O}(\lambda \log \lambda). \quad (5.15)$$

To find the explicit functional form of $p(k, \ell_y)$, we use the WKB approximation [222–224], so that the probability distribution takes the form

$$p(k, \ell_y) \simeq \begin{cases} A \exp(-2 \int d\ell \tilde{p}_y), & k \lesssim k_{\text{crit}}, \\ B \sin^2(\int d\ell p_y), & k > k_{\text{crit}} \end{cases} \quad (5.16)$$

where we denote the critical value of k where the particle description of the system in the WKB approximation has vanishing momenta (i.e. $p_y = 0$ in (3.52)) as,³³

$$k_{\text{crit}} = \begin{cases} \frac{1}{\sqrt{y}} \operatorname{sech} \frac{\ell_y}{2}, & \eta = +1, \\ \frac{1}{\sqrt{y}} \sec \frac{i\ell_y}{2}, & \eta = -1, \end{cases} \quad (5.18)$$

and A, B are normalization constants, such that (5.13) is satisfied; i.e.

$$A = \frac{1}{2\pi} \begin{cases} \sqrt{\frac{yk^2}{\operatorname{sech}^2 \frac{\ell_y}{2} - yk^2}}, & \eta = +1 \\ \sqrt{\frac{yk^2}{\sec^2 \frac{i\ell_y}{2} - yk^2}}, & \eta = -1 \end{cases}, \quad B = \frac{2}{\pi} \begin{cases} \sqrt{\frac{yk^2}{yk^2 - \operatorname{sech}^2 \frac{\ell_y}{2}}}, & \eta = +1 \\ \sqrt{\frac{yk^2}{yk^2 - \sec^2 \frac{i\ell_y}{2}}}, & \eta = -1 \end{cases}. \quad (5.19)$$

Meanwhile, p_y and \tilde{p}_y in (5.16) are the momenta in the allowed and disallowed regions of the corresponding Schrödinger equations for the DSSYK chord Hamiltonian in the Krylov chord number basis (3.52) in the IR limit, namely,

$$\sin^2 p_y = -\sinh^2 \tilde{p}_y = \begin{cases} \frac{yk^2 - \operatorname{sech}^2(\ell_y/2)}{\tanh^2(\ell_y/2)}, & \eta = +1, \\ \frac{\sec^2(i\ell_y/2) - yk^2}{\tan^2(i\ell_y/2)}, & \eta = -1, \end{cases} \quad (5.20a)$$

where we used that $\sqrt{1 - yk^2} = \tanh(\ell_y/2) \cos p_y$ for $\eta = +1$. We work in the regimes where

$$\eta = +1: \quad \operatorname{sech} \frac{\ell_y}{2} \gg yk \text{ for } k \lesssim k_{\text{crit}}; \quad \operatorname{sech} \frac{\ell_y}{2} \ll yk \text{ for } k \gtrsim k_{\text{crit}}, \quad (5.21a)$$

$$\eta = -1: \quad \sec \frac{i\ell_y}{2} \gg yk \text{ for } k \lesssim k_{\text{crit}}; \quad \sec \frac{i\ell_y}{2} \ll yk \text{ for } k \gtrsim k_{\text{crit}}. \quad (5.21b)$$

Then, we recover from (5.20) that

$$\sin^2 p_y \simeq \begin{cases} yk^2, & \eta = +1, \\ \csc^2 \frac{i\ell_y}{2}, & \eta = -1, \end{cases} \quad \sinh^2 \tilde{p}_y \simeq \begin{cases} \operatorname{csch}^2 \frac{\ell_y}{2}, & \eta = +1, \\ yk^2, & \eta = -1. \end{cases} \quad (5.22)$$

Thus, (5.16) with normalization constants in (5.19) and the limit (5.21) becomes

$$p(k, \ell_y) \simeq \begin{cases} 0, & k \lesssim k_{\text{crit}}, \\ \frac{2}{\pi} \sin^2(\ell_y \arcsin(yk)) \simeq \frac{1}{\pi}, & k > k_{\text{crit}}. \end{cases} \quad (5.23)$$

The algebraic entanglement entropy (5.14) with the explicit probability distribution (5.23) results in,³⁴

$$S + S_{\text{ren}} \xrightarrow{IR} \pi \int_0^{k_{\text{crit}}} dk = \frac{1}{\pi\sqrt{y}} \begin{cases} \operatorname{sech}\left(\frac{\ell_y}{2}\right), & \eta = +1 \\ \sec\left(i\frac{\ell_y}{2}\right), & \eta = -1, \end{cases} \quad (5.24)$$

³³We are using $k = \theta_{\text{IR}}/\lambda$ and the spectrum in (2.21), (2.23):

$$E_{\text{IR},y} = \begin{cases} \frac{1}{y} \left(1 - \sqrt{1 - yk^2}\right), & \eta = +1, \\ \frac{1}{y} \left(1 - \sqrt{yk^2 - 1}\right), & \eta = -1. \end{cases} \quad (5.17)$$

³⁴The result (5.24) in the $y \rightarrow 0$ limit reproduces the renormalized entropy in (dS) JT gravity [98, 99].

where $S_{\text{ren}} \equiv \pi \int_0^\infty dk$, corresponding to a regularization of the entanglement entropy in momentum space due to the IR energy limit taken in this approximation.

Next, we analyze the bulk dual of the above result.

5.3 Bulk Perspective: Ryu-Takayanagi Formula

In the following, we search for the minimal area surface γ in the (A)dS₂ space, using the finite cutoff boundary as the entangling surface to evaluate holographic entanglement entropy. The extremal surfaces in two-dimensional quantum gravity are point-like. We investigate the different configurations depending on the location of boundary cutoff surfaces in the corresponding spacetime.

Timelike Boundaries in an AdS Black Hole First, considering timelike finite cutoff boundaries, as illustrated in Fig. 3 (c) as the entangling surface to evaluate the RT formula in JT gravity, which corresponds to (2.1) with $U(\Phi) = 2\Phi$,

$$S_{\text{AdS}} \equiv \frac{\Phi_{\text{AdS}}(\gamma)}{4G_N} , \quad (5.25)$$

with G_N in (2.1), Φ_{AdS} is the dilaton in JT gravity, and γ the extremal surface. To locate the latter, we use global and Rindler-AdS₂ coordinates,

$$ds^2 = -(1 + X^2)dT^2 + \frac{dX^2}{1 + X^2} = -(r^2 - r_{\text{BH}}^2)dt_{L/R}^2 + \frac{dr^2}{r^2 - r_{\text{BH}}^2} , \quad (5.26)$$

where $t_{L/R}$ corresponds to the time asymptotic boundary time in the left/right patches of Rindler-AdS₂; the dilaton in JT gravity is given by

$$\Phi_{\text{AdS}} = r_{\text{BH}} \sqrt{1 + X^2} \cos T . \quad (5.27)$$

Due to symmetry, γ is located at $X = 0$ in global AdS₂ coordinates for a given Cauchy slice, as seen by minimizing the dilaton (5.27) ($\partial_X \Phi_{\text{AdS}} = 0$ with T fixed).

Let us then relate the time t and T at the location of the entangling region, $r = r_B$, using the following coordinate transformation between global and Rindler-AdS coordinates,

$$\tan T = \frac{r_{\text{BH}}}{r} \sqrt{\frac{r^2}{r_{\text{BH}}^2} - 1} \sinh\left(\frac{r_{\text{BH}} t}{2}\right) , \quad r < r_{\text{BH}} , \quad (5.28)$$

where we are fixing the gauge $t_L = t_R \equiv t/2$ in (5.26).

Next, from the explicit form of the wormhole length in terms of Rindler-AdS₂ time t and the metric in (5.26) (see App. B),

$$L \equiv \int d\xi \sqrt{g_{\mu\nu} \frac{dx^\mu}{d\xi} \frac{dx^\nu}{d\xi}} = 2 \operatorname{arcsinh}\left(\sqrt{\frac{r_B}{r_{\text{BH}}}} - 1 \cosh \frac{r_{\text{BH}} t}{2}\right) , \quad (5.29)$$

we have that the RT formula (5.25) from the dilaton at $X = 0$ is

$$S_{\text{AdS}} = \frac{r_B}{4G_N} \operatorname{sech} \frac{L}{2} . \quad (5.30)$$

Thus, we find exactly the same result as the boundary theory (5.24) following the holographic dictionary between DSSYK and sine dilaton gravity [112], including the relationship between the rescaled chord number ℓ_y with the geodesic length L (5.29) and the deformation parameter y and r_B in (2.17) for the counterterm $G(\Phi_B) = \Phi_B^2$ (2.3) in JT gravity

$$\ell_y = L, \quad \lambda = 8\pi G_N, \quad \frac{1}{\sqrt{y}} = r_B, \quad (5.31)$$

which is consistent with (2.36).

In particular, the limit $r_B \rightarrow r_{\text{BH}}$ leads to the Bekenstein-Hawking (BH) entropy of a Bañados-Teitelboim-Zanelli (BTZ) black hole,

$$S_{\text{BH}} = \frac{2\pi r_{\text{BH}}}{4G_3}, \quad (5.32)$$

where the two and three-dimension Newton's constants are related by $G_3 = 4\pi G_N$ [192], and we can recognize the factor $2\pi r_{\text{BH}}$ as the codimension-two area of the BTZ black hole, corresponding to the perimeter of a circle with radius r_{BH} . This can be interpreted from the boundary theory answer (5.30) when $y \rightarrow y_0$.

Spacelike Boundaries in an AdS Black Hole Next, we return to the JT gravity case with spacelike cutoff boundaries inside the black hole interior, illustrated in Fig. 3 (d), interpreted as the bulk dual to a $T^2 + \Lambda_1$ deformed DSSYK model in the IR limit.

An attempt might be made to evaluate the holographic entanglement entropy of (5.25) in a similar way to the previous case. However, if we extremize the dilaton (5.27) with T fixed and varying X to obey the homology constraint ($\partial_T \Phi = 0$) one would find $T = 0$ as the location for the RT surface. This corresponds to a maximum dilaton value instead of a minimum one. In fact, the minimum value is reached when $T = \pm\pi/2$, where $\Phi = 0$ for any X . However, the dilaton in the minimal area surface cannot describe holographic entanglement entropy, it would not even be smoothly connected to the extremal area when the timelike boundaries approach the black hole horizon (5.30). This means that the RT formula does not apply when the boundaries are located in the black hole interior. Thus, while we expect that the algebraic entanglement entropy for a chord number in the $T^2 + \Lambda_1$ deformed DSSYK (5.24) has a bulk interpretation, it does not correspond to the minimal area in the RT formula measured by the dilaton at the corresponding extremal surface.

6 Stretched Horizon Holography From the Deformed DSSYK Model

We collect the lessons from the previous sections to explicitly realize the stretched horizon conjecture by Susskind [1]. We perform the T^2 and $T^2 + \Lambda_1$ deformation procedure in the DSSYK chord Hamiltonian in the UV triple-scaling limit (3.28), which is isomorphic to the dS JT gravity generator of spatial translations along \mathcal{I}^\pm . After the $T^2 + \Lambda_1$ deformation, the finite cutoff boundary moves inside the static patch of dS_2 space, which takes the role of the cosmological stretched horizon [1]. We evaluate the rate of growth of the Krylov spread

complexity for the HH state defined in Sec. 3.2; OTOCs (based on Sec. 4.2), as well as the algebraic entanglement entropy for the chord number state in Sec. 5.2. We show that the Krylov complexity and OTOCs display hyperfast growth and hyperfast scrambling respectively, as the boundary approaches the cosmological horizon. Meanwhile, the entanglement entropy matches the dilaton in dS JT gravity at finite cutoff if the boundaries are spacelike, and it reproduces the expected formula in the Gibbon-Hawking entropy in dS₃ space in the stretched horizon limit.

Outline In Sec. 6.1 we compare general aspects and the thermodynamic properties between the UV limit of the deformed DSSYK model after T^2 and $T^2 + \Lambda_1$ deformations with dS₂ JT gravity with a stretched horizon in the static patch. In Sec. 6.2 we discuss Krylov complexity of the deformed HH state and its bulk interpretation as a geodesic length; particularly its hyperfast growth. In Sec. 6.3 we evaluate the OTOCs in the UV triple-scaling limit and its Lyapunov exponent. At last, in Sec. 6.4 we evaluate algebraic entanglement entropy for a chord number state in the Krylov basis; we match it to the dilaton in dS₂ JT gravity, confirming the RT formula.

A summary of results in this section in connection with the stretched horizon holographic proposal [1] is shown in Tab. 1.

6.1 UV Limit of the DSSYK Model vs dS Space at Finite Cutoff

To realize the stretched horizon proposal in the UV limit (3.28), as explained in Sec. 3.2, we apply the T^2 deformation into the UV chord Hamiltonian (3.28). Once the deformation parameter reaches the critical value $y = y_0$ (3.57), we apply the $T^2 + \Lambda_1$ deformation. We thus specialize in (3.54a) in the UV triple scaling limit (3.28a),

$$\hat{H}_{\text{UV},y} \equiv \begin{cases} \frac{1}{y} \left(1 - \frac{1}{2} \left(\tanh \left(\frac{\lambda \hat{n}_y}{2} \right) e^{-i\hat{p}_y} + e^{i\hat{p}_y} \tanh \left(\frac{\lambda \hat{n}_y}{2} \right) \right) \right) & 0 \leq y \leq y_0, \\ \frac{1}{y} \left(1 + \frac{1}{2} \left(\tanh \left(\frac{\lambda \hat{n}_y}{2} \right) e^{-i\hat{p}_y} + e^{i\hat{p}_y} \tanh \left(\frac{\lambda \hat{n}_y}{2} \right) \right) \right) & y \geq y_0, \end{cases} \quad (6.1)$$

where $y_0 \equiv \theta_{\text{UV}}^{-2}$ in the regime of interest. We may now interpolate between dS₂/CFT₁ holography at finite cutoff and static patch holography. In particular, when $y = y_0 + \delta$ for $0 < \delta \ll 1$ we recover the stretched horizon conjecture.³⁵

As emphasized in [99], the UV limit of the DSSYK model is an explicit example of a unitary theory which contrasts the dS/CFT correspondence [225–229] in higher dimensions, where a non-unitary CFT dual is expected to live at future/past infinity \mathcal{I}^\pm .³⁶ Work in this

³⁵This resonates with similar ideas presented in [150], which views $T\bar{T} + \Lambda_2$ deformations in dS₃/CFT₂ as a way to unify it with static patch holography.

³⁶There have been explicit realizations of the dS/CFT correspondence in different approaches, including higher spin gravity [230, 231] where dS₄ space [232–234] is dual to Sp(N) CFT₃s; as well as a dS₃ space higher spin proposal being dual to a SU(2) Wess-Zumino-Witten model [235–238] from an analytic continuation of Euclidean AdS₃ space; and from transitions between Euclidean AdS₄ space to dS₄ space [239–241]. A different approach involves geometries interpolating from asymptotically AdS₂ and dS₂ spacetimes, often referred to as centaur geometries [157, 172, 242–246], whose holographic dual has been recently investigated in [247, 248]. See [249] for a review and references therein.

area indicates that the renormalization group (RG) flow in the dual CFT at \mathcal{I}^\pm allows for an emergent notion of time evolution from the bulk [250] (recently debated by [183]). Similarly, the T^2 flow in (6.1) indicates one can associate an emergent global time generated by the T^2 deformation.

Next, we apply our results in Sec. 2 to compare the thermodynamics in the deformed boundary theory (6.1) to those in the bulk at a finite cutoff, discussed below.

First, consider the geometry of the dS_2 static patch (resulting from the s-wave reduction of dS_3 space), which is given by:

$$ds^2 = -f(r)dt_{L/R}^2 + \frac{dr^2}{f(r)}, \quad f(r) = r_{\text{CH}}^2 - r^2, \quad \Phi = r \in [0, r_{\text{CH}}], \quad (6.2)$$

where r_{CH} is a parametrization of the cosmological horizon radius.³⁷ We illustrate the geometry of dS_2 and the cosmological stretched horizon in Fig. 1 (d). Note that in writing (6.2) we may assume a gauge fixing where $t_L = t_R \equiv t/2$. Adopting a gauge-fixing choice for the coordinate system is not necessary for the evaluation of diffeomorphism invariant observables, all other gauge choices are equivalent.

Let us now evaluate the Euclidean on-shell action of the half-reduction dS_2 JT gravity model with a finite time-like Dirichlet surface, $r = r_B$, using (6.2, 2.32) with $U(\Phi) = -2\Phi$, and a counterterm $G(\Phi_B) = \Phi_B^2$ for the dual T^2 deformation, or $G(\Phi_B) = -\Phi_B^2$ for $T^2 + \Lambda_1$,³⁸ which, like (2.32), results in

$$I_E = S_{\text{dS}} - \beta_T E_{\text{BY}}(r_B), \quad (6.3)$$

where $S_{\text{dS}} = r_{\text{CH}}/(4G_N)$ is the Gibbons-Hawking (GH) entropy [252, 253] (which does not include a topological contribution, unlike the term Φ_0 in (2.25)). Meanwhile the BY [188] quasi-local energy with respect to the Dirichlet wall is given by

$$E_{\text{BY}} = \begin{cases} \frac{1}{8\pi G_N} \left(r_B + \sqrt{r_{\text{CH}}^2 - r_B^2} \right), & \text{when } r_{\text{CH}} > r_B, \\ \frac{1}{8\pi G_N} \left(r_B + \sqrt{r_B^2 - r_{\text{CH}}^2} \right), & \text{when } r_{\text{CH}} < r_B, \end{cases} \quad (6.4)$$

which is directly related to the energy spectrum of the triple-scaled SYK (3.28b) as expected from the holographic dictionary at a finite cutoff (2.34).

The corresponding inverse Tolman temperature is then given by

$$\beta_T = \beta \begin{cases} \sqrt{r_B^2 - r_{\text{CH}}^2}, & \text{when } r_{\text{CH}} > r_B, \\ \sqrt{r_{\text{CH}}^2 - r_B^2}, & \text{when } r_{\text{CH}} < r_B, \end{cases} \quad \beta = \frac{2\pi}{r_{\text{CH}}}. \quad (6.5)$$

³⁷This parameter is associated with the mass of SdS_3 space [251], where a value $r_{\text{CH}} \neq 1$ implies the existence of a conical deficit.

³⁸Note that this is the same boundary term choice as [38], which can be motivated for defining a notion of ADM mass for SdS_3 space with respect to \mathcal{I}^+ , as elaborated in [251], and it has also been applied in $T\bar{T} + \Lambda_2$ deformations in [153, 155].

Performing a similar analysis of the heat capacity with a Dirichlet wall with a fixed radial location $r = r_B$, as in (2.29), results in

$$C_{r_B} = -\frac{r_B}{8\pi G_N} \frac{4\pi^2 \beta_T^2}{(4\pi^2 - \beta_T^2)^{3/2}} . \quad (6.6)$$

Notice that the heat capacity for fixed location r_B is always negative, which corresponds to the $\eta = -1$ case in (2.29).

Thermodynamic properties of dS_2 space are indeed in agreement with the analysis of the UV behavior of the deformed boundary theory in Sec. 3.2. Particularly, given $G(\Phi_B) = \pm\Phi_B^2$ then the dictionary entry for the deformation parameter (2.17)

$$y = \pm 1/r_B^2 , \quad (6.7)$$

allow us to explicitly check of the dictionary (2.34) relating BY quasi-local energy (6.4) and Tolman temperature (6.5) to the energy spectrum of the T^2 deformed (2.21) and $T^2 + \Lambda_1$ deformed (2.23) theories and microcanonical temperature (2.26) respectively, as well as the corresponding heat capacity at fixed y (2.30) with that at fixed r_B (6.6). Thus, there is an exact match at the level of thermodynamic properties. We will extend this to dynamical observables and holographic entanglement entropy in the rest of the section.

6.2 Hyperfast Krylov Spread Complexity Growth

Let us now discuss the expectation value of the Krylov spread complexity (3.53) in the HH state in the UV limit (3.56) in the microcanonical ensemble, which we repeat for the convenience of the reader,

$$\begin{aligned} \mathcal{C}_S(t) &\equiv \sum_{n=0}^{\infty} n \frac{\left| \langle \Omega | e^{-\tau^* \hat{H}_y} | K_n^{(y)} \rangle \right|^2}{Z_y(\beta)} \Bigg|_{\tau = \frac{\beta(\theta)}{2} + it} \\ &\xrightarrow{UV} \begin{cases} \frac{2}{\lambda} \operatorname{arcsinh} \left(\sqrt{\frac{1}{y\theta_{UV}^2} - 1} \cosh \left(\frac{\theta_{UV} t}{2} \right) \right) , & 0 \leq y \leq y_0 , \\ \frac{2}{\lambda} \operatorname{arcsin} \left(\sqrt{1 - \frac{1}{y\theta_{UV}^2}} \cosh \left(\frac{\theta_{UV} t}{2} \right) \right) , & y \geq y_0 . \end{cases} \end{aligned} \quad (6.8)$$

We display the growth of this observable in Fig. 7. Similar to the IR case there is eternal growth in the $\eta = +1$ case, and a limit in the evolution for the $\eta = -1$. The first observation is in agreement with [82] (for the seed theory case), who finds that the expectation value of the chord number in the regime we have considered as the Krylov spread complexity of the corresponding state. The authors interpret this as a dual observable to a geodesic length in dS_2 space, which is thus a concrete manifestation of the CV conjecture [97]. It eternally evolves in terms of the spacelike coordinate t in (6.2). Our results can be seen as a finite cutoff realization. Meanwhile, by performing the $T^2 + \Lambda_1$ deformation, the rescaled chord number has a finite range of time evolution. In the bulk interpretation, this means that the corresponding geodesic curves become spacelike instead of timelike. This indicates that the cutoff surface

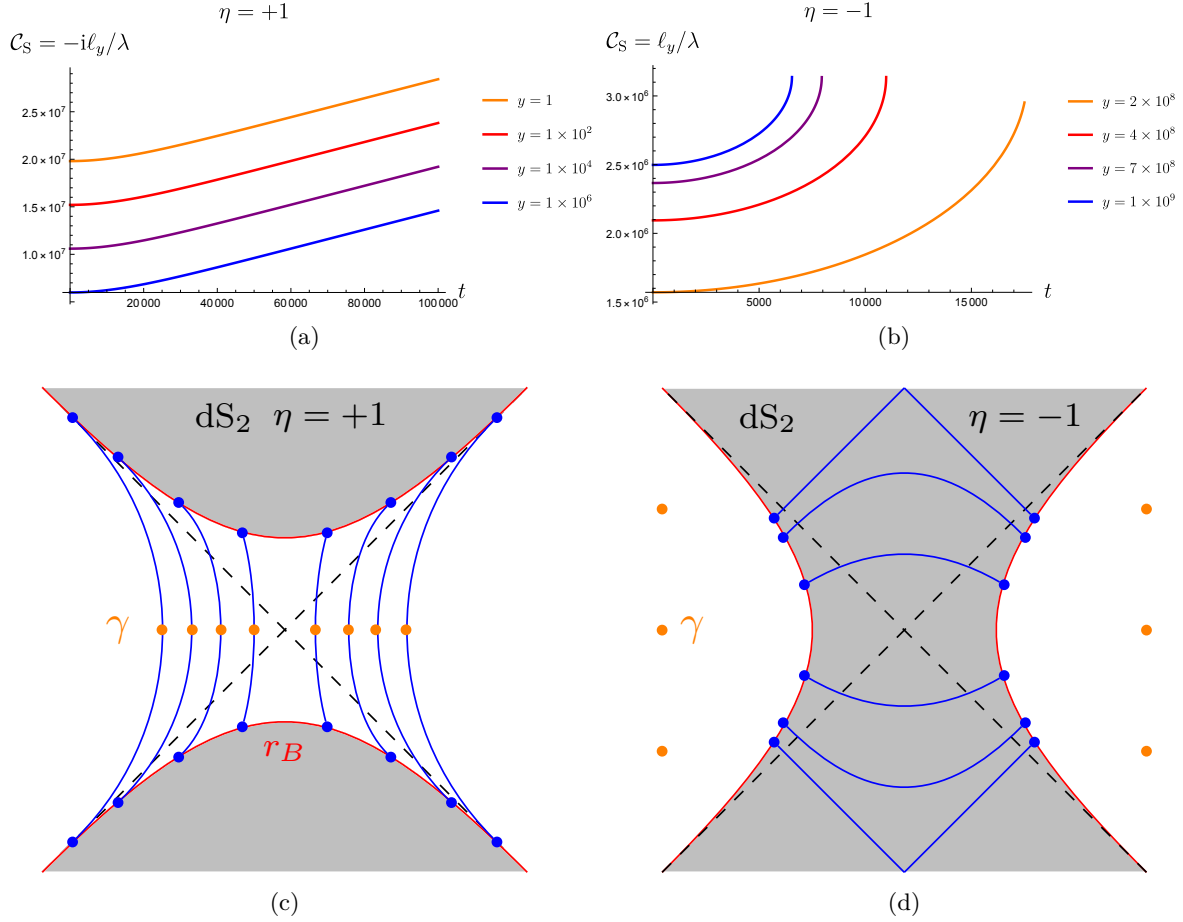


Figure 7. *Top:* UV triple-scaling limit of Krylov spread complexity (3.53) in the HH state from (a) T^2 , and (b) $T^2 + \Lambda_1$ deformations of the DSSYK model using $\theta_{UV} = 10^{-4}$. *Bottom:* Corresponding bulk interpretation of the T^2 and $T^2 + \Lambda_1$ deformations in terms of (c) timelike and (d) spacelike extremal length geodesics at a finite cutoff in dS_2 space. We marked minimal codimension-two area (measured by the dilaton) points γ homologous to the finite boundaries as orange dots, and the entangling surfaces as blue dots in the corresponding boundaries.

has crossed the cosmological horizon in the bulk dual, as depicted in Fig. 7, which is consistent with the $T\bar{T} + \Lambda_2$ interpretation [148, 150] in one lower spacelike dimension, as well as our findings in the AdS_2 case (Fig. 3). However, note that there is no enhanced growth as the cutoff surface approaches the cosmological horizon since we work in the canonical ensemble which does not include the corresponding redshift factor. Additionally, one finds from (6.8) that the maximal range of evolution is:

$$t \in [-t_{\text{crit}}, t_{\text{crit}}], \quad t_{\text{crit}} \equiv \frac{1}{\theta_{UV}} \text{arccosh} \left(\sqrt{1 - \frac{1}{y\theta_{UV}^2}} \right). \quad (6.9)$$

The result agrees with the hyperfast complexity growth conjecture (iii) and (iv) in Sec. 1; the Krylov spread complexity reaches its maximum at a critical time t_{crit} which is order one in units of the dS length scale.

In the bulk interpretation, (6.9) is consistent with previous results in the CV conjecture in $\text{dS}_{d+1 \geq 3}$ with a cosmological stretched horizon [145]. While the previous proposal does not discuss an explicit boundary dual, it was noticed that the extremal volume surfaces do not evolve eternally since there is a maximum value for the timelike coordinate, similar to $t = t_{\text{crit}}$ above. At this point, the extremal surfaces reach \mathcal{I}^\pm , as seen in Fig. 1 which diverges in higher dimensions. Thus, our results provide an explicit confirmation of the CV proposal in dS_2 space, and it displays the hyperfast growth expected by [1].

6.3 Hyperfast Scrambling From OTOCs

The crossed four-point function of the deformed DSSYK model in the semiclassical limit was calculated in (4.24) and its scrambling time in (4.28). Now, we are interested in its UV triple-scaling limit (3.28), where $\tilde{\theta}_{\text{UV}} \equiv (\pi - \theta)/\lambda$ is fixed as $\lambda \rightarrow 0$. Since the analysis follows similarly to the IR limit of the crossed four-point function (4.22) with two operators of conformal dimension Δ_0 and two with dimension Δ_1 , we specialize in the OTOC case, where $t_L = -t_R \equiv t$, as explained in (4.24). Using the corresponding canonical variables, the UV triple-scaling limit of (4.22) becomes

$$G_4(t, -t; \theta, \pi - \theta) \xrightarrow{UV} \left(\frac{e^{-\ell_0/2}}{1 + \left(1 - \frac{2e^{-\ell_0}}{\tilde{\theta}_{\text{UV}}^2}\right) \sinh^2\left(\frac{\lambda_L t}{2}\right)} \right)^{2\Delta_0}, \quad (6.10)$$

where $\lambda_L \equiv 2\pi/\tilde{\beta}_y$ is the corresponding Lyapunov exponent in the scrambling phase of the OTOC (4.24), and similar to (4.33), the constant ℓ_0 above is

$$e^{-\ell_0} \equiv e^{-\ell_*(q^{\Delta_1}, \theta, \pi - \theta)} \xrightarrow{UV} \frac{1}{2} \left(\tilde{\theta}_{\text{UV}}^2 + \Delta_1^2 - \Delta_1 \sqrt{2\tilde{\theta}_{\text{UV}}^2 + \Delta_1^2} \right), \quad (6.11)$$

with ℓ_* defined in (4.23). The scrambling time is obtained by Taylor expanding (6.10) in powers of $e^{\lambda_L t}$ by

$$G_4 \simeq \left(\frac{2\tilde{\theta}_{\text{UV}}^2 e^{-\ell_0}}{\tilde{\theta}_{\text{UV}}^2 + 2e^{-\ell_0}} \right)^{2\Delta_0} \left(1 - \Delta_0 \frac{\tilde{\theta}_{\text{UV}}^2 - 2e^{-\ell_0}}{\tilde{\theta}_{\text{UV}}^2 + 2e^{-\ell_0}} e^{\lambda_L t} \right), \quad t \ll t_{\text{sc}}, \quad (6.12)$$

where

$$\lambda_L \equiv \frac{2\pi}{\tilde{\beta}_y} \xrightarrow{UV} \begin{cases} \frac{\tilde{\theta}_{\text{UV}}}{\sqrt{1 - y\tilde{\theta}_{\text{UV}}^2}}, & 0 \leq y_0 \leq y_0, \\ \frac{\tilde{\theta}_{\text{UV}}}{\sqrt{y\tilde{\theta}_{\text{UV}}^2 - 1}}, & y \geq y_0, \end{cases} \quad (6.13a)$$

$$t_{\text{sc}} \xrightarrow{UV} \frac{1}{\lambda_L} \log \frac{2(\tilde{\theta}_{\text{UV}}^2 + 2e^{-\ell_0})}{\tilde{\theta}_{\text{UV}}^2 - 2e^{-\ell_0}}. \quad (6.13b)$$

Note that the latter expression is consistent with (3.83) in [70]. Manifestly, the result (6.13b) agrees with the hyperfast scrambling conjecture (ii) and (iv) in Sec. 1. The scrambling time of the OTOC is order one, corresponding to the dS scale, instead of order $t_{\text{sc}} \sim \log S \propto \log N$ [99, 191] the expected scrambling time for fast scrambler, which diverges in the double-scaling limit. Next, we see that the presence of the redshift factor in λ_L , the limit $y \rightarrow y_0$ reproduces the infinite temperature limit, confirming the hyperfast conjecture in [1].

6.4 Holographic Entanglement Entropy and dS Space

In this section, we discuss the algebraic entanglement entropy (5.6) of the DSSYK model in the UV limit and its holographic interpretation. Similar to the previous discussion, we focus on the chord number state $|K_n^{(y)}\rangle$.

Chord Number State From the boundary side, the algebraic entanglement entropy given the state $|K_n^{(y)}\rangle$ in the UV triple-scaling limit (3.28) can be evaluated using very analogous steps as in Sec. 5.2 with the corresponding limit of the Hamiltonian (3.28a) using the symmetry in the integration measure $\mu(\theta)$ (3.18) around $\theta = \pi/2$. Specifically, (5.24) extends to the UV case as

$$S \xrightarrow{UV} \frac{2\pi}{\lambda\sqrt{y}} \sec \frac{\ell_y}{2} . \quad (6.14)$$

Now, we discuss its bulk interpretation, including its limit as the GH entropy in the stretched horizon limit.

RT Surfaces From Spacelike Boundaries We are interested in evaluating the RT formula in dS JT gravity, i.e. (2.1) with $U(\Phi) = -2\Phi$ as

$$S_{\text{dS}} \equiv \frac{\Phi_{\text{dS}}(\gamma)}{4G_N} , \quad (6.15)$$

where the finite cutoff boundaries are spacelike, as displayed in Fig. 7 (c).

First, consider global coordinates, where the metric and the dilaton take the form

$$ds^2 = -dT^2 + \cosh^2 T d\varphi^2 , \quad \Phi_{\text{dS}} = r_{\text{CH}} \sin \varphi \cosh T . \quad (6.16)$$

To map to static patch coordinates in (6.2) (with gauge fixing $t_L = t_R \equiv t/2$) describing the Milne patch (i.e. outside the cosmological horizon in Fig. 1 (d)) we need to use $r_{\text{CH}} t \rightarrow r_{\text{CH}} t + i\frac{\pi}{2}$ [254], so that

$$\sqrt{\frac{r^2}{r_{\text{CH}}^2} - 1} \cosh \frac{r_{\text{CH}} t}{2} = \sinh T , \quad \text{when } r > r_{\text{CH}} , \quad (6.17a)$$

$$\sqrt{\frac{r^2}{r_{\text{CH}}^2} - 1} \sinh \frac{r_{\text{CH}} t}{2} = \cos \varphi \cosh T . \quad (6.17b)$$

From symmetry of dS_2 space the finite cutoff boundaries are located at $T = 0$ in global coordinates, as displayed in Fig. 7 (c). Following the same derivation as in App. B for the

dS₂ space with $r = r_B > r_{\text{CH}}$ for geodesics anchored at spacelike boundaries in the Milne patch (Fig. 1), we find

$$L_{\text{dS}} \equiv \int d\xi \sqrt{g_{\mu\nu} \frac{dx^\mu}{d\xi} \frac{dx^\nu}{d\xi}} = -2i \operatorname{arcsinh} \sqrt{\left(\frac{r_B}{r_{\text{CH}}} - 1\right) \cosh \frac{r_{\text{CH}} t}{2}}. \quad (6.18)$$

Then, using the relation between the coordinates in (6.17) with $r = r_B > r_{\text{CH}}$ for the entangling surface we get

$$\Phi_{\text{dS}} \Big|_{T=0} = r_B \sec \frac{L_{\text{dS}}}{2}. \quad (6.19)$$

Then, the evaluation of the RT formula in dS₂ space (6.15) gives

$$S_{\text{dS}} = \frac{r_B}{4G_N} \sec \frac{L_{\text{dS}}}{2}. \quad (6.20)$$

Note that the only difference with respect to the JT gravity setting (5.30) is in replacing $L \rightarrow -iL_{\text{dS}}$, which is consistent with the boundary evaluation. In particular, note that in the stretched horizon limit, i.e. $r_B \rightarrow r_{\text{CH}}$, we recover the GH entropy of dS₃ space, since $L_{\text{dS}} \rightarrow 0$ (6.19)

$$S_{\text{dS}} = \frac{2\pi r_{\text{CH}}}{4G_3}, \quad (6.21)$$

where we again used that $2\pi G_N = G_3$ [192], and $2\pi r_{\text{CH}}$ is the corresponding codimension-two area in dS₃ space. Due to the general correspondence with the entanglement entropy in the deformed theory (6.14) the GH entropy can indeed be interpreted as entanglement entropy from the perspective of the microscopic theory. The BH entropy in the $y \rightarrow 0$ limit can also be recovered as explained in [99].

RT Surfaces From Timelike Boundaries At last, we search to evaluate the RT formula for dS JT gravity (2.1) (with $U(\Phi) = -2\Phi$) in (6.15) using global coordinates (6.16) when the entangling surface are points along the finite cutoff boundaries that reside in the static patch (e.g. the cosmological stretched horizon case) in Fig. 7 (d).³⁹ The relationship between static patch coordinates and global dS₂ coordinates in the case of interest is similar to (6.17) without the analytic continuation between Milne and static patch, namely

$$\sqrt{1 - \frac{r^2}{r_{\text{CH}}^2}} \sinh \frac{r_{\text{CH}} t}{2} = \sinh T, \quad \text{when } r < r_{\text{CH}} \quad (6.22a)$$

$$\sqrt{1 - \frac{r^2}{r_{\text{CH}}^2}} \cosh \frac{r_{\text{CH}} t}{2} = \cos \varphi \cosh T. \quad (6.22b)$$

Analogous to the AdS case in Sec. 5.3, the homology constraint with r timelike boundaries implies that the dilaton in dS JT gravity (6.16) is extremized in the φ direction ($\partial_\varphi \Phi_{\text{dS}} = 0$)

³⁹Note that while we use entangling surface points in the two-dimensional context, in higher dimensions one can adopt spatial subregions, which may lead to a larger variety of the minimal codimension-two area with boundaries in the static patch [150, 255].

and for a fixed T coordinate. This leads to $\varphi = \pi/2$, which is a maximum value for the dilaton (6.16), while the minimum value is reached when $\varphi = 0$ or π , corresponding to the poles of the static patch. However, since the dilaton is trivial for this minimum, this would not even be connected to the previous result the extremal value of the dilaton with spacelike boundaries (6.20), and neither to the boundary result for the algebraic entanglement entropy. This indicates that the RT formula does not apply after the $T^2 + \Lambda_1$ deformation, and one might need to search for a different geometric quantity dual to the algebraic entanglement entropy found in (6.14).

Thus, the result differs from Susskind’s conjectures (i) and (iv) in Sec. 1, which expected the RT formula to hold when the corresponding boundary is inside the static patch instead of the Milne patch. However, in the strict limit where the boundary is at the cosmological horizon one recovers the expected GH entropy. Meanwhile, in higher dimensions, one can have subregions in the stretched horizon and develop a different form of the RT formula in [1], which is not accessible from the two-dimensional analysis.

7 Discussion

In summary, we developed chord Hamiltonian deformations based on general dilaton gravity theories with Dirichlet boundaries and different boundary counterterms. In particular, this recovers T^2 deformations in (0+1)-dimension, as well as a lower-dimensional analog of $T\bar{T} + \Lambda_2$ deformations (“ $T^2 + \Lambda_1$ ”) as special cases. The latter deformation might clarify the relationship and differences in the bulk interpretation of $T\bar{T} + \Lambda_2$ by [153] and [148]. Namely, one recovers the same deformation by either changing the dilaton potential, or the counterterm in the dilaton gravity action (2.1), which modifies the location of the finite cutoff boundaries, crossing the location of the corresponding horizon [148]. While the procedure can be applied in general (0+1)-dimensional quantum mechanical systems with a bulk dual, we specialized most of the study in the DSSYK model for concreteness.

We evaluated the semiclassical thermodynamic properties of the deformed model from its partition function. We investigated the Krylov spread complexity of the HH state in the deformed theory and matched it to a wormhole length in finite cutoff holography. We also deduced expressions for general and semiclassical correlation functions in the deformed theory. Remarkably, the algebraic entanglement entropy between the double-scaled algebras of the DSSYK given the new chord number basis precisely matches the dilaton at the extremal surface in the JT and dS JT gravity once we restrict to the IR and UV triple-scaling limits respectively. By combining the previous results in the UV limit of the DSSYK chord spectrum and applying a sequence of T^2 and $T^2 + \Lambda_1$ deformations, we explicitly realize the stretched horizon proposal by Susskind [1], including its characteristic hyperfast growth for dynamical observables. This provides a direct link between Susskind’s conjectures [1] with sine dilaton gravity, which recovers dS₂ space in a specific limit [109] associated with our UV triple-scaling limit, and therefore also with Schwarzschild-dS₃ holography [112]. This leads to a more precise connection between different proposals for the bulk dual of the DSSYK model.

Now, we discuss directions for future investigation.

7.1 Outlook

Krylov operator complexity In the main text, we discussed Krylov spread complexity, which has a bulk interpretation in terms of bulk geodesics at finite cutoff in (A)dS₂ space. This connects with literature on holographic complexity with a finite cutoff in the bulk, e.g. [145, 159–163, 165, 166, 205, 256]. In the main text, we also explored the effect of the deformations in the semiclassical correlation function, which are only affected by a modification in the inverse temperature to be the Tolman temperature. It is then natural to investigate what would be the effect of the Hamiltonian deformation in Krylov operator complexity.

For concreteness, consider the one-particle HH state in (4.9b) for $m = 1$ which can be expressed as

$$|\Psi_{\Delta_1}(\tau_L = \kappa\tau, \tau_R = \tau)\rangle = e^{-\hat{\mathcal{L}}_\kappa\tau} |\Delta_1; 0, 0\rangle = \sum_n \Psi_n^{(\kappa)}(\tau) |K_n^{(\kappa)}\rangle, \quad (7.1)$$

where

$$\hat{\mathcal{L}}_\kappa \equiv \hat{H}_{R,y} + \kappa \hat{H}_{L,y}, \quad \kappa \equiv \tau_L/\tau_R. \quad (7.2)$$

is a Liouvillian operator. Note that

$$\kappa = 1: \quad |\Psi_{\Delta_1}(\tau_L = \tau, \tau_R = \tau)\rangle = e^{-\tau(\hat{H}_L + \hat{H}_R)} |\Delta_1; 0, 0\rangle, \quad (7.3a)$$

$$\kappa = -1: \quad |\Psi_{\Delta_1}(\tau_L = -\tau, \tau_R = \tau)\rangle = e^{-\frac{\beta}{2}\hat{H}_{L,y}} \hat{\mathcal{O}}_{\Delta_1}(t) e^{-\frac{\beta}{2}\hat{H}_{L,y}} |\Omega\rangle. \quad (7.3b)$$

where

$$\hat{\mathcal{O}}_{\Delta_1}(t) \equiv e^{it\hat{H}_L} \hat{\mathcal{O}}_{\Delta_1} e^{-it\hat{H}_L}, \quad \tau \equiv \frac{\beta}{2} + it. \quad (7.4)$$

The $\kappa = +1$ case corresponds to Schrödinger evolution with respect to a total Hamiltonian $\hat{H}_L + \hat{H}_R$ in complex-valued time τ ; while $\kappa = -1$ corresponds to Heisenberg evolution with respect to the single-sided Hamiltonian \hat{H}_L . For this reason, based on the Liouvillian evolution operator $\hat{\mathcal{L}}_\kappa$, we can evaluate Krylov complexity for states and operators depending on the value of κ . Other choices of κ are associated with generalized notions of Krylov complexity [72]. We will focus on $\kappa = \pm 1$.

Meanwhile, we refer to $\{|K_n^{(\kappa)}\rangle\}$ as the Krylov basis for the reference state $|K_0^{(\kappa)}\rangle \equiv |\Delta_1; 0, 0\rangle$, which are defined to satisfy a Lanczos algorithm

$$\hat{\mathcal{L}}_\eta |K_n^{(\kappa)}\rangle = a_n^{(\kappa)} |K_n^{(\kappa)}\rangle + b_{n+1}^{(\kappa)} |K_{n+1}^{(\kappa)}\rangle + b_n^{(\kappa)} |K_{n-1}^{(\kappa)}\rangle, \quad (7.5)$$

with $b_0^{(\kappa)} = 0$, $a_0^{(\kappa)} = \langle K_0^{(\kappa)} | K_0^{(\kappa)} \rangle$, while $a_n^{(\kappa)}$ and $b_n^{(\kappa)}$ are called Lanczos coefficients. We define Krylov operator complexity as

$$\mathcal{C}(t) \equiv \frac{\langle \Psi_{\Delta}(-\tau, \tau) | \hat{\mathcal{C}}^{(\kappa)} | \Psi_{\Delta}(-\tau, \tau) \rangle}{\langle \Psi_{\Delta}(-\tau, \tau) | \Psi_{\Delta}(-\tau, \tau) \rangle} \Bigg|_{\tau = \frac{\beta}{2} + it}, \quad \hat{\mathcal{C}}^{(\kappa)} \equiv \sum_n n |K_n^{(\kappa)}\rangle \langle K_n^{(\kappa)}|. \quad (7.6)$$

Similar to the spread complexity case, the effect of the deformation in the Liouvillian operator (7.2) is to scramble the Krylov basis $|K_n^{(\kappa)}\rangle$. It would be interesting to deduce the semiclassical Krylov operator and spread complexity with a one-particle insertion. In particular, this could be useful to learn about these deformations in higher dimensional examples. For instance, it was reported in [257] that the exponential growth of Krylov operator complexity for CFTs might not agree with the OTOC chaos bound [144] when the deformation parameter has the sign associated to superluminal motion [258], unlike in finite cutoff holography.

It would also be interesting to compare the standard definition of Krylov operator complexity above with the work by [259], where the authors use a notion of Krylov operator complexity in a microcanonical window in JT gravity. They find that at leading order in the approximation, the Lanczos coefficients display linear growth, and Krylov complexity grows exponentially with a simple modification in the inverse temperature, which includes the corresponding redshift factor, similar to our findings for the semiclassical correlation functions. This suggests that one might find a redefinition of Krylov operator complexity (7.6) in a microcanonical window which can be expressed as the first derivative of the OTOC at finite temperature in (4.24) based on the seed theory result [72] where one would incorporate the fake temperature with the corresponding redshift factor in (4.21). This redefinition of Krylov operator complexity would be associated to the wormhole length connecting the asymptotic boundaries of an AdS₂ black hole instead of the one with finite Dirichlet boundary (5.29) even when $\Delta \rightarrow 0$. For this reason, it might also be fruitful to develop in detail the definition of Krylov operator complexity in (7.6) without fixing an energy window, which might be more closely related to finite cutoff holography.

Generalized Boundary Conditions in Finite Cutoff Holography Our work has focused on the finite cutoff interpretation of Hamiltonian deformations, when the bulk dual has Dirichlet boundary conditions. There is literature regarding how to extend holography between Dirichlet through multitrace deformations, which is expected to modify the boundary conditions in the bulk [43–45, 48, 260, 261]. In particular, there has been significant interest in developing conformal boundary conditions and its extensions [46, 47, 156, 156, 262–271, 271, 272] to obtain well-posed solutions in general relativity when Dirichlet boundary conditions are ill-posed. Finite cutoff in AdS space with conformal boundary conditions was investigated in [44–47]. Given that the DSSYK model is a useful analytically solvable model at different energy scales, it might be convenient to generalize our study, incorporating cutoff holography with conformal boundary conditions instead of Dirichlet in the dilaton-gravity theories, possibly along the lines of [268], and analyze how the thermodynamics properties of the model and its correlation functions are modified. Given the connection between the deformations in the DSSYK model and stretched horizon holography, this study could help us gain general lessons for static patch holography, since, as we saw, the theory is otherwise thermodynamically unstable. It is also relevant to study the perturbative stability of the solutions under background fluctuations [156], which could be incorporated following previous studies in the dilaton-gravity context by [273, 274].

Additionally, it should be possible to adapt our study in the mixed boundary condition interpretation where the DSSYK would stay at the original asymptotic boundary location (i.e. r_B). The development of this interpretation in the Schwarzian of JT gravity has been previously performed in [33]. We hope to come back to this point in future work to implement this interpretation in sine dilaton gravity.

Entanglement entropy in $T^2 + \Lambda_1$ Deformation As emphasized in the main text, the algebraic entanglement entropy in the double-scaled algebras associated to a chord number state (which reproduces bulk geodesics at a finite cutoff) leads to a precise matching between the bulk entanglement entropy in the T^2 deformed theory and the dilaton in JT and dS JT gravity at the extremal surface predicted by the RT formula. However, once we move to $T^2 + \Lambda_1$ deformations, the RT formula does not longer apply as the minimal value of the dilaton becomes trivial, as explained in Secs. 5.3 and 6.4. It would be interesting to find a geometric quantity that one can associate with the corresponding algebraic entanglement entropy (5.6) given the chord number state in the Krylov basis $|K_n^{(y)}\rangle$ in the $T^2 + \Lambda_1$ case, although the system is not even thermodynamically stable. For instance, a central part in Susskind’s conjectures are rules to implement RT formula calculations in stretched horizon holography in the bilayer vs monolayer proposals [1, 169–171]. These rules rely on angular dependence in dS₃ space, and they are thus inaccessible from the dS₂ perspective which is dual to the UV limit of the DSSYK model. In principle one may connect these additional RT proposals with the dS₃ embedding of sine dilaton gravity [112].

Additionally, we suspect that one does not need to limit the evaluations to a triple-scaling limit to be able to interpret the algebraic entanglement entropy in the chord number state holographically. We would like to extend this result for the semiclassical regime in the DSSYK model [58], which is expected to have a bulk interpretation in sine dilaton gravity. One might derive further results in this direction by developing a Lewkowycz-Maldacena path integral derivation of the corresponding RT formula in the bulk [275], or possibly through a factorization map [276–281].

Deforming Before Averaging Throughout our analysis, we deformed the DSSYK model after ensemble averaging since the Hamiltonian deformation can be interpreted as a radial bulk flow in the sine dilaton gravity theory. However, one might investigate the differences in the theory by applying first the deformation and then the averaging. This would mean a transformation in the SYK Hamiltonian (3.1)

$$\hat{H}_{\text{SYK}} \rightarrow \hat{H}_{\text{SYK},y} = \frac{1}{y} \left(1 - \sqrt{1 - 2y\hat{H}_{\text{SYK}}} \right). \quad (7.7)$$

The ensemble average evaluation is more complicated due the square root factor, although one can make much progress by working in the $G\Sigma$ -formalism, as in [33]. It would be interesting to consider in this alternative case how the different thermodynamic properties and dynamical observables in our study are modified, such as Krylov spread complexity and correlation functions, and to understand the corresponding bulk geometry.

Verifying Sine Dilaton at Finite Cutoff Our work has mostly taken a boundary perspective without requiring a specific bulk dual to the DSSYK model beyond its IR and UV triple-scaling limits, as long as it corresponds to a dilaton gravity theory. Nevertheless, we found explicit results that suggest a natural bulk interpretation in terms of sine dilaton gravity, where Krylov spread complexity for the HH state in the deformed DSSYK in the semiclassical limit (3.53) describes a wormhole geodesic at finite cutoff (5.29), as well as the RT formula verification for the UV and IR triple-scaling limits in Sec. 3.2; see App. C for further exploration. As a next step, one could perform a bulk analysis of correlations functions to provide a concrete bulk dual interpretation of some of our other results. A simple start would be studying the functional dependence of correlation functions in the microcanonical ensemble and an overall redshift factor associated to the Tolman temperature in the semiclassical limit, as in the existing literature in JT gravity and higher dimensional cutoff holography [32–34, 38, 148, 207]. However, it is important to make further checks outside the AdS₂ regime of the bulk dual theory. For instance, in sine dilaton gravity, one could carry out a gravitational path integral calculation in the bulk, or study solutions to the WDW equation in the bulk at finite cutoff (similar to [34]) to verify our boundary theory results for the partition functions and correlation functions.

Additionally, it was previously pointed out by [92] that there is a defect interpretation of the thermodynamics in sine dilaton gravity related to an infinite degeneracy in the black hole and cosmological horizons due to the periodicity in the dilaton potential. Meanwhile, the finite cutoff interpretation of the Hamiltonian deformations in this work might allow to remove the degeneracy by placing the boundaries in appropriate locations in the complex-valued geometry. It would be interesting to investigate how the properties of the conical defect associated with the removed horizons can be matched with the exact deformed partition function in (2.24).

Moreover, while the practical computations are semiclassical, one could repeat our analysis of correlation functions and partition functions beyond the on-shell level by including one-loop corrections as in [191] for the T^2 deformed DSSYK, and comparing them with recent developments [42, 111]. It is also important to extend our investigation with non-perturbative series expansions of our results in terms of Borel resummation and instanton processes following analogous studies in JT gravity [37] to better understand the spectrum of the deformed theory and the putative bulk dual at a finite cutoff.

At last, a related interesting extension would be to explore finite cutoff holography using the chord Hamiltonian (3.13) when $q = e^{ib}$ (where $b \in \mathbb{R}$) (instead of $q \in [0, 1]$ in the main text) which is argued to be dual to a $\sinh \Phi$ dilaton gravity theory [282, 283], and it is closely connected with Liouville gravity [284–289]; see [42] for recent progress.

Narovlansky-Verlinde Model Another interesting proposal for the bulk dual of the DSSYK model was made by V. Narovlansky and H. Verlinde in [115] (see also [95, 96, 112, 117]), who developed an approach towards dS₃ holography by considering a two-copy SYK model with an equal energy constraint. In the double-scaling limit and after ensemble-

averaging, the system can be described by the zero-particle chord Hamiltonian (3.13).

In the bulk proposal of [115], the dual dilaton gravity theory has a potential (C.1) of the form:

$$U(\Phi) = -2 \cosh(\Phi) . \quad (7.8)$$

The T^2 deformation parameter is given by (2.17) for the potential with the counterterm (2.3) is

$$y = -\frac{\lambda}{\sinh \Phi_B} . \quad (7.9)$$

It would be interesting to test our boundary theory findings with finite cutoff holography in the NV model to check if it leads to manifestly different thermodynamics or correlation functions with respect to those in sine dilaton gravity at finite cutoff and compare both with our boundary theory results. In particular, our results about entanglement entropy at a finite cutoff have a clear geometric interpretation for (A)dS space when we zoom in the UV and IR triple-scaling limits. These limits are naturally compatible with sine dilaton gravity; it would be interesting to find if there are similar limit that can be associated to the dilaton gravity theory described by (7.8), or whether one can show there are none unless $\Phi \rightarrow i(\Phi)$ which would recover an equivalent theory to sine dilaton gravity. It would also be interesting to relate the NV model at finite cutoff to a dimensionally reduced version of the $T\bar{T} + \Lambda_2$ deformations [153, 155] similar to our proposal for $T^2 + \Lambda_1$ deformations of the DSSYK model in the triple-scaling limit (3.28a).

Relational Holographic Flow In the future, we would like to study the relational interpretation in the T^2 flow, focusing on the dressed observables and the finite cutoff holographic dictionary. It has been noticed that quantum reference frame (QRF) transformation will significantly affect the thermodynamics, and algebraic operator structure of general systems [290, 291] (see also [292]). Given the explicit knowledge of the solution for the DSSYK model, it would be intriguing to study QRF transformations in this system explicitly and how the semiclassical thermodynamics studied here will be modified. More generally, it would be interesting to study the algebra of observables for the T^2 -deformed DSSYK model with matter, as a microscopic realization of [154].

If one interprets the boundary in terms of an observer to define expectation values of gravitationally dressed operators in the bulk algebra, we might view that as we change the location of the cutoff boundary, the observer also changes due to the Hamiltonian deformation of the boundary theory. For instance, based on recent work by [112], we could re-express sine dilaton gravity theory by a pair of Liouville fields; and we study how the flow in the Schrödinger evolution is captured by relational observables. The effect of the $T\bar{T}$ deformation is to change the Hamiltonian but not the proper time measured by a boundary observer. From the relational interpretation of the Liouville-CFT formulation of sine dilaton gravity this means that the collective field description of the DSSYK is modified, but not the time parameter itself corresponding to the observer's clock in the Liouville theory. It would thus be interesting to explore how the $T\bar{T}$ deformation changes the Page-Wootters mechanism

[293, 294] in the bulk theory. We expect there is a relational description in the bulk in terms proper time in sine dilaton gravity. In contrast, the boundary theory just experiences Schrödinger evolution since it only has access to gauge-invariant data of the bulk.

Deforming Matrix Models T^2 deformations in an ensemble of matrix models have been previously considered in the JT gravity context by [36]; which allowed them to study the energy spectrum of the deformed model for all real values of the deformation parameter without recurring to a mixed boundary condition interpretation in the bulk. It would be interesting to generalize the previous work of [36] to explore how this type of interpretation works in a matrix model dual to the sine dilaton gravity model with a higher genus expansion, which is not well developed. It might also be interesting to perform the T^2 deformation of the two-matrix model of [295, 296] that reproduces certain DSSYK amplitudes (and which has been further developed in [297–299]), to compare with our findings on semiclassical thermodynamics in Sec. 2.3, and possibly to investigate recent connections between JT gravity at finite cutoff with matrix models [42].

Charged DSSYK model and \overline{JT} deformations In line with our analysis of T^2 deformations in the DSSYK model, there also exist \overline{JT} deformations [300] in the literature [301], where J is a chiral $U(1)$ current. It would be interesting to investigate the nature of the bulk dual to the DSSYK model with a $U(1)$ charge [302] (see also [303–305]), which has been recently discussed in [114, 132]. One could then introduce \overline{JT} deformations, or alternatively a combination of T^2 , \overline{JT} deformations in the DSSYK model and study the thermodynamic properties and correlation functions we have encountered in this work. In particular, it would be interesting to evaluate the corresponding Krylov spread complexity (away from the vanishing deformation parameter $y \rightarrow 0$ limit, discussed by [76]). A related possibility in this direction is using the $\mathcal{N} = 2$ extension of the DSSYK model [306] which counts with an R-charge. It would be very interesting to extend the results deforming the theory and finding the corresponding bulk length at finite cutoff, particularly for the BPS sector [307], its interpretation as chord number [91] and in terms of Krylov spread complexity [77].

Stretched Horizon in Higher Dimensions Recently, [149] found an extension of $T\overline{T} + \Lambda_2$ deformations in higher dimensions, which we denote $T^2 + \Lambda_d$ deformations. Explicitly, consider deformation the action of a CFT_d as

$$\frac{dI_{\text{bdry}}}{dy} = \int d^{d-1}x \sqrt{-h} \left[\frac{\pi y}{d} : \left(\tilde{T}_{\mu\nu} \tilde{T}^{\mu\nu} - \frac{1}{d-1} (\tilde{T}^\mu{}_\mu)^2 \right) : - \frac{d^2(d-1)\eta-1}{4\pi} \frac{1}{y} + \frac{d}{4\pi} \left(\frac{C_d^2}{y^{d-2}} \right)^{1/d} R^{(d)} \right]. \quad (7.10)$$

with $h_{\mu\nu}$ being the metric of the boundary theory in d space-time dimensions, with an associated Ricci scalar $R^{(d)}$; y is the deformation parameter and the stress tensor is $\tilde{T}_{\mu\nu} = T_{\mu\nu} + \tilde{T}_{\mu\nu}^{\text{CT}}$ where $: \ :$ represents large- N normal ordering as described in [27], where CT denotes the counterterm contribution, and η is a parameter corresponding to T^2 ($\eta = +1$) and $T^2 + \Lambda_d$ ($\eta = -1$) deformations.

The authors associate the deformed theory (7.10) to Einstein gravity in (A)dS_{d+1} space at finite cutoff:

$$I_{\text{bulk}} = \frac{1}{16\pi G_N} \int_{\mathcal{M}} d^{d+1}x \sqrt{-g} \left(R^{(d+1)} + \frac{d(d-1)}{\ell^2} \eta \right) + \frac{1}{8\pi G_N} \int_{\partial\mathcal{M}} d^d x \sqrt{-h} (K + \text{counterterm}) , \quad (7.11)$$

where \mathcal{M} represents the spacetime manifold, G_N Newton's constant, $g_{\mu\nu}$ the bulk metric, $R^{(d+1)}$ the Ricci scalar, and K the mean curvature.

The authors find an associated (dimensionless) energy spectrum for the deformed theory, which takes the form

$$\mathcal{E}_y = \frac{d(d-1)}{2\pi y} \left[\sqrt{1 + \Omega^{2/(d-1)} (C_d y)^{2/d}} \Big|_{y^{(\lceil d-2 \rceil)/d}} \mp \sqrt{\eta + \Omega^{2/(d-1)} (C_d y)^{2/d} - \frac{4\pi}{d(d-1)} y \mathcal{E}_0} \right] , \quad (7.12)$$

where C_d represents constants determined by the counterterms and \mathcal{E}_0 is the (dimensionless) energy spectrum of the seed theory. Using the available tools to repeat the analysis in this work in higher dimensional settings, it would be interesting to verify our findings on the stretched horizon, such as the hyperfast scrambling in the OTOCs and holographic entanglement entropy from the algebraic perspective in the higher dimensional settings. One difficulty is to identify a specific boundary theory in the dS_{d+1} case.

Acknowledgments

I thank Andrew Svesko, and Manus Visser for previous collaboration on [38], which partially motivated this work; to Gonalo Araujo-Regado, Philipp A. Hohn, Francesco Sartini, Jiayue Yang and Ming Zhang for collaboration in other works with related themes; to Takanori Ane-gawa, Andreas Blommaert, Klaas Parmentier, and Jiuci Xu for useful comments on an earlier version of the draft; and to Dio Anninos, Luis Apolo, Micha Berkooz, Arghya Chattopadhyay, Chuanxin Cui, Victor Franken, Damian A. Galante, Eleanor Harris, Taishi Kawamoto, Simon Lin, Masamichi Miyaji, Sangjin Sin, Andrew Rolph, and Gopal Yadav for insightful discussions/comments. I also thank the organizers of the ‘‘V Siembra-HoLAGrav Young Frontiers Meeting’’, the ‘‘Quantum Extreme Universe: Matter, Information and Gravity 2024’’ workshop in Okinawa Institute of Science and Technology Graduate University (OIST), ‘‘New Avenues in Quantum Many-body Physics and Holography’’ in Asia-Pacific Centre (APCTP) for Theoretical Physics, the ‘‘Young Researchers of Quantum Gravity’’ online seminars, ‘‘Strings 2025’’ in New York University Abu Dhabi; the ‘‘QISS 2025 Conference’’ in Vienna University, and ‘‘2025 East Asia Joint Workshop on Fields and Strings’’ in OIST, and the joint Israeli seminars at Neve Shalom where part of the work was presented in different formats; to the ‘‘XX Modave summer school’’ for allowing relevant discussions with other participants; to the high energy physics groups at Rikkyo University and the Weizmann Institute of Science for hospitality while this work was in finishing stages. SEAG acknowledges support from the APCTP, the Office of Scholarships and the QISS consortium for travel support; as well as

partial support by the FWO Research Project G0H9318N and the inter-university project iBOF/21/084 when this project started. SEAG is supported by the Okinawa Institute of Science and Technology Graduate University. This work was made possible through the support of the WOST, WithOut SpaceTime project (<https://withoutspacetime.org>), supported by Grant ID# 63683 from the John Templeton Foundation (JTF), and ID#62312 grant from the JTF, as part of the ‘The Quantum Information Structure of Spacetime’ Project (QISS), as well as Grant ID# 62423 from the JTF. The opinions expressed in this work are those of the author(s) and do not necessarily reflect the views of the John Templeton Foundation.

A Notation

Acronyms

- ADM: Arnowitt–Deser–Misner.
- (A)dS: (Anti-)de Sitter.
- AGH: Almheiri-Goel-Hu
- ASC: Al-Salam Chihara.
- BTZ: Bañados-Teitelboim-Zanelli.
- BH: Bekenstein-Hawking.
- BY: Brown-York.
- CFT: Conformal field theory.
- CV: Complexity=volume.
- (DS)SYK: (Double-scaled) Sachhev-Ye-Kitaev
- ETW: End-Of-The-World
- GH: Gibbons-Hawking.
- HH: Hartle-Hawking
- IR: Infrared
- JT: Jackiw-Teitelboim
- OTOC: Out-of-time-order correlations.
- QFT: Quantum field theory
- SC: Square correlators.
- RT: Ryu-Takayanagi.
- WKB: Wentzel-Kramers-Brillouin.
- UV: Ultraviolet
- WDW: Wheeler–DeWitt

Notation

- $F(r)$ (2.31): Blackening factor.
- $G(\Phi_B)$ (2.1): Boundary counterterm, where $\Phi_B(\equiv r_B)$ denotes the dilaton at the finite or asymptotic boundary.
- $h_{\mu\nu}$ (2.1): Induced metric.

- γ_{ab} (2.14): Boundary metric.
- $U(\Phi)$ (2.1): Dilaton potential.
- \mathcal{H} (2.11): Hamiltonian constraint.
- \tilde{T}_{ab} (2.8a): Bulk matter stress tensor.
- T_{ab} (2.13): Boundary matter stress tensor.
- \mathcal{O}_{Φ_B} (2.8b): Dilaton source.
- K, \mathcal{R} (2.1): Mean curvature, and Ricci scalar.
- $Z_y(\beta)$ (2.28a): Deformed partition function without matter.
- y and η (2.17): Deformation parameters.
- $E(\theta) = \frac{-2J \cos(\theta)}{\sqrt{\lambda(1-q)}}$ (2.25): DSSYK energy spectrum, where θ is a parametrization.
- E_y (2.16): Deformed energy spectrum.
- $\hat{H}_y = f_y(\hat{H})$ (2.18): Deformed Hamiltonian, with f_y a generic analytic function.
- $S(\theta)$ (2.25): Thermodynamic entropy.
- ρ_y (2.28b): Density of states of the deformed theory.
- β_y (2.26): Microcanonical inverse temperature.
- C_y (2.29): Heat capacity for fixed deformation parameter.
- N , and p (3.1): Number of Majorana fermions and all-to-all interactions respectively.
- $q \in [0, 1)$ (3.6): q -deformation parameter, the penalty factor associated to DSSYK Hamiltonian interceptions in chord diagrams.
- $\lambda = 2N/p^2 \equiv -\log q$: Parameter in the double-scaling limit (3.6).
- \mathcal{H}_m and $\mathcal{H}_{\text{chord}}$ (3.19): Chord space with m operators, and an all-operator extension.
- $|K_n^{(y)}\rangle$ (3.56): Krylov basis in the deformed DSSYK model.
- \hat{n}_y (3.54b): Chord number operator in the deformed DSSYK model.
- $|K_n^{(\kappa)}\rangle, a_n^{(\kappa)}, b_n^{(\kappa)}$ (7.5): Krylov basis and Lanczos coefficients, where κ is a parametrization for one-particle states.
- \mathcal{C} (3.31): Cost function.
- \mathcal{C}_S (3.38), a_n, b_n (3.33b): Krylov spread complexity in the zero-particle chord space.
- ℓ_y (3.39): Expectation value of the rescaled chord number in the HH state.
- L (B.1), L_{dS} (6.18): Minimal geodesic lengths between the asymptotic boundaries in the bulk.
- $|n\rangle, |\theta\rangle$ (3.15): Chord number and energy basis for zero-particle states respectively.
- $|\Omega\rangle$ (3.8): Tracial (zero chord number) state.
- $[n]_q = \frac{1-q^n}{1-q}$ (3.10): q -deformed integer.
- $(a; q)_n = \prod_{k=0}^{n-1} (1 - aq^k)$ (3.16): q -Pochhammer symbol.
- $(a_1, a_2, \dots, a_m; q)_n = \prod_{i=1}^m (a_i; q)_n$ (3.16).
- $\tilde{\beta}_y = \frac{\pi}{J \sin \theta}$ (4.21): Fake temperature of the deformed theory.
- $H_n(x|q)$ (3.17): q -Hermite polynomials.
- $\mu(\theta)$ (3.18): Integration measure in the energy parametrization basis θ .
- $\hat{\mathcal{O}}_\Delta$ (3.4): Matter chord operator with conformal dimension Δ .
- \hat{n} (3.11): Chord number operator in the zero-particle sector \mathcal{H}_0 .

- dE/dE_y (2.27): Redshift factor.
- $\hat{H}_{\text{IR/UV}}$ (3.28): Chord Hamiltonian in the IR and UV triple-scaling limit respectively.
- $\theta_{\text{IR}} \equiv \theta \ll 1$ and $\theta_{\text{UV}} \equiv \pi - \theta \ll 1$ (3.28b): IR and UV triple-scaled energy parametrizations respectively in the seed theory.
- \hat{a}_i^\dagger and \hat{a}_i (3.23a): Non-Hermitian conjugate creation and annihilation operators in \mathcal{H}_m .
- $\tau_{L/R} = \frac{\beta_{L/R}}{2} + it_{L/R}$ (4.7): Complex-valued time, with $\beta_{L/R}$ the inverse temperature and $t_{L/R}$ as real time.
- $|\Psi_\Delta(\tau_L, \tau_R)\rangle$ (4.9b): Generalization of the HH state with matter chord insertions.
- $\tilde{\Delta} = \{\Delta_1, \dots, \Delta_m\}$ (3.20): Collective index of conformal dimensions.
- \hat{N} (3.21): Total chord number with one or more particle chords.
- $\hat{n}_i^> \equiv \sum_{j=i+1}^m (\hat{n}_j + \Delta_j)$ and $\hat{n}_i^< \equiv \sum_{j=0}^{i-1} (\hat{n}_j + \Delta_{j+1})$ (3.22).
- $\hat{H}_{L/R,y}$ (4.1): Deformed two-sided chord Hamiltonian
- G_{2m} (4.6): $(2m)$ -point correlation function.
- ℓ_* (4.23), ℓ_0 (4.33): Constants in the crossed-correlation function in the double-scaling and triple-scaling limits respectively.
- λ_L (6.13a): Lyapunov exponent.
- t_{sc} (4.28): Scrambling time.
- $\mathcal{A}_{L/R} \equiv \{\hat{H}_{L/R}, \hat{\mathcal{O}}_\Delta^{L/R}\}$ (5.1): Double-scaled algebras.
- Tr (5.2): Type II algebraic trace.
- S (5.6): Entanglement entropy between double-scaled algebras given a chord state.
- $\hat{\rho}$ (5.5): Reduced density matrix.
- r_{BH} (5.26), r_{CH} (6.2): AdS black hole and cosmological horizon radial locations.
- $\Phi_{(\text{A})\text{dS}}$ (5.25): Dilaton Φ (2.1) in (dS) JT gravity.
- γ (5.25): RT surface.
- $\hat{\varphi}_i$ (E.4): Constraints selecting symmetry sectors in the chord Hilbert space.
- \hat{H}_{ASC} (E.1): ASC Hamiltonian. X, Y : Parameters in the ASC Hamiltonian.
- $\tilde{\mu}(\theta)$ (E.13): Integration measure factor in energy basis in systems with ETW branes.
- $Q_l(\cos \theta|X, Y; q)$ (E.11): ASC polynomials.
- $Z_{\text{ETW}}^{(y)}(\beta|X, Y)$ (E.19): Disk partition function with ETW brane.
- χ (C.4): Stretched horizon parameter.

B Matching Time/Space-like Geodesics with (3.53)

In this appendix, we show that the Krylov spread complexity of the HH state in the deformed DSSYK model in (3.53) describes both spacelike and timelike geodesic lengths connecting the finite cutoff boundaries of AdS₂ black hole, which are illustrated in Fig. 3.

We define geodesic lengths as

$$L = \int d\xi \mathcal{L}(\xi), \quad \mathcal{L} \equiv \sqrt{g_{\mu\nu} \dot{x}^\mu \dot{x}^\nu} = \sqrt{-f(r) \dot{v}_{L/R}^2 + 2\dot{v}_{L/R} \dot{r}}, \quad (\text{B.1})$$

where ξ is a general parameterization, $\dot{x} \equiv \frac{dx}{d\xi}$, the index L/R indicates left/right patches, while

$$ds^2 \equiv g_{\mu\nu} dx^\mu dx^\nu = -f(r) dv_{L/R}^2 + 2dv_{L/R} dr = -f(r) dt_{L/R}^2 + \frac{dr^2}{f(r)}. \quad (\text{B.2})$$

Here we will be interested in the blackening factor

$$f(r) = r^2 - r_{\text{BH}}^2, \quad (\text{B.3})$$

although, we keep some expressions with $f(r)$ general unless otherwise specified.

There is a conserved charge

$$P = \frac{\delta \mathcal{L}}{\delta \dot{v}_{L/R}} = \frac{-f(r) \dot{v}_{L/R} + \dot{r}}{\mathcal{L}}. \quad (\text{B.4})$$

Note that \mathcal{L} is a diffeomorphism invariant function, and it can be thus gauged fixed to any value. In the literature, one commonly chooses $\mathcal{L} = \pm 1$ where $+1$ corresponds to the spacelike case, and -1 to timelike [308]. However, given that \mathcal{L} is diffeomorphism invariant, it is not necessary to make any particular gauge-choice, all will give the same answer, and thus, regardless of the geodesic being spacelike or timelike, they will have the same functional expression, as we show below by combining \mathcal{L} in (B.2) with (B.4). This gives

$$\dot{r}^2 = (P^2 + f(r)) \mathcal{L}^2. \quad (\text{B.5})$$

Then, we can evaluate the geodesic length functional as

$$L = \int_{\xi_*}^{\xi_B} \mathcal{L} d\xi = \int_{r_*}^{r_B} \frac{dr}{\sqrt{P^2 + f(r)}}, \quad (\text{B.6})$$

where ξ_B is the parametrization of the boundary cutoff value where $r(\xi_B) = r_B$, and $r(\xi_*) = r_*$ represents the turning-point i.e. when $\dot{r} = 0$ in (B.5)

$$r_* = f^{-1}(-P^2), \quad (\text{B.7})$$

where we are using that P is a conserved charge. Meanwhile, using the relation between t and v in (B.2), we have that $f(r) \dot{t}_{L/R} = -\mathcal{L}P$, i.e.

$$t = -P \int_{\xi_*}^{\xi_B} \frac{dr}{f(r) \sqrt{P^2 + f(r)}}, \quad (\text{B.8})$$

where we are gauge-fixing $t_L = t_R \equiv t$.

We can now specialize in the cases of interest in the AdS₂ black hole (B.3), where (B.6) and (B.8) gives

$$L = 2 \operatorname{arccosh} \frac{r_B}{r_*}, \quad (\text{B.9a})$$

$$\frac{r_{\text{BH}} t}{2} = \arctan \frac{r_B \sqrt{r_*^2 - r_{\text{BH}}^2}}{r_{\text{BH}} \sqrt{r_B^2 - r_*^2}}. \quad (\text{B.9b})$$

Note that in the case of timelike geodesics ($r_* < r_B$) L (B.9a) becomes complex-valued, while t remains real-valued; while both L and t remain real-valued for spacelike geodesics, where $r_* > r_B$. One can simplify the above expressions by inverting $r_*(t)$ from (B.9a), plugging it back in (B.9b) and using hyperbolic trigonometric identities, which gives

$$L(t) = 2 \operatorname{arcsinh} \left(\sqrt{\frac{r_B}{r_{\text{BH}}} - 1} \cosh \frac{r_{\text{BH}} t}{2} \right). \quad (\text{B.10})$$

This indeed agrees with Krylov spread complexity in (3.53), where time includes the corresponding redshift factor. The geodesic length at finite cutoff has been previously noticed for the spacelike case in e.g. [42, 157].

C Sine Dilaton Gravity at Finite Cutoff

In this appendix, we explore the putative duality between the deformation of the DSSYK model and sine dilaton gravity at the disk topology level from finite cutoff holography. We are interested in the reality properties of the theory. Recent progress relating sine dilaton gravity and the DSSYK chord model can be found in [66, 71, 82, 92, 109, 113, 283] among others.

Sine dilaton gravity (in Euclidean-like signature) is described by (2.1) where the dilaton potential takes the form

$$U(\Phi) = 2 \sin \Phi. \quad (\text{C.1})$$

Since the metric and the dilaton in this model are complex-valued, the holographic dictionary implies that the deformation parameter in the deformed DSSYK model can be complex. Thus, we are particularly interested in the conditions for the energy spectrum of the deformed theory to be real, and its corresponding interpretation in the Lorentzian signature bulk spacetime. We also search for locations in the complex plane where the model has positive and near constant curvature, corresponding to first implementing the deformation and then taking the UV triple-scaling limit of the DSSYK model, which we applied in previous sections.

Reality Conditions One might be concerned that the Euclidean path integral of the theory might not converge when the energy spectrum is generically complex-valued. For instance, consider the partition

$$\int dE e^{S(E) - \beta E_y}, \quad (\text{C.2})$$

where $S(\theta) = S_0 - \frac{(\pi - 2\theta)^2}{\lambda}$ [191], S_0 is a constant; and $E(\theta)$ appears in (3.14). In principle, due to the complex spectrum (C.2) could diverge along the flow. After all, this what happens for instance in JT gravity (and other set-ups) when the finite cutoff reaches the black hole horizon in the bulk, where instanton effects need to be taken into account [37]. However, the model that we study is UV finite, and (C.2) is well-defined even when the exponent of the integral is complex.⁴⁰

⁴⁰If the Hamiltonian has a complex-valued spectrum, one needs to include its left and right-eigenstates, in contrast to the past sections where we considered the eigenbasis for a Hermitian Hamiltonian.

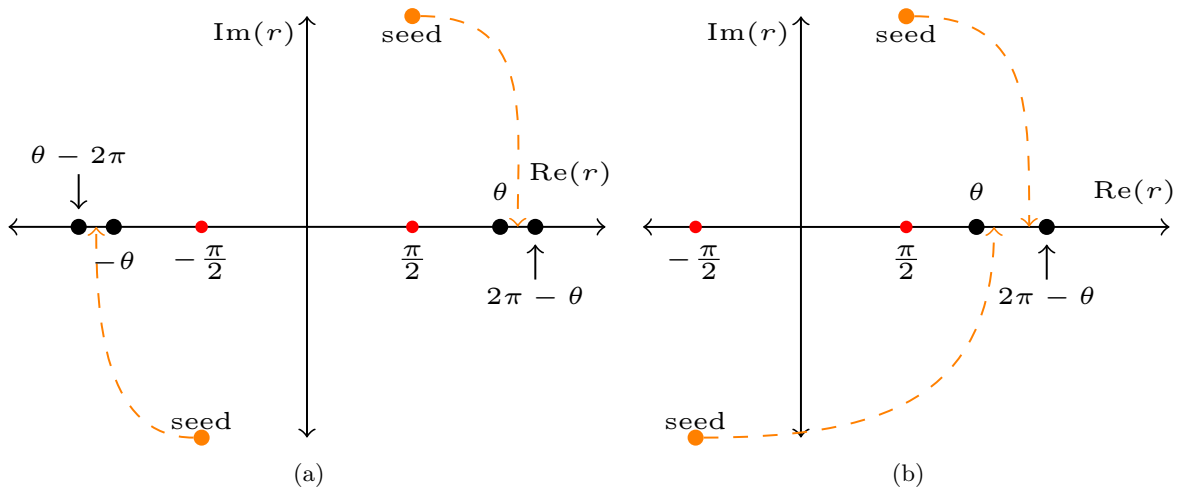


Figure 8. Moving the boundaries in the complex r -plane by T^2 deforming the DSSYK model according to the dictionary entry (2.17). The seed DSSYK model is initially located at $r \rightarrow \pm(\frac{\pi}{2} + i\infty)$, and it can be moved in the indicated contours (dashed orange lines) close to the horizons at (a) $r = \pm\theta$, and (b) $r = \theta, 2\pi - \theta$. Both ways can be used to probe the positive curvature regions between the black hole and cosmological horizons when $\theta \simeq \pi$ (see the respective Penrose diagrams in Fig. 10).

For the above reasons, we now analyze the constraints to recover a unitary energy spectrum (2.20) by considering that the radial bulk flow is described by the HJ equation (2.11). A diagram of the paths generating these flows is shown in Fig. 8,⁴¹ where we choose as the final radial location for the boundary theories to be the black hole and cosmological stretched horizon in (C.10), and (C.11). To be more explicit about the trajectory, one can, for instance, use

$$\Phi_B = \pm \left(\frac{\pi}{2} + i \log(v + i \cos r_B) \right), \quad (\text{C.3})$$

to connect $r = \frac{\pi}{2} + i\infty$ (the asymptotic boundary) with $r = r_B$. Meanwhile, the trajectory from the black hole horizon at $r = \theta$ and the boundary location $r = r_B$ can be expressed by

$$r = \theta\chi + (1 - \chi)r_B, \quad \chi \in [0, 1]. \quad (\text{C.4})$$

Here χ is a parametrization that allows us to interpolate between the location of the cosmological horizon (i.e. $\chi = 1$ in $r_B(\theta)$) and black hole horizon (i.e. $\chi = 0$ in $r_B(\theta)$)⁴² in $r \in [-2\pi, 2\pi]$.

⁴¹As mentioned in Sec. 1, this is not the only possible way to place the seed theories; for instance, one could consider placing the boundaries in between the black hole region; or between several black hole and cosmological patches (similar to [166] in the extended SdS spacetime). Given that our focus is to probe the positive curvature region between the black hole and cosmological horizons, we leave these other possibilities for future directions (Sec. 7.1).

⁴² $\chi = 0$ implies $r_{B_1}^{(1)} = -\theta$, which is a 2π displacement (also referred to as a duplicate in [92]) of the cosmological horizon at $r = 2\pi - \theta$, so we will attribute it as a cosmological horizon as well.

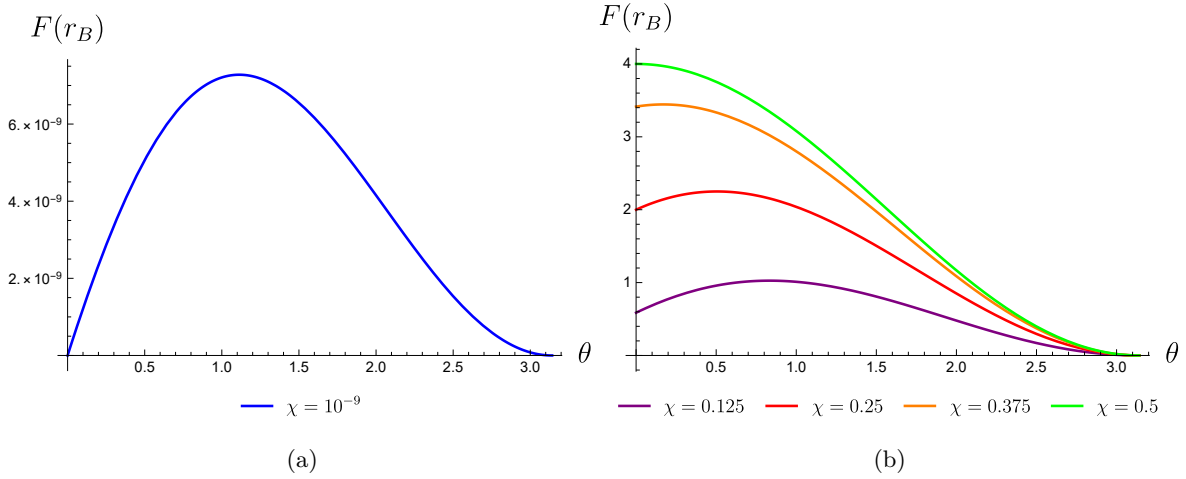


Figure 9. Evaluation of the blackening factor (C.5) at the stretched horizon defined in (C.10) in terms of the parameter χ (for the different values shown in the legend). It remains positive $\forall \theta \in [0, \pi]$.

As we flow the boundary theory from $r_B \rightarrow \pm(\frac{\pi}{2} + i\infty)$ to a generic location $r_B \in \mathbb{C}$ in Fig. 8, the energy spectrum (2.21) becomes complex; however, one should notice that the metric (2.31) is also complex along this flow, and there is no Lorentzian interpretation where we could associate the complex energy spectrum, e.g. a dissipation process.⁴³ Once we reach the real line, we must study the locations where we can have a thermodynamic description of the system. First, notice that if we use the parametrization of the stretched horizon in (C.10) as the location of the boundary, we need to account for the functional dependence of $r_B(\theta)$. We can see that the blackening factor

$$F(r_B) = 2(\cos \theta - \cos(\theta + 2\chi(\pi - \theta))) , \quad (\text{C.5})$$

remains positive for $\chi \in [0, 1]$ and $\theta \in [0, \pi]$, as shown in Fig. 9.

In what follows, we search the reality constraints for unitary evolution in (2.20), meaning that

$$1 \geq 2yE(\theta) . \quad (\text{C.6})$$

For concreteness, consider $\pi/2 \leq \theta \leq \pi$ so $E(\theta) \geq 0$. We identify different possibilities for the location r_B given the condition (C.6), as we list below.

- When $y > 0$,

$$\theta < r_B . \quad (\text{C.7})$$

⁴³In higher dimensions, a non-unitary energy spectrum with T^2 deformations has been studied in *Cauchy slice holography* [180, 181, 309]. The interpretation is that if one deforms a CFT living on the boundary of a Euclidean Cauchy slice, its energy spectrum is inherently complex. Once the deformation is large enough, the extrinsic curvature $K_{\alpha\beta}$ becomes timelike, resulting in a real energy spectrum, corresponding to a Lorentzian signature in the bulk.

However, in this case, the blackening factor in the metric (C.5) is $F(r_B) < 0$, so that r is a timelike coordinate and τ spacelike. Thus, the quantity (2.20) would be related to a conserved momentum instead of the energy spectrum of the system. One might attempt a double Wick rotation in $\tau \rightarrow it$ and $r \rightarrow i\tilde{r}$, but in that case, $F(r_B) \in \mathbb{C}$. For this reason, we will not consider this case. Notice that if we take $r_B = \pi + ir_0$ with $r_0 \in \mathbb{R}$, we will face a similar problem.

- When $y \leq 0$, there are no restrictions, and $F(r_B) > 0$. We can then perform the Wick rotation $\tau \rightarrow it$ in the metric (2.31) so that $E_y(\theta)$ in (2.20) along the real line indeed can be interpreted as conserved energy.

To draw the Penrose diagram, we consider the timelike Eddington–Finkelstein coordinates:

$$v = t + r^*(r), \quad u = t - r^*(r),$$

$$r^*(r) = \int_{r_0}^r \frac{dr'}{F(r')} = \frac{1}{2 \sin \theta} \log \left| \frac{\sin \frac{\theta-r}{2}}{\sin \frac{\theta+r}{2}} \right|, \quad (\text{C.8})$$

where $r^*(r)$ is the tortoise coordinate, and we have chosen r_0 such that $r^*(r=0) = 0$. We then define Kruskal coordinates

$$U = e^u, \quad V = -e^{-v}, \quad (\text{C.9})$$

for the first quadrant of the Penrose diagram, Fig. 10, while $U = e^u, V = e^{-v}$ in the second; $U = -e^u, V = e^{-v}$ third; and $U = -e^u, V = -e^{-v}$ fourth. At last, we define compact coordinates $U = \tan \tilde{U}$ and $V = \tan \tilde{V}$ to generate the Penrose diagram. Notice that the location of the horizons is $UV = 0$, and the periodic nature of the diagram shares similarities with the (extended) full-reduction dS₂ spacetime (see e.g. [310–312]).

Probing the Bulk Interior We now probe the positive curvature region in Fig. 10 (and (8)) using two configurations for the *cosmological* and *black hole* stretched horizons where we move the boundaries into the locations:⁴⁴

$$r_{B_1}^{(1)} = r_B(-\theta), \quad r_{B_2}^{(1)} = r_B(\theta), \quad \text{where } r_B(\theta) = (1 - \chi)\theta + \chi(\theta - 2\pi), \quad (\text{C.10})$$

$$r_{B_1}^{(2)} = r_B(\theta), \quad r_{B_2}^{(2)} = r_B(2\pi - \theta). \quad (\text{C.11})$$

As seen from Fig. 10, by setting the boundary locations to be $r_B = r_{B_1}^{(1)}, r_B = r_{B_2}^{(1)}$ in (C.10), the deformed DSSYK model can be located at a very close distance with respect to the cosmological ($\chi \ll 1$) or black hole ($\chi \simeq 1$), where the bulk thermodynamics with respect to the boundary locations can be associated with the respective black hole or cosmological horizon.

⁴⁴A similar definition as (C.10) was first proposed in [166] in the context of the extended Schwarzschild-de Sitter (SdS) black hole geometries. It allows us to generalize the notion of the stretched horizon in [1] for pure dS space to spacetimes with multiple horizons.

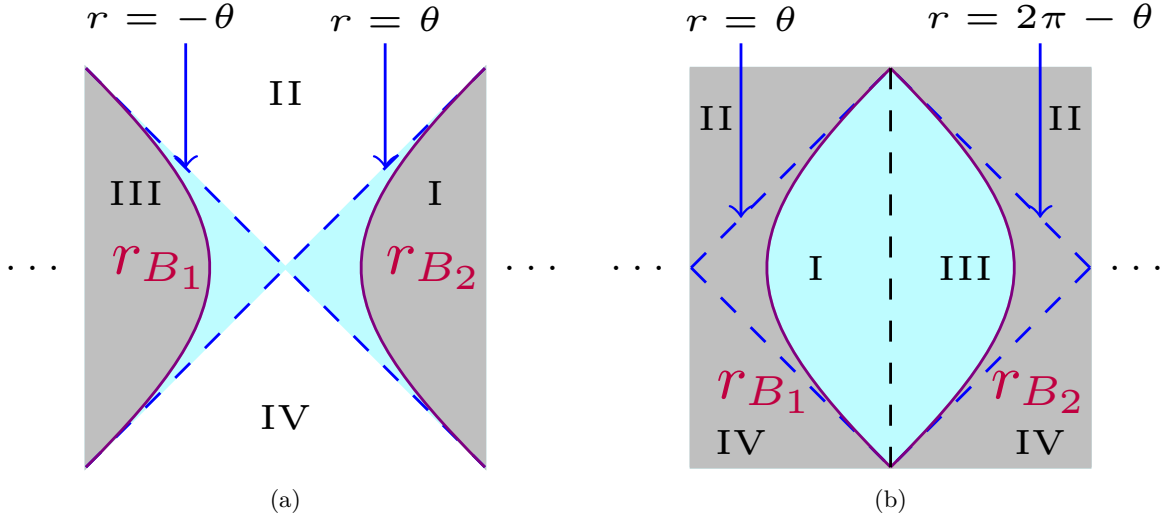


Figure 10. Penrose diagram in the \tilde{U}, \tilde{V} coordinates below (C.9) for all the quadrants (Roman numerals). The energy spectrum of the dual T^2 deformed dual DSSYK models (3.14) have a relative (a) $-$, and (b) $+$ sign. We have placed the Dirichlet boundaries (purple) in (a) (C.10), and (b) (C.11), corresponding to the respective bulk radial flow paths. The gray region represents the part of the bulk that has been cut out in the bulk interpretation of the T^2 deformation, and the light blue area between the stretched horizon and the black hole and cosmological horizons (dashed blue lines) represents the bulk positive curvature region (for $\theta \simeq \pi$). The dashed black line in (b) only serves to separate the respective quadrants, and the dots indicate the $2n\pi$ periodicity of the spacetime.

By taking $\theta \simeq \pi$, the region $r \in [-2\pi + \theta, -\theta] \cup [\theta, 2\pi - \theta]$ has a positive and near constant scalar curvature $\mathcal{R} \simeq 2$ [66]. This is equivalent to implementing the UV triple-scaling limit after performing the $T^2(+\Lambda_1)$ deformation in the DSSYK model, which we applied in previous sections, albeit without assuming the correspondence between sine dilaton gravity and the DSSYK model. The procedure in this section allows us to be more explicitly explore the structure of the finite cutoff holography with a concrete bulk dual for the range of its energy spectrum of the DSSYK model.

D An Alternative Chord Number Basis

In this appendix, we define a new chord number basis, an alternative to the Krylov basis (3.33) in the deformed DSSYK model, which is motivated by finite cutoff holography. Concretely, consider

$$|n\rangle_y \equiv g_n \left(\frac{\sqrt{\lambda(1-q)} \hat{H}}{-J} \right) |\Omega\rangle, \quad (\text{D.1})$$

where \hat{H} is the zero-particle chord Hamiltonian of the seed theory (3.9) and $g_n(x)$ is a polynomial function defined recursively

$$x g_n(x) = g_{n+1}(x) + \left(1 - R(y)^2 \operatorname{sech}^2 \frac{\lambda n}{2}\right) g_{n-1}(x) , \quad (\text{D.2})$$

with $R(y)$ a constant dependent on the deformation parameter y , and we impose as initial conditions,⁴⁵

$$g_0(x) = 1 , \quad g_{-1}(x) = 0 . \quad (\text{D.4})$$

There is a map between the different chord basis, given by

$$|n\rangle_y = g_n(\hat{h}) |\Omega\rangle = \sum_{m=0}^{\infty} a_{nm} |m\rangle , \quad (\text{D.5})$$

where

$$a_{nm} \equiv \langle m | n \rangle_y = \int_0^\pi d\theta \mu(\theta) g_n(2 \cos \theta) \frac{H_n(\cos \theta | q)}{\sqrt{(q; q)_n}} . \quad (\text{D.6})$$

The explicit holographic dictionary between the arbitrary parameter $R(y)$ and the bulk radial cutoff will be determined below. Using the basis (D.1), the seed theory Hamiltonian is then expressed as,⁴⁶

$$\hat{H} = \frac{-J}{\sqrt{\lambda(1-q)}} \left(2 \cos \hat{P}_y - R(y)^2 e^{i\hat{P}_y} \operatorname{sech}^2 \frac{\lambda \hat{n}_y}{2} \right) , \quad (\text{D.8})$$

where

$$e^{\mp i \hat{P}_y} |n\rangle_y \equiv |n \pm 1\rangle_y , \quad \hat{n}_y |n\rangle_y \equiv n |n\rangle_y . \quad (\text{D.9})$$

The resulting representation for the chord Hamiltonian (D.8) relates to recent findings by [42], since, as seen below, the triple-scaling limit of the chord Hamiltonian recovers the canonically quantized JT gravity ADM Hamiltonian [42]. However, we emphasize that the chord Hamiltonian representation (D.8) only connects with finite cutoff holography once we study the deformed Hamiltonian \hat{H}_y (3.29), either with the chord number basis $|n\rangle_y$ or a different one.⁴⁷ In contrast, the construction of the Krylov basis for the deformed DSSYK in Sec. 3.2 does not incorporate auxiliary parameters associated to a spacetime foliation in the bulk, and indeed the Krylov spread complexity of the HH state reproduces the minimal geodesic length

⁴⁵For instance:

$$g_1(x) = R(y)^2 \operatorname{sech}^2 \left(\frac{\lambda}{2}\right) x , \quad (\text{D.3})$$

and the higher-order polynomials, $g_{n \geq 2}$, follow iteratively.

⁴⁶Note that by imposing

$$\lim_{y \rightarrow 0} \frac{\cosh(L_y/2)}{R(y)} = e^{L/2}/2 , \quad (\text{D.7})$$

one recovers the corresponding chord Hamiltonian in the appropriate limit after a canonical transformation [72]. Importantly, (D.8) remains as a Hermitian Hamiltonian with respect to the chord inner product [73, 74].

⁴⁷We expect that the choice of chord number basis $|n\rangle_y$ corresponds to the foliation in terms of the auxiliary parameter y in the bulk dual, such that the regularized geodesic length between the asymptotic boundaries for chosen foliation reproduces the minimal length geodesic length connecting finite boundaries. We will explore this interpretation in upcoming work.

at finite cutoff (3.53). As we will see in the semiclassical analysis of the next subsection, the chord number in the $|n\rangle_y$ basis is related to an Einstein-Rosen bridge connecting the boundaries of an AdS₂ black hole with a finite radial cutoff with Dirichlet boundary conditions [42] (7.5) (see also App. B).

Outline We investigate the path integral of the theory in App. D.1 and we evaluate the expectation value of the chord number, which reproduces the wormhole length in the bulk. In App. D.2 we study the triple scaling limits of the chord Hamiltonian, and we show it reproduces the canonically quantized ADM Hamiltonian of JT gravity at a finite cutoff in a different ensemble with respect to the one found in the main text. At last, App. D.3 contains an evaluation of algebraic entanglement entropy (5.6) using the chord number basis $|n\rangle_y$ which, in the IR/UV triple-scaling reproduces the dilaton in JT and dS JT gravity in the bulk dual, respectively.

D.1 Path Integral Formulation

We study the path integral of the deformed DSSYK chord theory using the representation (D.8), which is

$$Z = \int [dL_y][dP_y] \exp \left[\int d\tau \left[\frac{i}{\lambda} P_y \partial_\tau L_y - H_y \right] \right], \quad (\text{D.10a})$$

$$H_y = f_y \left(\frac{J}{\lambda} \left(2 \cos P_y - \frac{R(y)^2 e^{iP_y}}{\cosh^2 \frac{L_y}{2}} \right) \right). \quad (\text{D.10b})$$

where $\tau \equiv \frac{\beta}{2} + it$. Here, we represent L_y as the semiclassical expectation value of the chord number in the deformed HH state $e^{-\tau \hat{H}_y} |\Omega\rangle$, namely

$$L_y \equiv \lambda \frac{\langle \Omega | e^{-\tau^* \hat{H}_y} \hat{\Pi}_y e^{-\tau \hat{H}_y} | \Omega \rangle}{\langle \Omega | e^{-\beta \hat{H}_y} | \Omega \rangle}, \quad (\text{D.11})$$

and P_y is the corresponding conjugate momenta. The saddle point solutions of (D.10a) are then

$$\frac{1}{\lambda} \frac{dL_y}{dt} = \frac{\partial H_y}{\partial P_y} = f'_y(H) \frac{\partial H}{\partial P_y}, \quad (\text{D.12a})$$

$$\frac{1}{\lambda} \frac{dP_y}{dt} = -\frac{\partial H_y}{\partial L_y} = -f'_y(H) \frac{\partial H}{\partial L_y}. \quad (\text{D.12b})$$

Note that we have used the chain rule. Using the explicit form in (D.8) we recover

$$\frac{dL_y}{dt_y} = 2i(\cos \theta - e^{iP_y}), \quad (\text{D.13a})$$

$$-i \frac{de^{-iP_y}}{dt_y} = R(y)^2 \operatorname{sech}^2 \left(\frac{L_y}{2} \right) \tanh \left(\frac{L_y}{2} \right), \quad (\text{D.13b})$$

where

$$t_y \equiv J f'_y(H) t . \quad (\text{D.14})$$

In particular for T^2 deformations (3.30) we have that the redshift factor is $f'_y(H) = 1/\sqrt{1 - 2yH}$, and for $T^2 + \Lambda_1$ $f'_y(H) = 1/\sqrt{2yH - 1}$.

The differential equations in (D.13) are supplemented by boundary conditions

$$L_y(0) \equiv L_0 , \quad L'_y(0) = 0 , \quad (\text{D.15})$$

Meanwhile, L_0 in (D.15) is a numerical constant determined from initial conditions and conservation of energy. Namely, consider (D.13a) and the second initial condition in (D.15) for $t = 0$ implies

$$\left. \frac{dL_y}{dt_y} \right|_{t_y=0} = 0 , \quad e^{iP_y(0)} = \cos \theta . \quad (\text{D.16})$$

Then, by introducing (D.16) and the first initial condition in (D.15) to (D.10b), it follows that

$$R(y)^2 \operatorname{sech}^2 \frac{L_0}{2} = \sin^2 \theta . \quad (\text{D.17})$$

Combining them, we recover

$$\frac{d^2 L_y}{dt_y^2} = 2R(y)^2 \tanh\left(\frac{L_y}{2}\right) \operatorname{sech}^2\left(\frac{L_y}{2}\right) . \quad (\text{D.18})$$

The solution to the above ordinary differential equation subject to the boundary conditions (D.15) is

$$L_y = 2 \operatorname{arcsinh} \left(\sqrt{\frac{R(y)^2}{\sin^2 \theta} - 1} \cosh(t_y \sin \theta) \right) , \quad (\text{D.19})$$

which is precisely the spacelike geodesic length between the finite cutoff boundaries of AdS_2 black holes [42, 157] with a black hole horizon at $\rho = \sin \theta$ in the coordinates

$$ds_{\text{eff}}^2 = (\rho^2 - \sin^2 \theta) d\tau^2 + \frac{d\rho^2}{\rho^2 - \sin^2 \theta} . \quad (\text{D.20})$$

In fact, we show that (D.19) is also valid to describe timelike geodesics connecting finite cutoff boundaries inside the AdS_2 black hole (D.20), see App. B.

In the AdS_2 interpretation, $\rho = R(y)$ (D.19) corresponds to the radial cutoff parameter in the effective AdS_2 metric. Thus, while the original chord Hamiltonian in canonical variables measure lengths/momenta with respect to the boundaries [58], we can implement the

canonical transformation in the Hamiltonian (D.8) to the new chord basis (D.1) to describe the deformed theory.⁴⁸

T^2 vs $T^2 + \Lambda_1$ Deformations Note that in the derivation of the semiclassical chord number (D.19) we have made no assumptions about the explicit form of f_y ; the expression is valid for both general deformations in finite cutoff holography. In particular, the difference between T^2 and $T^2 + \Lambda_1$ deformation is contained in the factor t_y (D.14) which depends on the explicit form of the deformation. Also, from the bulk perspective, we will be interested in the cases where $R(y) \geq \sin \theta$ for the T^2 case, and $R(y) \leq \sin \theta$ for $T^2 + \Lambda_1$, resulting real-valued and pure imaginary lengths.

D.2 IR/UV Triple-Scaling Limits and $T^2(+\Lambda_1)$ Deformations

To examine more closely the chord number in the $|n\rangle_y$ basis, we now define the IR/UV triple-scaling limit to further examine its properties:

$$\text{IR : } \quad \text{sech}^2 \frac{\lambda \hat{n}_y}{2} \rightarrow \lambda^2 \text{sech}^2 \frac{\hat{L}_{\text{IR}}}{2}, \quad \hat{P}_y \rightarrow \lambda \hat{P}_{\text{IR}}, \quad (\text{D.23a})$$

$$\text{UV : } \quad \text{sech}^2 \frac{\lambda \hat{n}_y}{2} \rightarrow \lambda^2 \text{sech}^2 \frac{i \hat{L}_{\text{UV}}}{2}, \quad \hat{P}_y \rightarrow \pi - i \lambda \hat{P}_{\text{UV}}, \quad (\text{D.23b})$$

where the eigenvalues of the operators \hat{L}_{IR} , \hat{P}_{IR} and \hat{L}_{UV} , \hat{P}_{UV} are fixed as $\lambda \rightarrow 0$.

We note that by subtracting the zero-energy contribution in the IR and UV limits of the chord Hamiltonian in the $|n\rangle_y$ basis (D.8) and considering leading order terms, we recover

$$\hat{H}_{\text{IR}} \equiv \frac{1}{2J\lambda} \left(\hat{H} + \frac{2J}{\sqrt{\lambda(1-q)}} \right) \Big|_{\mathcal{O}(1), \text{IR}} = \frac{\hat{P}_{\text{IR}}^2}{2} + \frac{R(y)^2}{2} \text{sech}^2 \frac{\hat{L}_{\text{IR}}}{2}, \quad (\text{D.24a})$$

$$\hat{H}_{\text{UV}} \equiv \frac{1}{2J\lambda} \left(\hat{H} - \frac{2J}{\sqrt{\lambda(1-q)}} \right) \Big|_{\mathcal{O}(1), \text{UV}} = -\frac{\hat{P}_{\text{UV}}^2}{2} + \frac{R(y)^2}{2} \text{sec}^2 \frac{\hat{L}_{\text{UV}}}{2}. \quad (\text{D.24b})$$

\hat{H}_{IR} is isomorphic to the canonically quantized JT gravity Hamiltonian at finite cutoff in [42] (\hat{H}_{IR}) in terms of the finite cutoff length and its canonical conjugate, and \hat{H}_{UV} is its dS_2 counterpart, which is the boundary operator dual to the generator of spatial translations along \mathcal{I}^\pm in dS JT gravity [82, 99], as a s-wave dimensional reduction of dS_3 space [82]. Note that both are manifestly Hermitian, since the spectrum of \hat{L}_{UV} is pure imaginary.

⁴⁸For example, in the specific case of the sine dilaton gravity proposal [92], the map between the AdS_2 black hole metric (D.20) to the geometry where we identified $y = 2\lambda/G(r_B)$ based on (2.17) and (2.36) is given by

$$r_B = \frac{\pi}{2} + i \log(R(y) + i \cos \theta), \quad y = \frac{-\lambda}{\cos(r_B)}, \quad (\text{D.21})$$

where we are using $G(x) = -2 \cos(x)$ (2.3) for sine dilaton gravity. The above relation means that

$$\frac{\lambda}{y} = \frac{i}{2} \left(R(y) + i \cos \theta - \frac{1}{R(y) + i \cos \theta} \right), \quad (\text{D.22})$$

if the DSSYK model were dual to sine dilaton gravity at the disk level.

Importantly, the need of the λ^2 factor in (D.23) signals that in the triple-scaling limit one is defining a two-sided geodesic length between the asymptotic boundaries. In contrast, as we found in Sec. 3.2, one does not need to implement a regularization in the canonical variables describing a finite cutoff geodesic length. In a similar way, the triple-scaling limit describing geodesic lengths connecting one asymptotic boundary to a matter particle or specifically an ETW brane, one requires introducing a regularized geodesic length with a λ^1 factor [59, 60, 74, 313] in contrast to the λ^2 factor in the two-sided case.

In either of the IR/UV limits, we can consider the sequence of a T^2 deformation and $T^2 + \Lambda_1$ deformation once the cutoff boundary reaches the corresponding AdS₂ black hole and dS₂ cosmological horizons (3.28a), namely

$$\hat{H}_{\text{IR/UV},y} = \begin{cases} \frac{1}{y} \left(1 - \sqrt{1 - 2y \hat{H}_{\text{IR/UV}}} \right) & 0 \leq y \leq y_0, \\ \frac{1}{y} \left(1 + \sqrt{2y \hat{H}_{\text{IR/UV}} - 1} \right) & y \geq y_0, \end{cases} \quad (\text{D.25})$$

We represent the energy spectrum introducing the parameters $\theta_{\text{IR}} \equiv \theta \ll 1$ and $\theta_{\text{UV}} \equiv \pi - \theta \ll 1$ in the corresponding triple-scaling limits, so that the deformed energy spectrum becomes

$$E_{\text{IR/UV},y} = \begin{cases} \frac{1}{y} \left(1 - \sqrt{1 - y \theta_{\text{IR/UV}}^2} \right), & 0 \leq y \leq y_0, \\ \frac{1}{y} \left(1 + \sqrt{y \theta_{\text{IR/UV}}^2 - 1} \right), & y \geq y_0, \end{cases} \quad (\text{D.26})$$

where y_0 appears in (3.57).

Chord Number We also define the expectation value of the IR and UV length operators in (D.23) in the deformed HH state $e^{-\tau \hat{H}_y} |\Omega\rangle$ ($\tau = \beta/2 + it$) as

$$L_{\text{IR}}(t) \equiv \frac{\langle \Omega | e^{-\tau^* \hat{H}_y} \hat{L}_{\text{IR}} e^{-\tau \hat{H}_y} | \Omega \rangle}{\langle \Omega | e^{-\beta \hat{H}_y} | \Omega \rangle}, \quad L_{\text{UV}}(t) \equiv \frac{\langle \Omega | e^{-\tau^* \hat{H}_y} \hat{L}_{\text{UV}} e^{-\tau \hat{H}_y} | \Omega \rangle}{\langle \Omega | e^{-\beta \hat{H}_y} | \Omega \rangle}, \quad (\text{D.27})$$

which can be seen as the UV and IR limits of expectation value of the chord number in the $|n\rangle_y$ basis in (D.19). To carry out their evaluation, we use the explicit solution for the wormhole length L_y in (D.19) with $R(y)$ identified as the boundary cutoff an AdS₂ black hole metric (D.20) in the IR and UV triple-scaling limits (D.23), which describe JT ($U(\Phi) = 2\Phi$) and dS JT gravity ($U(\Phi) = -2\Phi$) respectively. Using the counterterm $G(\Phi_B)$ (2.3) (corresponding to $\eta = +1$) and the deformation parameter y through (2.17) we have that

$$\eta = +1 : \quad \text{IR} : y = R(y)^{-2}, \quad \text{UV} : y = -R(y)^{-2}. \quad (\text{D.28})$$

Meanwhile, for $T^2 + \Lambda_1$ deformations, we invert the sign of $G(\Phi_B)$ in both the IR and UV cases (2.23), resulting in

$$\eta = -1 : \quad \text{IR} : y = -R(y)^{-2}, \quad \text{UV} : y = R(y)^{-2}. \quad (\text{D.29})$$

It follows that the wormhole length (D.19) in each of the corresponding triple-scaling limits (D.27) becomes⁴⁹

$$L_{\text{IR}}(t) = \begin{cases} 2\text{arcsinh}\left(\sqrt{\frac{1}{y\theta_{\text{IR}}^2} - 1} \cosh\left(\frac{J\theta_{\text{IR}}t}{\sqrt{1-y\theta_{\text{IR}}^2}}\right)\right), & 0 \leq y \leq y_0, \\ 2i \arcsin\left(\sqrt{1 - \frac{1}{y\theta_{\text{IR}}^2}} \cosh\left(\frac{J\theta_{\text{IR}}t}{\sqrt{y\theta_{\text{IR}}^2-1}}\right)\right), & y \geq y_0, \end{cases} \quad (\text{D.30a})$$

$$L_{\text{UV}}(t) = \begin{cases} 2i \text{arcsinh}\left(\sqrt{\frac{1}{y\theta_{\text{UV}}^2} - 1} \cosh\left(\frac{J\theta_{\text{UV}}t}{\sqrt{1-y\theta_{\text{UV}}^2}}\right)\right), & 0 \leq y \leq y_0, \\ 2\text{arcsin}\left(\sqrt{1 - \frac{1}{y\theta_{\text{UV}}^2}} \cosh\left(\frac{J\theta_{\text{UV}}t}{\sqrt{y\theta_{\text{UV}}^2-1}}\right)\right), & y \geq y_0. \end{cases} \quad (\text{D.30b})$$

Note that L_{IR} and L_{UV} are real and pure imaginary respectively for the T^2 deformation, and they exchange to pure imaginary and real for the $T^2 + \Lambda_1$ flow. The results show that the rescaled chord number in the IR triple-scaling limit L_{IR} grows eternally in the $\eta = +1$ case, while in the $\eta = -1$, there is a finite growth in terms of the t parametrization. In both cases, the deformation parameter y modifies the rate of growth of L_{IR} . This reflects that the Tolman temperature in the bulk is the thermal scale accompanying t . In the $\eta = +1$ case as we approach $y \rightarrow y_0$ the rate of growth increases since the cutoff surface approaches the black hole horizon, increasing the Tolman temperature. Meanwhile, in the $\eta = -1$ case, corresponding to the interior of the black hole in the AdS₂ description, the imaginary value of L_{IR} can be interpreted in terms of the growth of the timelike geodesics. Note the growth of L_{IR} stops when the argument in arcsin of (D.30a) is greater than 1 (which we discuss further in Sec. 6.2). This signals that the geodesics in the bulk dual reach $r \rightarrow \infty$ in Rindler-AdS₂ space, as this corresponds to the maximum value of the renormalized length in the AdS₂ description in Fig. (3). Similar findings occur in dS₂ space, as discussed in Sec. 6.3.

Next, one sees that $L_{\text{IR/UV}}$ (D.30) takes the same form as ℓ_y (3.53), with a rescaling in the time parameter

$$\frac{J\theta_{\text{IR/UV}}t}{\sqrt{1-y\theta_{\text{IR/UV}}^2}} \rightarrow \frac{\theta_{\text{IR/UV}}\tilde{t}}{2}, \quad (\text{D.31})$$

where the different time parametrizations have been interpreted in the JT gravity case in terms of different ensembles in [42]. Similar to our analysis, the left-hand side in (D.31) corresponds to a microcanonical ensemble incorporating the redshift factor due to the fixed energy (4.21), while the right-hand side to a canonical ensemble, where the redshift factor is not present in the Krylov complexity growth. Thus, if one instead evaluates Krylov spread complexity in the microcanonical ensemble, then one needs to incorporate the redshift factor in the rescaled time.

D.3 Algebraic Entanglement Entropy

In this subappendix, we show that the entanglement entropy between the double-scaled algebras (5.6) for the chord number state $|n\rangle_y$ leads to the same result as using the Krylov basis

⁴⁹Note that in (D.30b) we are using the fact that the conformal transformation between Rindler-AdS₂ (D.20) and static patch coordinates is given by a $-$ sign, instead applying the map in sine dilaton gravity of (D.22).

in the deformed DSSYK model in the triple-scaling limit. Thus, our starting point is

$$|\Psi\rangle = |n\rangle_y = g_n(\hat{h}) |\Omega\rangle, \quad \hat{\rho} = g_n(\hat{h})^2, \quad (\text{D.32})$$

where g_n appears in (D.2).

From the general expression for algebraic entanglement entropy (5.6), we get

$$S(L) \equiv - \int_0^\pi d\theta \mu(\theta) \frac{g_n(2 \cos \theta)^2}{\langle \Psi | \Psi \rangle} \log \frac{g_n(2 \cos \theta)^2}{\langle \Psi | \Psi \rangle}, \quad (\text{D.33})$$

where the energy measure appears in (3.18).

For analytic progress, we study the triple-scaling limit of $S(L)$; see [98] for similar considerations, and [99].⁵⁰ For concreteness, we focus on the IR triple-scaling limit (D.23); very similar arguments can be implemented for the UV limit, which we discuss in Sec. 6.4.

To study the IR triple-scaling limit of the different terms in (D.33), let us first find solutions to the inner product $\langle k | L \rangle$, where $|L\rangle$ represents the eigenstates of \hat{L}_{IR} , and $|k\rangle \equiv |\theta = \lambda k\rangle$ the eigenstates of \hat{H}_{IR} , i.e.

$$\hat{L}_{\text{IR}} |L\rangle = L_{\text{IR}} |L\rangle, \quad \hat{H}_{\text{IR}} |k\rangle = \frac{k^2}{2} |k\rangle, \quad (\text{D.34})$$

Plugging these states in the corresponding Hamiltonian in (D.24),

$$\langle k | \hat{H}_{\text{IR}} |L\rangle = \left(\frac{-1}{2} \partial_{L_{\text{IR}}}^2 + \frac{R(y)^2}{2} \text{sech}^2 \frac{L_{\text{IR}}}{2} \right) \langle k | L \rangle = \frac{k^2}{2} \langle k | L \rangle, \quad (\text{D.35})$$

where we used $\hat{P}_{\text{IR}} = -i\partial_{L_{\text{IR}}}$, and $\theta \equiv k\lambda$ in the IR triple-scaling limit (D.23), so that (D.35) can be seen as a Schrödinger equation. The solutions are associated Legendre functions of first ($P_\nu^\mu(x)$) and second ($Q_\nu^\mu(x)$) kind,

$$\langle k | L \rangle = c_1 P_{\frac{1}{2}(\sqrt{1-16R(y)^2}-1)}^{2ik} \left(\tanh \left(\frac{L_{\text{IR}}}{2} \right) \right) + c_2 Q_{\frac{1}{2}(\sqrt{1-16R(y)^2}-1)}^{2ik} \left(\tanh \left(\frac{L_{\text{IR}}}{2} \right) \right), \quad (\text{D.36})$$

where c_1 and c_2 are constants. We are interested in solutions that are square integrable, so we keep $c_2 = 0$ and take c_1 such that

$$c_1 = \left(\int_0^\infty dk \rho(k) \left| P_{\frac{1}{2}(\sqrt{1-16R(y)^2}-1)}^{2ik} \left(\tanh \left(\frac{L_{\text{IR}}}{2} \right) \right) \right|^2 \right)^{-1/2}, \quad (\text{D.37})$$

where $\rho(k)$ is the density of states of JT gravity

$$\rho(k) \equiv 4k \sin(2\pi k). \quad (\text{D.38})$$

Then, (D.33) becomes

$$S \xrightarrow{\text{IR}} -\lambda \int_0^\infty dk p(L_{\text{IR}}, k) \log \frac{p(L_{\text{IR}}, k)}{\mu(\theta \equiv \lambda k)}. \quad (\text{D.39})$$

⁵⁰We expect that the evaluation in the $\lambda \rightarrow 0$ limit leads to a RT formula in sine dilaton gravity at finite cutoff, which has not been addressed even in the seed theory case.

where we use that

$$\mu(\theta \equiv \lambda k) \xrightarrow{IR} \frac{\lambda^{1/2}}{\sqrt{2\pi}} e^{-\frac{\pi^2}{2\lambda}} (\rho(k) + \mathcal{O}(\lambda)) , \quad (\text{D.40a})$$

$$\mu(\theta) \frac{g_n(2 \cos \theta)^2}{\langle \Psi | \Psi \rangle} \xrightarrow{IR} p(L_{IR}, k) . \quad (\text{D.40b})$$

Here, (D.40a) is known in [58], and (D.40b) follows the fact that $\langle \theta | n \rangle_y$ satisfies the recurrence relation (D.2) where $x = -\lambda E(\theta)/(2J)$, while $\langle k | L \rangle$ satisfies the IR triple-scaled version of the same equation, namely (D.35).

To make more analytic progress, we apply the WKB approximation, where we look for semiclassical solutions to the Schrödinger equation (D.35). We consider energy scales away from the one where the kinetic energy vanishes, meaning $\hat{P}_{IR}^2 = 0$ in (D.24). This can be expressed in terms of a cutoff scale

$$k_{\text{crit}} \equiv R(y) \operatorname{sech} \frac{L_{IR}}{2} , \quad (\text{D.41})$$

so that the wavefunction in (D.35) can be approximately described by a particle trapped in a potential given by the $R(y)^2 \operatorname{sech}^2 \frac{L_{IR}}{2}$ term in the Schrödinger equation (D.35), resulting in

$$p(L_{IR}, k) \simeq \begin{cases} \frac{1}{2\pi} \sqrt{\frac{k^2}{R(y)^2 \operatorname{sech}^2 \frac{L_{IR}}{2} - k^2}} \exp\left(-2 \int_{L_{IR}}^{L_0} dL \sqrt{R(y)^2 \operatorname{sech}^2 \frac{L}{2} - k^2}\right) & k \lesssim k_{\text{crit}} , \\ \frac{2}{\pi} \sqrt{\frac{k^2}{k^2 - R(y)^2 \operatorname{sech}^2 \frac{L_{IR}}{2}}} \sin^2\left(\int^{L_{IR}} dL \sqrt{k^2 - R(y)^2 \operatorname{sech}^2 \frac{L}{2}}\right) & k > k_{\text{crit}} , \end{cases} \quad (\text{D.42})$$

where

$$L_0 \equiv 2 \operatorname{arccosh}\left(\frac{R(y)}{k}\right) \quad (\text{D.43})$$

results from inverting (D.41), and the proportionality constant in (D.42) is chosen for normalization. By evaluating the integrals in the approximation where

$$\begin{aligned} R(y) \operatorname{sech} \frac{L_{IR}}{2} \gg k , \quad k \lesssim k_{\text{crit}} , \\ R(y) \operatorname{sech} \frac{L_{IR}}{2} \ll k , \quad k > k_{\text{crit}} , \end{aligned} \quad (\text{D.44})$$

then the corresponding probability distribution in the WKB approximation (D.42) becomes

$$p(L_{IR}, k) \simeq \begin{cases} 0 & k \lesssim k_{\text{crit}} , \\ \frac{2}{\pi k} \sin^2(L_{IR} k) & k > k_{\text{crit}} . \end{cases} \quad (\text{D.45})$$

We can now evaluate the following entropy difference based on (D.39)

$$\Delta S \equiv S(L) - S(L \rightarrow \infty) , \quad (\text{D.46})$$

using the triple-scaled probability distribution in the following terms inside (D.39),

$$\lambda \int_0^\infty dk (p(L_{\text{IR}}, k) \log p(L_{\text{IR}}, k) - p_\infty(k) \log p_\infty(k)) = \mathcal{O}(\lambda) , \quad (\text{D.47})$$

where

$$p_\infty(k) \equiv p(L_{\text{IR}} \rightarrow \infty, k) = \frac{1}{\pi} , \quad (\text{D.48})$$

as seen from (D.45); and the last equality in (D.47) follows from $p(L_{\text{IR}}, E) \sim \mathcal{O}(1)$.

Thus, the leading order terms contributing to the entropy difference (D.46) are

$$\Delta S \simeq 2 \int_0^\infty dk (p(L_{\text{IR}}, k) - p_\infty(k)) \lambda \log(\mu(\theta = \lambda k)) . \quad (\text{D.49})$$

We can implement the following relation from (D.40a)

$$\lambda \log \mu(\theta = \lambda k) \xrightarrow{UV} -\frac{1}{2} \pi^2 + \mathcal{O}(\lambda \log \lambda) . \quad (\text{D.50})$$

Therefore, to leading order in the semiclassical expansion, the entropy difference (D.49) with (D.45, D.47, D.50) becomes

$$\Delta S \simeq -\pi^2 \int_0^\infty dk (p(L_{\text{IR}}, k) - p_\infty(k)) \simeq \pi \int_0^{k_{\text{crit}}} dk . \quad (\text{D.51})$$

Then, the WKB approximation gives

$$\Delta S \simeq \pi R(y) \operatorname{sech} \frac{L_{\text{IR}}}{2} . \quad (\text{D.52})$$

Moreover, since, in general, traces are defined up to a proportionality constant (equivalently with respect to the choice of normalization of $|\Omega\rangle$), we can perform the following rescaling

$$\operatorname{Tr} \rightarrow \frac{2}{\lambda} \operatorname{Tr} , \quad (\text{D.53})$$

so that (D.52) after the rescaling becomes

$$\Delta S \xrightarrow{IR} \frac{2\pi}{\lambda} R(y) \operatorname{sech} \frac{L_{\text{IR}}}{2} . \quad (\text{D.54})$$

The specific choice of overall constant is motivated by the RT formula (5.30).

E Deformations with End-Of-The-World Branes and Wormholes

As emphasized in the main text, Hamiltonian deformations modify the energy and micro-canonical temperature of the chord auxiliary theory while keeping the thermodynamic entropy the same. There is a complementary situation where the thermodynamic entropy with respect to the seed theory is modified while keeping the same energy spectrum. This occurs when applying constraints in the chord Hilbert space of the DSSYK model [74], which

lead to ETW brane Hamiltonians in sine dilaton gravity [94]. In this section, we implement Hamiltonian deformations in the DSSYK model with matter in constrained chord states, resulting in the ETW branes in the finite cutoff bulk theory,⁵¹ and we develop its connection with the double trumpet geometry in the DSSYK model and sine dilaton gravity [60, 94, 113, 296, 298, 299, 315, 316].

Outline We begin App. E.1 with a brief review of the ETW brane Hamiltonian from implementing Hilbert space constraints used in Dirac quantization (see [317, 318] for reviews). In App. E.2 we investigate the semiclassical partition function based on the Al-Salam Chihara (ASC) polynomials and two-point correlation functions with the ETW branes in the DSSYK model. In App. E.3 we extend the results for trumpet geometries resulting from a Hilbert space trace.

E.1 Matter Chords as ETW Branes from Deformed DSSYK Model

We investigate Hamiltonian deformations in the ETW brane Hamiltonian for the DSSYK model, first studied by [313], and followed up by [60, 74, 94, 316], among others. The seed theory of interest is described by the ASC Hamiltonian [74, 94, 113],

$$\hat{H}_{\text{ASC}} = \frac{J}{\sqrt{\lambda(1-q)}} \left(e^{-i\hat{P}} + (X+Y)e^{-\hat{\ell}} + (1-XYe^{-\hat{\ell}})e^{i\hat{P}}(1-e^{-\hat{\ell}}) \right), \quad (\text{E.1})$$

which can be derived by imposing constraints in the chord Hilbert space (3.20) with one particle insertion [74], and X and Y are constant parameters which depend on the specific symmetry sector under consideration. Details about the gauging procedure which fixes X and Y in (E.1) can be found in [74], which we briefly summarize below for completeness. We begin considering the one particle chord state

$$\mathcal{H}_1 = \text{span}\{|\Delta; n_L, n_R\rangle\}, \quad (\text{E.2})$$

and the corresponding one-particle chord Hamiltonian (3.24). We may study symmetry sectors in the one-particle chord space to recover the basis $|H_n\rangle$ (E.7) and the ASC Hamiltonian (E.1). By a symmetry we refer to a transformation, \hat{U}_i , that leaves a set of states $\{|\psi\rangle\}$ in the system invariant i.e.

$$\hat{U}_i : |\psi\rangle \rightarrow |\psi\rangle. \quad (\text{E.3})$$

One generates the physical Hilbert space $\mathcal{H}_{\text{phys}}$ from the set of states $\{|\psi\rangle\}$ that are annihilated by the generator of the corresponding transformation (E.3), which we refer to as constraints $\hat{\varphi}_i$:

$$\hat{\varphi}_i |\psi\rangle = 0, \quad |\psi\rangle \in \mathcal{H}_{\text{phys}}. \quad (\text{E.4})$$

There are different constraints leading to a basis where the one-particle Hamiltonian adopts the ASC form (E.1), which we summarize below (based on [74]):

⁵¹There are higher dimensional analogs, such as in double holography [314] where both effects result in intricate dynamical observables.

One-sided branes Let $\hat{\varphi}_A := \hat{P}_L - \delta \hat{\hat{P}}_L$, $\hat{\varphi}_B := \hat{\ell}_L - \hat{\hat{\ell}}_L/\delta$, where δ is a constant so that $[\hat{\ell}_L, \hat{P}_L] = [\hat{\hat{\ell}}_L, \hat{\hat{P}}_L]$ is invariant under the constraint, even under the limit $\delta \rightarrow 0$; and let $\hat{P}_R = \hat{P}$, $\hat{\ell}_R = \hat{\ell}$. By applying these constraints to build the physical Hilbert space, one of the chord Hamiltonians (3.24) takes the representation

$$\hat{H}_R \rightarrow \hat{H}_{\text{ASC}}^{(1s)} = \frac{J}{\sqrt{\lambda(1-q)}} \left(e^{-i\hat{P}} + e^{i\hat{P}} (1 - e^{-\hat{\ell}}) + q^\Delta e^{-\hat{\ell}} \right), \quad (\text{E.5})$$

while \hat{H}_L becomes constant.

Two-sided branes We can take $\hat{\varphi}_A^{(L/R)} := \hat{P}_{L/R} - \hat{P}$, $\hat{\varphi}_B^{(L/R)} := \hat{\ell}_{L/R} - \hat{\ell}$, so that the total Hamiltonian can be represented as

$$\hat{H}_L + \hat{H}_R \rightarrow \hat{H}_{\text{ASC}}^{(2s)} = \frac{2J}{\sqrt{\lambda(1-q)}} \left(e^{-i\hat{P}} + (1 + q^{\Delta+1} e^{-\hat{\ell}}) e^{i\hat{P}} (1 - e^{-\hat{\ell}}) \right). \quad (\text{E.6})$$

States in the Constrained Chord space Next, we summarize the general structure of the states $\{|H_n\rangle\}$ in the Hilbert space where the ASC Hamiltonian (E.1) acts. The operators in the Hamiltonian above can be represented by

$$e^{-i\hat{P}} |H_n\rangle = |H_{n+1}\rangle, \quad e^{i\hat{P}} |H_n\rangle = |H_{n-1}\rangle, \quad \hat{n} |H_n\rangle = n |H_n\rangle. \quad (\text{E.7})$$

We can also look for a basis that diagonalizes the Hamiltonian

$$\hat{H}_{\text{ASC}} |\theta\rangle = E(\theta) |\theta\rangle, \quad (\text{E.8})$$

where $\theta \in [0, \pi]$ is a parametrization of the energy. Next, by acting with the basis $\{|H_n\rangle\}$ and $|\theta\rangle$ in (E.1), we recover

$$2 \cos \theta Q_n = Q_{n+1} + (X + Y) q^n Q_n + (1 - XY q^{n-1})(1 - q^n) Q_{n-1}, \quad (\text{E.9})$$

where

$$\langle \theta | H_n \rangle := Q_n(\cos \theta | X, Y; q), \quad E(\theta) = \frac{2J}{\sqrt{\lambda(1-q)}} \cos \theta, \quad \theta \in [0, \pi]. \quad (\text{E.10})$$

By requiring $Q_0 = 1$ and $Q_{-1} = 0$, the recurrence relation is solved by the ASC polynomials [319], which are given by

$$Q_l(\cos \theta | X, Y; q) = \frac{(XY; q)_l}{X^l} \sum_{n=0}^{\infty} \frac{(q^{-l}, X e^{\pm i\theta}; q)_n}{(XY, q; q)_n} q^n. \quad (\text{E.11})$$

The ASC polynomials satisfy the relation

$$\int_0^\pi d\theta \tilde{\mu}(\theta) \frac{Q_{l_1}(\cos \theta, X, Y | q)}{\sqrt{(q, XY; q)_{l_1}}} \frac{Q_{l_2}(\cos \theta, X, Y | q)}{\sqrt{(q, XY; q)_{l_2}}} = \delta_{l_1, l_2}, \quad (\text{E.12})$$

where

$$\tilde{\mu}(\theta) = \mu(\theta) \frac{(XY; q)_\infty}{(Xe^{\pm i\theta}; Y e^{\pm i\theta}; q)_\infty}, \quad \int_0^\pi d\theta \tilde{\mu}(\theta) |\theta\rangle \langle \theta| = \mathbb{1}. \quad (\text{E.13})$$

The integration measure can be expressed as

$$\langle \Omega | B_{X,Y} \rangle = \int_0^\pi d\theta \tilde{\mu}(\theta), \quad (\text{E.14})$$

where $|B_{X,Y}\rangle$ refers to the ETW brane state, a generalized q -coherent state, which is defined to satisfy the relation:⁵²

$$(\hat{a} + XY \hat{a}^\dagger) |B_{X,Y}\rangle \equiv \frac{X+Y}{\sqrt{1-q}} |B_{X,Y}\rangle, \quad (\text{E.15})$$

with \hat{a} , \hat{a}^\dagger being annihilation and creation operators in the zero-particle chord space in (3.12)

$$\hat{a} \equiv e^{i\hat{p}} \sqrt{[\hat{n}]_q}, \quad \hat{a}^\dagger \equiv \sqrt{[\hat{n}]_q} e^{-i\hat{p}}. \quad (\text{E.16})$$

E.2 Deformed ETW Brane theory

We consider deforming the Hamiltonian after gauging the corresponding symmetry sector in the chord Hilbert space⁵³

$$\begin{aligned} \text{Gauging : } & \hat{H}_{L/R} \rightarrow \hat{H}_{\text{ASC}}, \\ \text{Deforming : } & \hat{H}_{\text{ASC}} \rightarrow \hat{H}_{\text{ASC}}^y = f_y(\hat{H}_{\text{ASC}}), \end{aligned} \quad (\text{E.18})$$

with f_y being the Hamiltonian deformation function (4.15a).

Now, we evaluate the disk partition function with the ETW brane based on (E.18), which is

$$\begin{aligned} Z_{\text{ETW}}^{(y)}(\beta|X, Y) & \equiv \langle H_0 | e^{-\beta \hat{H}_{\text{ASC}}^y} | H_0 \rangle = \int_0^\pi d\theta \frac{(XY, e^{\pm 2i\theta}; q)_\infty e^{-\beta E_y(\theta)}}{2\pi (Xe^{\pm i\theta}, Y e^{\pm i\theta}; q)_\infty} \\ & \stackrel{\lambda \rightarrow 0}{=} \int_0^\pi d\theta \sqrt{\frac{8\pi(1-XY) \sin^2 \theta}{\lambda(1+X^2-2X \cos \theta)(1+Y^2-2Y \cos \theta)}} e^{S_\Delta(\theta) - \beta E_y(\theta)}, \end{aligned} \quad (\text{E.19})$$

where the thermodynamic entropy, and microcanonical temperature are respectively

$$\begin{aligned} S_{\text{ETW},y}(\theta) & = S(\theta) + \frac{1}{\lambda} \left(\text{Li}_2(XY) + \frac{\pi^2}{6} + \sum_{\varepsilon=\pm} \left(\text{Li}_2(X e^{i\varepsilon\theta}) + \text{Li}_2(Y e^{i\varepsilon\theta}) \right) \right), \\ \frac{dS_{\text{ETW},y}}{dE_y} & = \frac{dE}{dE_y} \left(\beta(\theta) + \frac{i}{2J \sin \theta} \log \frac{(1 - X e^{i\theta})(1 - Y e^{i\theta})}{(1 - X e^{-i\theta})(1 - Y e^{-i\theta})} \right), \end{aligned} \quad (\text{E.20})$$

⁵²See e.g. [316]; the dictionary relating our notation with theirs is $\beta_{\text{There}} = (1-q)/((1+X)(1+Y))$ and $\delta_{\text{There}} = -(1-q)XY/((1+X)(1+Y))$. The relation between X, Y to ETW brane parameters in sine dilaton gravity has been explored in [74].

⁵³Alternatively, one may deform the chord Hamiltonian with matter (4.1)

$$\hat{H}_{L/R} \rightarrow \hat{H}_{L/R,y} = f(\hat{H}_{L/R}), \quad (\text{E.17})$$

and then gauge the corresponding symmetry $\hat{H}_{L/R,y} \rightarrow \hat{H}_{\text{ASC}}$.

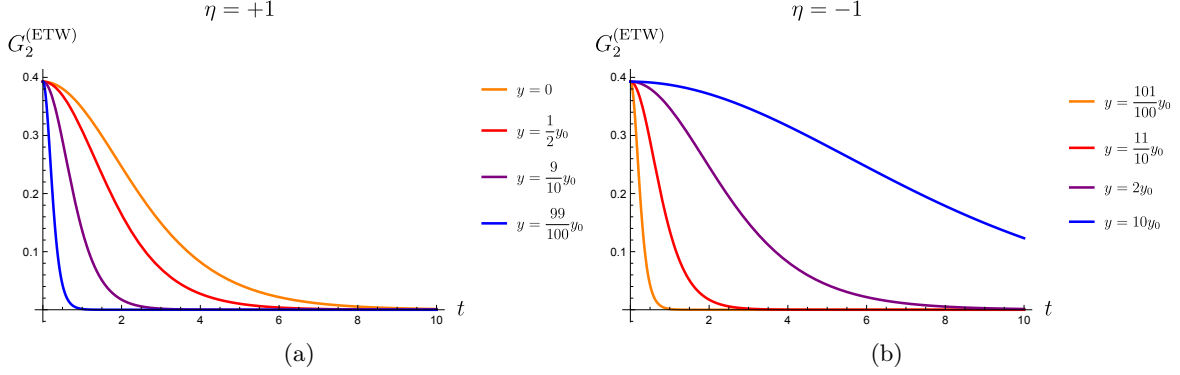


Figure 11. Two-point correlation function (E.21) resulting from (a) T^2 deformation ($\eta = +1$) and (b) $T^2 + \Lambda_1$ deformation ($\eta = -1$). We display the enhanced rate of decay of the two-point function as the deformation parameter approaches the critical value y_0 (3.57) due to the redshift factor in the fake temperature (4.21). The parameters in the plot are $\lambda = 10^{-4}$, $J = 1$, $\lambda\Delta_1 = 1$, $\Delta_2 = 1$ and $\theta = 3\pi/4$ for one-sided ETW brane ($X + Y = q^\Delta$ and $XY = 0$ in (E.21)). Similar results are recovered for two-sided ETW branes.

and $S(\theta)$, $\beta(\theta)$ appear in (2.25), (2.26).

Applying the constraints in the crossed four-point function (4.21), the corresponding two-point function in presence of an ETW brane contains redshift factor in (4.18) gives

$$G_2^{(ETW)}(t, \theta) \equiv \frac{\langle H_0 | e^{-\left(\frac{\beta(\theta)}{2} - it\right) \hat{H}_{ASC}^y} q^{\Delta \hat{n}} e^{-\left(\frac{\beta(\theta)}{2} + it\right) \hat{H}_{ASC}^y} | H_0 \rangle}{\langle H_0 | e^{-\beta(\theta) \hat{H}_{ASC}^y} | H_0 \rangle} \quad (\text{E.21})$$

$$\stackrel{\lambda \rightarrow 0}{=} \left(\frac{2 \sin^2 \theta}{1 + XY - (X + Y) \cos \theta + \cosh\left(\frac{2\pi t}{\tilde{\beta}_y(\theta)}\right) \prod_{X_i=X, Y} \sqrt{X_i^2 - 2X_i \cos \theta + 1}} \right)^\Delta,$$

with $\tilde{\beta}_y$ in (4.21). We display the behavior of the two-point function in Fig. 11.

From the figure, it can be seen that, as expected in finite cutoff holography [23], once the deformation parameter approaches its critical value y_0 (3.57), it will experience an enhanced decay rate, while it leads to an enhanced rate of growth for crossed-four point functions (4.24). This is also expected since the growth of OTOCs is bounded by that of the two-point correlation functions [129]. We discussed its implications in the IR and UV regimes in Sec. 4.3 and 6.3 respectively.

E.3 Euclidean Wormholes from the DSSYK Model

Now, we proceed by studying the trumpet geometries from the deformed theory perspective.

The ASC Hamiltonian (E.1) can be used to evaluate partition functions and correlation functions for Euclidean wormhole geometries [74, 94]. In this subsection, we will study how the thermodynamics and correlation functions in the ETW brane and Euclidean wormhole theories are modified after implementing the deformations in the corresponding Hamiltonians.

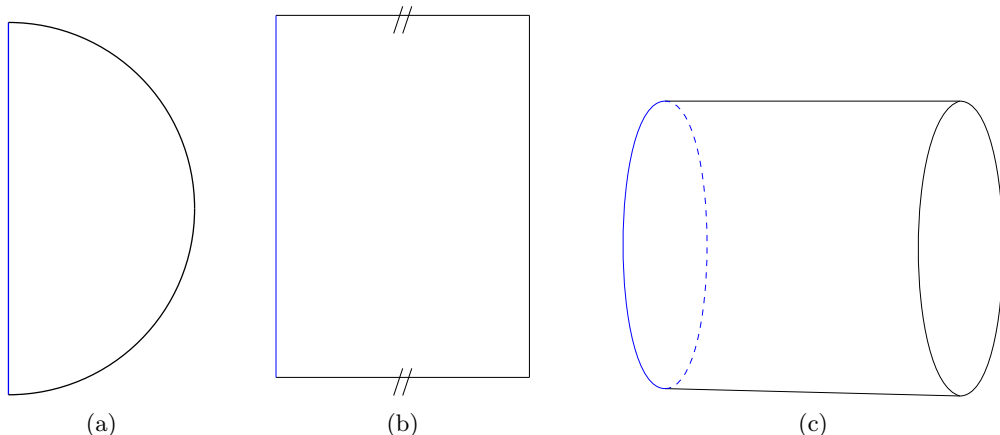


Figure 12. Construction of the cylinder partition function (E.22). (a) The disk topology with an ETW brane (blue solid line) is mapped to (b) a rectangle. The identification between two of its edges represents the Hilbert space trace $\sum \langle H_n | \cdots | H_n \rangle$, which is glued together to form (c) the cylinder, which leads to the divergence in (E.22).

T^2 deformations in JT gravity with non-trivial topology have been recently considered in [37, 259]. This motivates us to look at the corresponding wormhole partition functions

$$\begin{aligned}
 Z_{X,Y}^{(y)}(\beta) &\equiv \text{Tr} \left[e^{-\beta \hat{H}_{\text{Asc}}^y} \right] \\
 &= \sum_{n=0}^{\infty} \int_0^{\pi} d\theta \tilde{\mu}(\theta) e^{-\beta E_y(\theta)} \langle H_n | \theta \rangle \langle \theta | H_n \rangle = \int d\theta \delta(\theta - \theta) e^{-\beta E_y(\theta)}, \tag{E.22}
 \end{aligned}$$

where we implemented $\mathbb{1} = \sum_{n=0}^{\infty} |H_n\rangle \langle H_n|$. This partition function can be visualized as cutting in half a partition function and gluing its ends, resulting in a trumpet geometry, as we illustrate in Fig. 12. While the above correlation function is singular, one can define a regularized version, which is the trumpet partition function

$$\begin{aligned}
 Z_b^{(y)}(\beta) &\equiv \frac{1}{2\pi i} \oint \frac{dY}{Y^{(b+1)}} Z_{X,Y}^{(y)}(\beta) \\
 &= \frac{2}{(q; q)_{\infty}} \sum_{n=0}^{\infty} \int_0^{\pi} d\theta 2 \cos(b\theta) e^{-\beta E_y(\theta)} q^{nb}, \tag{E.23}
 \end{aligned}$$

which we display in Fig. 13.

The above expression is not simple to evaluate; it would be interesting to use the techniques of resurgence, similar to the JT gravity analog [37], to complete the evaluation. One would be able to use the result to determine the double trumpet amplitude in the bulk

$$Z_b^{(y)}(\beta) := \frac{(q; q)_{\infty} (1 - q^b)}{2} \tilde{Z}_b^{(y)}(\beta), \tag{E.24}$$

and construct a partition function for multiple-boundaries Euclidean wormhole [74]

$$Z_y(\beta_1, \beta_2, \dots, \beta_m) := \sum_{b=1}^{\infty} b Z_b^{(y)}(\beta_1) Z_b^{(y)}(\beta_2) \cdots Z_b^{(y)}(\beta_m), \tag{E.25}$$

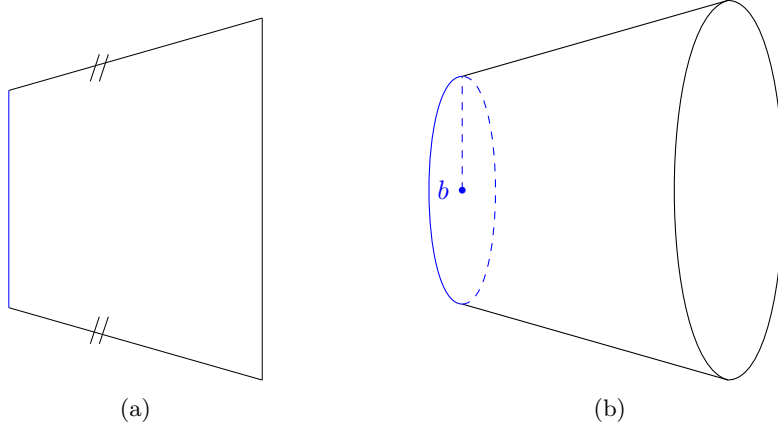


Figure 13. The regularization implemented in the trumpet partition function (E.23) can be seen as reducing the length of the ETW brane (solid blue line) in Fig. 12 to a finite size and gluing appropriately the edges of the plane.

which reduces to a double-trumpet partition function in the $m = 2$ case. Relevant evaluations for this quantity in finite cutoff holography have recently appeared in [42].

We move on to a unnormalized thermal two-point correlation function in the trumpet configuration, given by gauging symmetries and implement the Hilbert space trace as

$$\begin{aligned}
G_{\text{cylinder}}^{(\Delta_w)} &= \text{Tr} \left(\hat{\mathcal{O}}_{\Delta_w} e^{-\beta_1 \hat{H}_{\text{ASC}}^y} \hat{\mathcal{O}}_{\Delta_w} e^{-\beta_2 \hat{H}_{\text{ASC}}^y} \right) \\
&= \sum_{n=0}^{\infty} \langle H_n | e^{-\beta_2 \hat{H}_{\text{ASC}}^y} q^{\Delta_w \hat{n}} e^{-\beta_1 \hat{H}_{\text{ASC}}^y} | H_n \rangle \\
&= \sum_{n=0}^{\infty} \left(\int_0^\pi \prod_{i=1}^2 d\theta_i \frac{(XY, e^{\pm 2i\theta_i}; q)_\infty}{(X e^{\pm i\theta_i}, Y e^{\pm i\theta_i}; q)_\infty} e^{-\beta_i E_y(\theta_i)} \right) \langle H_n | \theta_1 \rangle \langle \theta_1 | q^{\Delta_w \hat{n}} | \theta_2 \rangle \langle \theta_2 | H_n \rangle .
\end{aligned} \tag{E.26}$$

Using (E.12) and defining $\beta = \beta_1 + \beta_2$ one recovers

$$G_{\text{cylinder}}^{(\Delta_w)}(\beta) = \int_0^\pi d\theta \tilde{\mu}(\theta) \langle \theta | q^{\Delta_w \hat{n}} | \theta \rangle e^{-\beta E(\theta)} , \tag{E.27}$$

where $\tilde{\mu}(\theta) = \frac{(XY, e^{\pm 2i\theta}; q)_\infty}{(X e^{\pm i\theta}, Y e^{\pm i\theta}; q)_\infty}$. This can be further simplified by inserting the identity $\sum_n |K_n^y\rangle \langle K_n^y| = \mathbb{1}$ and $\hat{n}_y |K_n^y\rangle = n_y |K_n^y\rangle$, resulting into

$$G_{\text{cylinder}}^{(\Delta_w)}(\beta) = \sum_{n=0}^{\infty} q^{\Delta_w n} \int_0^\pi d\theta \tilde{\mu}(\theta) |\langle \theta | K_n \rangle|^2 e^{-\beta E_y(\theta)} . \tag{E.28}$$

It might be possible to simplify the result using saddle point method where the semiclassical solution takes the form

$$G_{\text{cylinder}}^{(\Delta_w)}(\beta) \underset{\lambda \rightarrow 0}{=} \sum_{n=0}^{\infty} q^{\Delta_w n} e^{-\beta E_y(\theta_{\text{s.p.}})} \int_0^\pi d\theta \tilde{\mu}(\theta) |\langle \theta | K_n \rangle|^2 , \tag{E.29}$$

where $\theta_{\text{s.p.}}$ denotes the corresponding saddle-point solution. This would result from a one-loop quantum corrected two-point correlation function similar to [74]. However, the details of the evaluation are outside the scope of the current investigation, and we leave them for future directions.

F Almheiri-Goel-Hu Model

In this appendix, we explore the previous results on T^2 deformation for the model developed in [184], which is significantly simpler than the one in the main text. We are interested in its thermodynamic properties, correlation functions, and the evolution of the chord number.

Motivated by the high-temperature limit of the DSSYK model, [184] studied the limit where its ensemble averaged theory can be approximately described by

$$\hat{H} = \frac{1}{\sqrt{2}}(\hat{a} + \hat{a}^\dagger) , \quad (\text{F.1})$$

with \hat{a}^\dagger , \hat{a} being creation and annihilation operators of the harmonic oscillator.

By matching correlation functions with bulk geodesics, a (non-local like) dilaton gravity theory dual to the model was proposed by [184], which is described by (2.1) with a potential

$$U(\Phi) = \frac{96\pi^2}{\beta^4}(1 - \Phi)^{-1/3} , \quad (\text{F.2})$$

where we have performed an overall rescaling in the dilaton field with respect to [184] to make it dimensionless as in the ansatz (2.31), where we now have

$$ds^2 = F(r)d\tau^2 + \frac{dr^2}{F(r)} , \quad F(r) = \frac{\beta^4}{4}(1 - (1 - r)^{2/3}) . \quad (\text{F.3})$$

We assume a counter term of the type (2.3) to keep the on-shell action finite at the asymptotic boundary, located at $\Phi_B = 1$.

Thermodynamics In the rest of the section, we investigate T^2 deformations of the AGH model (F.1). We can directly use the thermodynamic results in [184], where

$$\beta = -2E , \quad S = -E^2 , \quad (\text{F.4})$$

to derive the boundary inverse temperature of the T^2 deformed model in terms of energy spectrum (3.14) and thermodynamic entropy (2.25)

$$\beta_y = E_y(-2 + yE_y)(1 - 2yE_y) = -2\sqrt{|S|}\sqrt{1 - 2y\sqrt{|S|}} . \quad (\text{F.5})$$

where the interpretation of the negative thermodynamic entropy is similar to [184], namely a relative entropy with respect to the maximal mixed state of the model. Similarly, the density of states (2.28b) and the heat capacity (2.29) can be calculated as:

$$\rho_y = e^S \sqrt{1 - 2y\sqrt{-S}} , \quad (\text{F.6})$$

$$C_y = \frac{(\beta_y)^2}{2 - 3yE_y(2 - yE_y)} . \quad (\text{F.7})$$

Moreover, using the dictionary entry (2.17), we can modify the boundary location from $r = 1$ to the stretched horizon (i.e. nearby $r = 0$). Note that since the potential (F.2) is obtained by matching geodesic lengths with two-point correlations, its boundary temperature will be modified $\beta \rightarrow \beta_y$, and the corresponding deformation parameter (2.17) is expressed as

$$y = \frac{16\pi G_N (\beta_y)^4}{144\pi^2 (1 - r_B)^{2/3}} . \quad (\text{F.8})$$

Note that the boundary temperature dependence is consistent with the non-local nature of the theory proposed by [184], and the factor G_N in (2.1) allows to match ADM energy and entropy in (2.32) with those of the DSSYK model (3.14, 2.25) when we set $16\pi G_N = \sqrt{2}$.

The evaluation of (3.4) for different boundary locations $r_B \in (0, 1)$ (i.e. between the event horizon and the asymptotic boundary) used in (F.8) are shown in Fig. 14. We emphasize that, for the purposes of the analysis, we are allowing the boundary inverse temperature to have a finite range of values, even though the connection with the DSSYK model occurs at high temperatures. As seen, for instance, in Fig. 14 the energy spectrum is real only under a finite range of boundary temperatures, which do not include strictly infinite boundary temperatures. Note also, there is a non-zero inverse boundary temperature where S and C_y will diverge, independent of the stretched horizon limit. Meanwhile, the fact that the model has a negative thermodynamic entropy (F.4, F.5) implies that the growth of the density of states is suppressed in the regime where S diverges. At last, it is seen in Fig. 14 (d) that the system is manifestly thermodynamically stable for generic values of r_B . Further discussion of the results is provided at the end of this subsection.

Correlation functions We now proceed to evaluate the T^2 deformed thermal two-point correlation function of matter operators \hat{V} with conformal dimension Δ_V and the corresponding OTOCs (see Fig. 15), to compare with our previous findings in Sec. 4.2 for the sine dilaton gravity model. Note that while in Sec. 4.2 we evaluate the correlation functions through saddle point methods in the $\lambda \rightarrow 0$ regime, since we are viewing the (F.1) as a model on its own; which is not necessarily related to the DSSYK model in the $\lambda \rightarrow 0$ regime, we will perform the evaluation without taking any limits. In general, these evaluations become intricate due to the $E_y(E)$ factor (except in the $y = 0$ case). Fortunately for us, we notice that we can approach a stretched horizon regime for $y \ll 1$ in (F.8) when $\beta_y \rightarrow 0$, which is the high temperature regime where the AGH model is expected to describe the DSSYK model. For this reason, in this subsection, we will be mostly interested in a perturbative y expansion, in contrast to most of the work, which is at non-perturbative order in y .

Similar to the identity (3.19), we can express the (Euclidean-signature) evolution of the oscillator number basis $\{|n\rangle\}$ (i.e. where $\hat{a}^\dagger \hat{a} |n\rangle = n |n\rangle$) of (F.1) in terms of a complete basis of energy eigenstates $|E\rangle$:

$$\left| \phi_n^{(y)}(\tau) \right\rangle \equiv e^{-\hat{H}_y \tau} |n\rangle = \int_{-\infty}^{\infty} dE \frac{e^{-E^2 - E_y(E)\tau} H_n(E)}{\sqrt{n! 2^n \pi}} |E\rangle , \quad (\text{F.9})$$

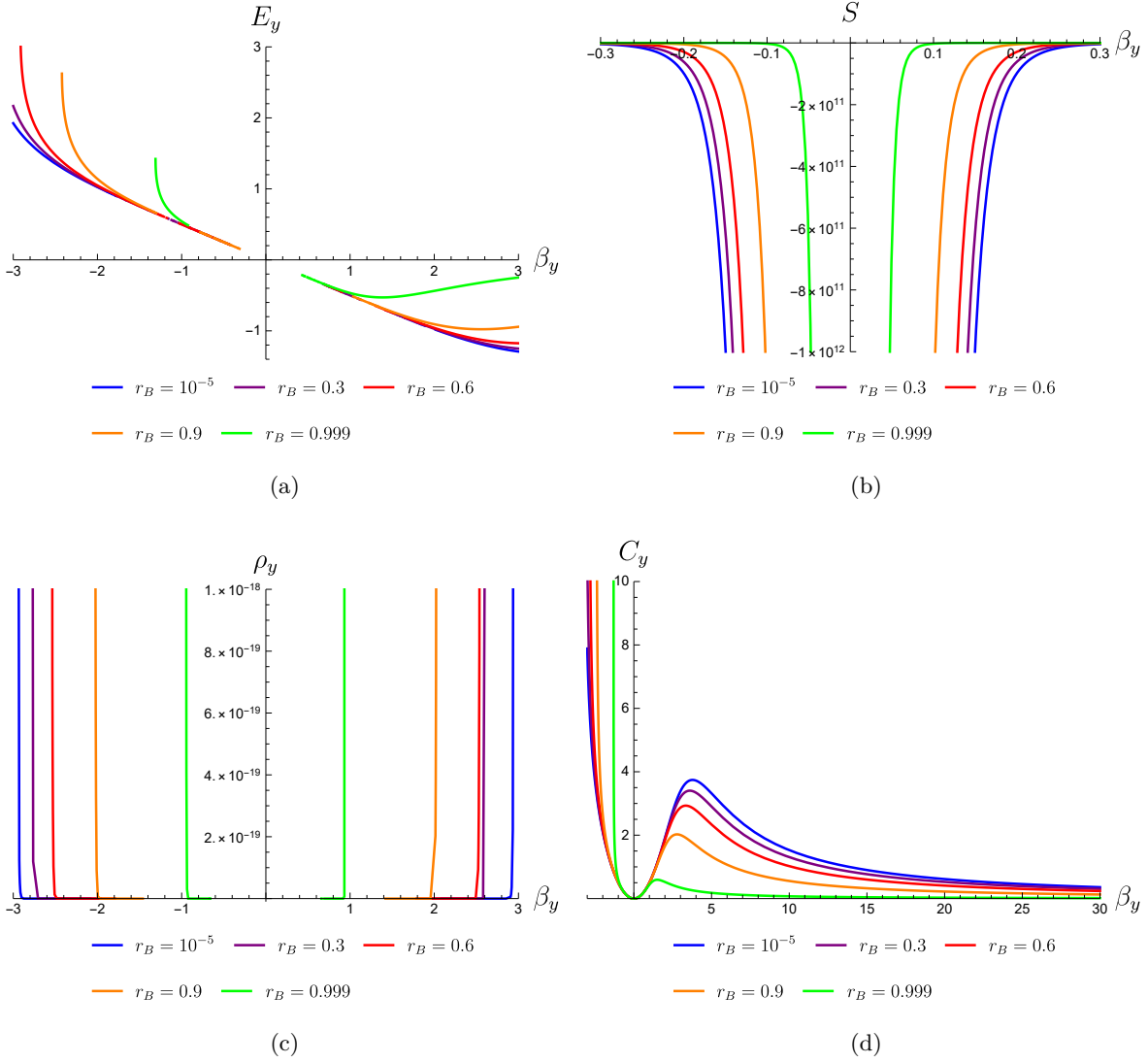


Figure 14. (a) T^2 deformed ($\eta = +1$ (2.17)) energy spectrum, (b) thermodynamic entropy, (c) density of states, and (d) heat capacity of the AGH model [184], using the map (F.8) for different values of the boundary location r_B .

where $H_n(E) = \langle E|n \rangle$ is the n -th order Hermite polynomial. Note that

$$\langle \Omega | \phi_n^{(y=0)}(\tau) \rangle = \frac{(-\tau)^n}{\sqrt{n! 2^n}} e^{\tau^2/4}. \quad (\text{F.10})$$

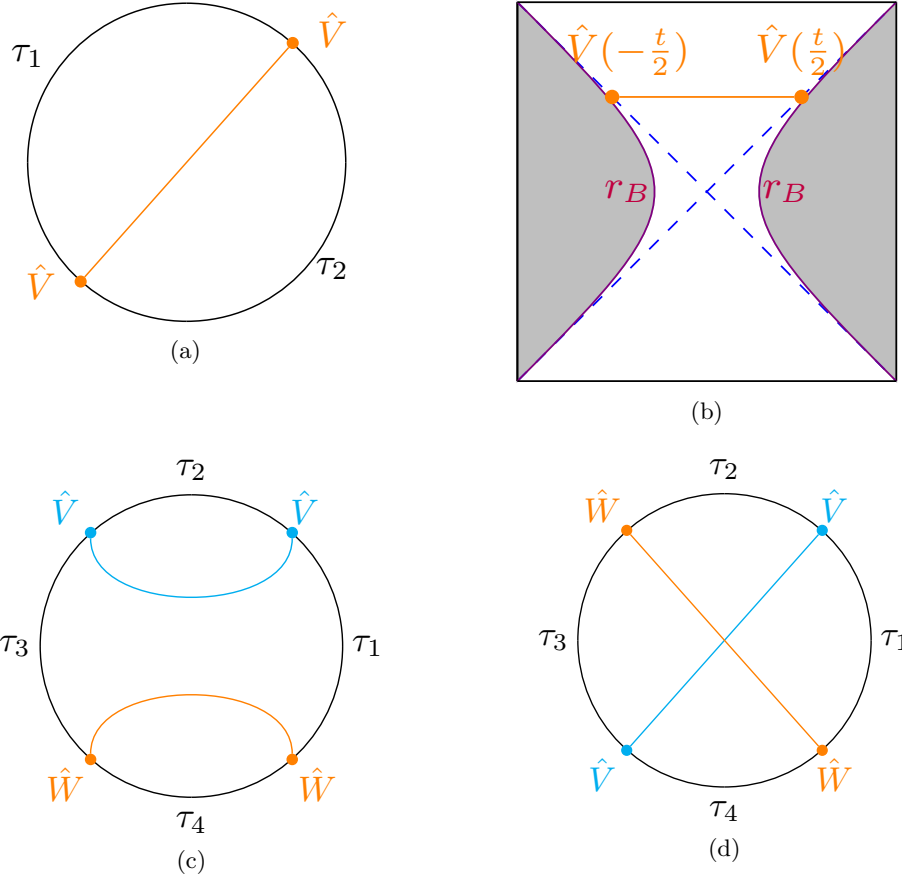


Figure 15. Correlation functions of matter field operators \hat{V} (cyan) and \hat{W} (orange) (with conformal dimension Δ_V and Δ_W respectively) in the AGH model: two-point correlation functions from the (a) boundary and (b) the Lorentzian-signature bulk perspectives (where $\hat{V}(t) = e^{i\hat{H}t}\hat{V}(0)e^{-i\hat{H}t}$); as well as the (c) uncrossed, and (d) crossed four-point correlation functions.

Two-point correlation functions We can then evaluate the correlation function in Fig. 15 (a) as:

$$\begin{aligned} \frac{1}{Z_y(\beta)} \langle \Omega | e^{-\tau_2 \hat{H}_y} \hat{V} e^{-\tau_1 \hat{H}_y} \hat{V} | \Omega \rangle &= \langle \Omega | e^{-\tau_2 \hat{H}_y} e^{-\Delta_V \hat{n}} e^{-\tau_1 \hat{H}_y} | \Omega \rangle \\ &= \sum_n \langle \phi_n^{(y)}(\tau_2) | \Omega \rangle \langle \Omega | \phi_n^{(y)}(\tau_1) \rangle e^{-\Delta_V n} . \end{aligned} \quad (\text{F.11})$$

To perform the evaluation above, we will first consider a perturbative y expansion, where $E_y(E) = E + \frac{y}{2}E^2 + \mathcal{O}(y^2)$. In this case (F.11) with (F.10) can be expressed as

$$\begin{aligned} &\langle \Omega | e^{-\tau_2 \hat{H}_y} \hat{V} e^{-\tau_1 \hat{H}_y} \hat{V} | \Omega \rangle \\ &= \exp \left[\frac{1}{4} \sum_{i=1}^2 \tau_i^2 \left(1 - \frac{y}{2} \tau_i \right) + \frac{e^{-\Delta_V}}{2} \tau_1 \tau_2 \left(1 - \frac{y}{4} (\tau_1 + \tau_2) \right) + \mathcal{O}(y^2) \right] . \end{aligned} \quad (\text{F.12})$$

We can then see the expansion $E_y(E) = E + \frac{y}{2}E^2 + \mathcal{O}(y^2)$ as the first order correction in y in the exponent of the correlation function.

To make the analytic continuation to Lorentzian signature, we take

$$\tau_1 = it + \frac{\beta}{2}, \quad \tau_2 = -it + \frac{\beta}{2}, \quad (\text{F.13})$$

so that the normalized two-point correlation function becomes

$$\begin{aligned} \mathcal{G}(t) &\equiv \frac{\langle \Omega | e^{-(\beta/2-it)\hat{H}_y} \hat{V} e^{-(\beta/2+it)\hat{H}_y} \hat{V} | \Omega \rangle}{\langle \Omega | e^{-\frac{\beta}{2}\hat{H}_y} \hat{V} e^{-\frac{\beta}{2}\hat{H}_y} \hat{V} | \Omega \rangle} \\ &= \exp \left(-\frac{t^2}{2} \left((1 - e^{-\Delta_V}) + \frac{y\beta}{8}(1 - e^{-2\Delta_V}) + \mathcal{O}(y^2) \right) \right). \end{aligned} \quad (\text{F.14})$$

We can then see the time dependence of the function in (F.14) remains unaffected, at least at the first order perturbation in y . Moreover, it follows from (F.14) that the temperature, defined as the rate of decay of the thermal correlation functions, is a fixed value

$$\tilde{\beta}_y = 2\pi\alpha, \quad \text{where} \quad \alpha = \left(1 - e^{-\Delta_V} + \frac{y\beta}{8}(1 - e^{-2\Delta_V}) \right) + \mathcal{O}(y^2). \quad (\text{F.15})$$

where we notice that even without the perturbation, the system's temperature and decay of correlation functions are different in general, as in the DSSYK case [92].

Performing the calculation (F.11) at the non-perturbative level in the deformation parameter y is in general complicated; however, to get the answer at any order in perturbation theory, we can carry out the expansion

$$e^{-E_y(E)\tau} = e^{-E\tau} \sum_{m=0}^{\infty} \tilde{c}_m(\tau, y) E^m, \quad (\text{F.16})$$

where $\tilde{c}_m(\tau, y)$ is a polynomial function in τ and y , which can be explicitly evaluated for the 1D T^2 deformation (3.14). One can then use (F.10) to evaluate:

$$\int_{-\infty}^{\infty} dE E^m e^{-\tau E - E^2} H_n(E) = \left(-\frac{d}{d\tau} \right)^m \left[\frac{(-\tau)^n}{\sqrt{\pi}} e^{\tau^2/4} \right], \quad (\text{F.17})$$

and obtain (F.11) at any order in perturbation theory in y . However, for the purpose of later computations, we find it more convenient to evaluate the y -corrections in the exponent (F.14), instead of the correlation function itself. Lastly, to find the full, non-perturbative answer for (F.11), one might also attempt a numerical evaluation of the integral corresponding to $\langle \Omega | \phi_n(\tau) \rangle$ from (F.9) and performing the sum in n . However, we do not pursue this direction, since perturbation theory is a good approximation to study the stretched horizon regime analytically in the $\beta \rightarrow 0$ regime.

Squared correlators We would like to evaluate the Lorentzian-signature squared correlator defined by

$$\text{SC}_y(t) \equiv \frac{1}{Z_y(\beta)} \langle \Omega | e^{-\beta \hat{H}_y} [\hat{W}(0), e^{i\hat{H}_y t} \hat{V}(0) e^{-i\hat{H}_y t}]^2 | \Omega \rangle, \quad (\text{F.18})$$

for the operators \hat{V} and \hat{W} with conformal dimensions Δ_V and Δ_W respectively. The diagrammatic techniques for the calculation have been worked out in App. B of [184], so we state the results after incorporating the T^2 deformation at order $\mathcal{O}(y)$, which essentially amounts to the modification $\tau_i \rightarrow \tau_i(1 - \frac{y}{4}\tau_i)$ inside the overall exponent. This allows us to express the uncrossed four-point correlation function (Fig. 15 (c)):

$$\begin{aligned} & \log \left(\langle \Omega | e^{-\hat{H}_y \tau_4} V e^{-\hat{H}_y \tau_3} W e^{-\hat{H}_y \tau_2} W e^{-\hat{H}_y \tau_1} V | \Omega \rangle \right) \\ &= \sum_{i=1}^4 \tau_i^2 + (\tau_2 + \tau_4) \left(\frac{e^{-\Delta_V}}{2} \tau_3 + \frac{e^{-\Delta_W}}{2} \tau_1 \right) + \frac{e^{-\Delta_V - \Delta_W}}{2} \tau_2 \tau_4 + \frac{\tau_1 \tau_3}{2} \\ & \quad - \frac{y}{8} \left(e^{-\Delta_V} \tau_1 (\tau_2 (\tau_2 + \tau_3) + \tau_4 (\tau_1 + \tau_4)) + (\tau_1^3 + \tau_3^3 + (\tau_2 + \tau_4) (\tau_2^2 + \tau_4^2)) \right) \\ & \quad - \frac{y}{8} e^{-\Delta_V - \Delta_W} \tau_3 \left(\tau_1 (\tau_1 + \tau_3) + (\tau_2 (\tau_1 + \tau_2) + \tau_4 (\tau_3 + \tau_4)) e^{\Delta_V} \right) + \mathcal{O}(y^2), \end{aligned} \quad (\text{F.19})$$

as well as the crossed four-point correlation function (Fig. 15 (d)):

$$\begin{aligned} & \langle \Omega | e^{-\hat{H}_y \tau_4} V e^{-\hat{H}_y \tau_3} W e^{-\hat{H}_y \tau_2} V e^{-\hat{H}_y \tau_1} W | \Omega \rangle \\ &= \sum_{i=1}^4 \tau_i^2 + \frac{e^{-\Delta_V}}{2} (\tau_1 \tau_2 + \tau_3 \tau_4) + \frac{e^{-\Delta_W}}{2} (\tau_2 \tau_3 + \tau_1 \tau_4) + \frac{e^{-\Delta_V - \Delta_W}}{2} (\tau_1 \tau_3 + \tau_2 \tau_4) - \Delta_V \Delta_W \\ & \quad - \frac{y}{8} \left((\tau_2 \tau_3 (\tau_2 + \tau_3) + \tau_1 \tau_4 (\tau_1 + \tau_4)) e^{-\Delta_W} + (\tau_1 \tau_2 (\tau_1 + \tau_2) + \tau_3 \tau_4 (\tau_3 + \tau_4)) e^{-\Delta_V} \right) \\ & \quad + \frac{y}{8} \left(\sum_{i=1}^4 \tau_i^3 - (\tau_1 \tau_3 (\tau_1 + \tau_3) + \tau_2 \tau_4 (\tau_2 + \tau_4)) e^{-\Delta_V - \Delta_W} \right) + \mathcal{O}(y^2). \end{aligned} \quad (\text{F.20})$$

Combining (F.19) and (F.20), and choosing the corresponding value for τ_i , we can evaluate (F.18) at order $\mathcal{O}(y)$ as

$$\begin{aligned} \text{SC}_y(t) &\equiv \frac{1}{Z_y(\beta)} \langle \Omega | e^{-\hat{H}_y \beta} [W(0), V(t)]^2 | \Omega \rangle \Big|_{\mathcal{O}(y)} \\ &= e^{\frac{1}{16}(-8t^2 - \beta t e^{-\Delta_V - \Delta_W} (e^{\Delta_V} (y(t(it y + \beta y - 4) - 2i\beta) + 8i) + 2i(\beta y - 4)) - \beta t e^{-\Delta_V} (y(t(it y + \beta y - 4) - 2i\beta) + 8i) - 2i\beta t(3\beta y - 4) - 2\beta^3 y)} \\ & \quad \left(e^{\frac{1}{32} t^2 e^{-\Delta_V - \Delta_W} (e^{\Delta_V} (y(2t^2 y + \beta(\beta y - 12)) + 32) + e^{\Delta_W} (y(2t^2 y + \beta(\beta y - 12)) + 32) + y(2t^2 y + \beta(12 - \beta y)) + 4(3\beta y - 4) e^{\Delta_V + \Delta_W} - 32)} \right. \\ & \quad \left(1 + e^{\frac{1}{8} i \beta t e^{-\Delta_V - \Delta_W} (2e^{\Delta_W} (e^{\Delta_V} (3\beta y - 4) + \beta(-y) + 4) - 2(e^{\Delta_V} - 1)(\beta y - 4))} \right) - \left(e^{\frac{1}{16} \beta t^2 y e^{-\Delta_V} (\beta y - 4)} \right. \\ & \quad \left. + e^{\frac{1}{16} \beta t^2 y e^{-\Delta_W} (\beta y - 4)} \right) e^{\frac{1}{32} t e^{-\Delta_V} (e^{\Delta_V} (16t + 4i\beta(3\beta y - 4)) - 4i\beta(e^{\Delta_V} - 1) e^{-\Delta_W} (\beta y - 4) - 4i\beta(\beta y - 4))} \Big). \end{aligned} \quad (\text{F.21})$$

Note that the $y \rightarrow 0$ limit reproduces one of the results in [184]

$$\begin{aligned} \text{SC}_{y \rightarrow 0}(t) &\equiv \frac{1}{Z(\beta)} \langle \Omega | e^{-\beta \hat{H}} [\hat{W}(0), \hat{V}(t)]^2 | \Omega \rangle \\ &= -2 + 2 \cos \left((1 - e^{-\Delta_V})(1 - e^{-\Delta_W}) \frac{\beta t}{2} \right) e^{-(1 - e^{-\Delta_V})(1 - e^{-\Delta_W})(1 + t^2)}. \end{aligned} \quad (\text{F.22})$$

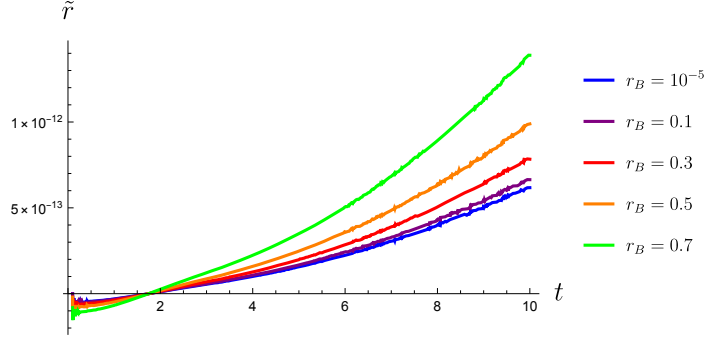


Figure 16. Real part of the relative difference between the out of time order correlator with the perturbative y correction (F.21) and the one in the seed theory (F.22), in terms of the ratio \tilde{r} (F.23), and the radial cutoff r_B related to the deformation parameter through (F.8) as it approaches the horizon located at $r = 0$. We have taken $\Delta_V = 1$, $\Delta_W = 2$, $\beta = 0.01$, and different values of r_B . The numerical noise is produced by the relative phases in (F.21)

A comparison between the evolution of (F.21) and (F.22) is shown in Fig. 16 in terms of a ratio

$$\tilde{r} \equiv \text{Re}((\text{SC}(t) - \text{SC}_{\text{AGH}}(t))/\text{SC}_{\text{AGH}}(t)) \quad (\text{F.23})$$

We notice that the increased rate of growth of the OTOC (F.21) is not significantly impacted in the stretched horizon limit $y \rightarrow \frac{2\sqrt{2}\beta^4}{144\pi^2}$. Moreover, one can evaluate the scrambling time in this model, defined as the time scale associated to the exponential decay in (F.21); one finds that it is not significantly different from the one corresponding to (F.22) $t_{\text{sc}} = \left((1 - e^{-\Delta_V})(1 - e^{-\Delta_W})\right)^{-1/2}$, given that it is a $\mathcal{O}(1)$ value that remains below the time scale where SC and SC_{AGH} start differing substantially (see Fig. 16).

Krylov Spread Complexity Meanwhile, the expectation value of the chord number operator (3.38) in the state $e^{-\hat{H}_y \tau} |\Omega\rangle$ can be evaluated directly from (F.11) by taking a derivative in Δ_V and taking the limit $\Delta_V \rightarrow 0$ (see e.g. [71]). This results in:

$$\begin{aligned} \frac{1}{Z} \langle \Omega | e^{-\hat{H}_y \tau_2} \hat{n} e^{-\hat{H}_y \tau_1} | \Omega \rangle &= \sum_{n=0}^{\infty} n \langle \phi_n^{(y)}(\tau_2) | \Omega \rangle \langle \Omega | \phi_n^{(y)}(\tau_1) \rangle \\ &= \frac{\tau_1 \tau_2}{2} (1 + 2y(\tau_1 + \tau_2)) . \end{aligned} \quad (\text{F.24})$$

Its analytic continuation to Lorentzian signature (F.13) allow us to evaluate the spread complexity as

$$\langle n \rangle_y(t) = \frac{\langle \Omega | e^{-\hat{H}_y \tau_2} \hat{n} e^{-\hat{H}_y \tau_1} | \Omega \rangle}{\langle \Omega | e^{-\hat{H}_y \beta_y} | \Omega \rangle} = \frac{1}{2} t^2 (1 + 2y\beta) + \mathcal{O}(y^2) . \quad (\text{F.25})$$

Note that the rate of growth of $\langle n \rangle_y(t)$ is faster when $y \rightarrow \frac{\sqrt{2}\beta^4}{144\pi^2}$ (i.e. the stretched horizon limit), similar to our results in the main text. In contrast, the thermodynamic properties in Fig. 14 do not display an enhancement in the same limit. Perhaps this is expected since [1]

associates the enhanced growth of observables in time with a hyperfast scrambling of information, which would not be exhibited in generic integrable models, such as this one. It had been noticed in [92] that the model proposed in [184] displays quite different observables with respect to the $\lambda \rightarrow 0$ limit in the sine dilaton gravity model, which should still describe the DSSYK model at high temperatures, without the Heisenberg algebra limit (F.1). Therefore, our findings in this section compared to Secs. 2.3 add further contrast between these two approaches, as different observables display rather different behaviors in the stretched horizon limit.

G First Law of Thermodynamics at Finite Cutoff

Motivated by recent developments on black hole thermodynamics in finite cutoff holography [320], we study the first law of thermodynamics in the deformed DSSYK model based on our results in Sec. 2.

We specialize in $T^2(+\Lambda_1)$ deformations, where the relevant deformation parameter $\eta = \pm 1$ (2.17). Let us use the semiclassical entropy in (2.25) to express the energy spectrum in (2.21) ($\eta = +1$) for the T^2 deformation, and (2.23) ($\eta = -1$) for the $T^2 + \Lambda_1$ deformation. This results in

$$E_y^\eta = \frac{1}{y} \left(1 - \eta \sqrt{\eta \left(1 - \frac{2y}{\pi V \sqrt{\lambda(1-q)}} \sin \sqrt{\frac{\lambda(S_0 - S)}{2}} \right)} \right), \quad (\text{G.1})$$

where we have defined $V \equiv \frac{2\pi}{f}$. By taking variations with respect to each of the parameters in (G.1) we can write the extended first law for the deformed DSSYK model as

$$dE_y = P_y dV + (\beta_y)^{-1} dS + \tilde{\mu}_y d\lambda + \nu_y dy, \quad (\text{G.2})$$

$$P_y \equiv - \frac{\eta^2 \sin \left(\frac{\sqrt{\lambda(S_0 - S)}}{\sqrt{2}} \right)}{\pi V^2 \sqrt{\lambda(1-q)} \sqrt{\eta - \frac{2\eta y \sin \left(\frac{\sqrt{\lambda(S_0 - S)}}{\sqrt{2}} \right)}{\pi V \sqrt{\lambda(1-q)}}}}, \quad (\text{G.3})$$

$$\tilde{\mu}_y \equiv - \frac{\eta^2 q \left(\frac{2(\lambda q - q + 1) \sqrt{\lambda(S_0 - S)} \sin \left(\frac{\sqrt{\lambda(S_0 - S)}}{\sqrt{2}} \right)}{q} + \frac{\sqrt{2} \lambda (1-q) (S - S_0) \cos \left(\frac{\sqrt{\lambda(S_0 - S)}}{\sqrt{2}} \right)}{q} \right)}{4\sqrt{\pi} \lambda (1-q) V \sqrt{\lambda(1-q)} \sqrt{\lambda(S_0 - S)} \sqrt{\pi \eta - \frac{2\eta y \sin \left(\frac{\sqrt{\lambda(S_0 - S)}}{\sqrt{2}} \right)}{V \sqrt{\lambda(1-q)}}}}, \quad (\text{G.4})$$

$$\nu_y \equiv \frac{\eta \sqrt{\eta - \frac{2\eta y \sin \left(\frac{\sqrt{\lambda(S_0 - S)}}{\sqrt{2}} \right)}{\pi V \sqrt{\lambda(1-q)}}} - 1}{y^2} + \frac{\eta^2 \sin \left(\frac{\sqrt{\lambda(S_0 - S)}}{\sqrt{2}} \right)}{\pi V y \sqrt{\lambda(1-q)} \sqrt{\eta - \frac{2\eta y \sin \left(\frac{\sqrt{\lambda(S_0 - S)}}{\sqrt{2}} \right)}{\pi V \sqrt{\lambda(1-q)}}}}, \quad (\text{G.5})$$

while β_y appears in (2.26). One may interpret $\tilde{\mu}_y$ as a chemical potential associated with variations in the parameter λ (3.6) for a fixed deformation parameter y ; and similarly for ν_y , where y is allowed to vary instead. Note that the notation suggests that V and P_y are analogs to thermodynamic volumes and pressures in the bulk [320]; however, they are viewed only as definitions of different combinations of parameters from our analysis.

References

- [1] L. Susskind, *Entanglement and Chaos in De Sitter Space Holography: An SYK Example*, *JHAP* **1** (2021) 1 [2109.14104].
- [2] J.M. Maldacena, *The Large N limit of superconformal field theories and supergravity*, *Adv. Theor. Math. Phys.* **2** (1998) 231 [hep-th/9711200].
- [3] A.B. Zamolodchikov, *Expectation value of composite field T anti- T in two-dimensional quantum field theory*, hep-th/0401146.
- [4] F.A. Smirnov and A.B. Zamolodchikov, *On space of integrable quantum field theories*, *Nucl. Phys. B* **915** (2017) 363 [1608.05499].
- [5] A. Cavaglià, S. Negro, I.M. Szécsényi and R. Tateo, *$T\bar{T}$ -deformed 2D Quantum Field Theories*, *JHEP* **10** (2016) 112 [1608.05534].
- [6] S. Dubovsky, R. Flauger and V. Gorbenko, *Solving the Simplest Theory of Quantum Gravity*, *JHEP* **09** (2012) 133 [1205.6805].
- [7] S. Dubovsky, V. Gorbenko and M. Mirbabayi, *Natural Tuning: Towards A Proof of Concept*, *JHEP* **09** (2013) 045 [1305.6939].
- [8] E. Tsoiakidis, *Massive gravity generalization of $T\bar{T}$ deformations*, *JHEP* **09** (2024) 167 [2405.07967].
- [9] S. Dubovsky, V. Gorbenko and M. Mirbabayi, *Asymptotic fragility, near AdS_2 holography and $T\bar{T}$* , *JHEP* **09** (2017) 136 [1706.06604].
- [10] S. Dubovsky, V. Gorbenko and G. Hernández-Chifflet, *$T\bar{T}$ partition function from topological gravity*, *JHEP* **09** (2018) 158 [1805.07386].
- [11] J. Cardy, *The $T\bar{T}$ deformation of quantum field theory as random geometry*, *JHEP* **10** (2018) 186 [1801.06895].
- [12] O. Aharony, S. Datta, A. Giveon, Y. Jiang and D. Kutasov, *Modular invariance and uniqueness of $T\bar{T}$ deformed CFT*, *JHEP* **01** (2019) 086 [1808.02492].
- [13] R. Conti, L. Iannella, S. Negro and R. Tateo, *Generalised Born-Infeld models, Lax operators and the $T\bar{T}$ perturbation*, *JHEP* **11** (2018) 007 [1806.11515].
- [14] R. Conti, S. Negro and R. Tateo, *The $T\bar{T}$ perturbation and its geometric interpretation*, *JHEP* **02** (2019) 085 [1809.09593].
- [15] A.J. Tolley, *$T\bar{T}$ deformations, massive gravity and non-critical strings*, *JHEP* **06** (2020) 050 [1911.06142].
- [16] G. Jafari, A. Naseh and H. Zolfi, *Path Integral Optimization for $T\bar{T}$ Deformation*, *Phys. Rev. D* **101** (2020) 026007 [1909.02357].

- [17] Y. Jiang, *A pedagogical review on solvable irrelevant deformations of 2D quantum field theory*, *Commun. Theor. Phys.* **73** (2021) 057201 [[1904.13376](#)].
- [18] S. He, Y. Li, H. Ouyang and Y. Sun, *$T\bar{T}$ Deformation: Introduction and Some Recent Advances*, [2503.09997](#).
- [19] M. Guica, *From black holes to solvable irrelevant deformations and back*, [2512.23620](#).
- [20] A. Giveon, N. Itzhaki and D. Kutasov, *$T\bar{T}$ and LST*, *JHEP* **07** (2017) 122 [[1701.05576](#)].
- [21] L. Apolo, S. Detournay and W. Song, *TsT, $T\bar{T}$ and black strings*, *JHEP* **06** (2020) 109 [[1911.12359](#)].
- [22] T. Araujo, E.Ó. Colgáin, Y. Sakatani, M.M. Sheikh-Jabbari and H. Yavartanoo, *Holographic integration of $T\bar{T}$ & $J\bar{T}$ via $O(d, d)$* , *JHEP* **03** (2019) 168 [[1811.03050](#)].
- [23] L. McGough, M. Mezei and H. Verlinde, *Moving the CFT into the bulk with $T\bar{T}$* , *JHEP* **04** (2018) 010 [[1611.03470](#)].
- [24] L. Apolo, P.-X. Hao, W.-X. Lai and W. Song, *Extremal surfaces in glue-on AdS/ $T\bar{T}$ holography*, *JHEP* **01** (2024) 054 [[2311.04883](#)].
- [25] L. Apolo, P.-X. Hao, W.-X. Lai and W. Song, *Glue-on AdS holography for $T\bar{T}$ -deformed CFTs*, *JHEP* **06** (2023) 117 [[2303.04836](#)].
- [26] M. Guica and R. Monten, *$T\bar{T}$ and the mirage of a bulk cutoff*, *SciPost Phys.* **10** (2021) 024 [[1906.11251](#)].
- [27] T. Hartman, J. Kruthoff, E. Shaghoulian and A. Tajdini, *Holography at finite cutoff with a T^2 deformation*, *JHEP* **03** (2019) 004 [[1807.11401](#)].
- [28] M. Taylor, *TT deformations in general dimensions*, [1805.10287](#).
- [29] T. Morone, S. Negro and R. Tateo, *Gravity and $T\bar{T}$ flows in higher dimensions*, *Nucl. Phys. B* **1005** (2024) 116605 [[2401.16400](#)].
- [30] G. Bonelli, N. Doroud and M. Zhu, *$T\bar{T}$ -deformations in closed form*, *JHEP* **06** (2018) 149 [[1804.10967](#)].
- [31] C. Ferko, J. Hou, T. Morone, G. Tartaglino-Mazzucchelli and R. Tateo, *TT^- -like Flows of Yang-Mills Theories*, *Phys. Rev. Lett.* **134** (2025) 101603 [[2409.18740](#)].
- [32] D.J. Gross, J. Kruthoff, A. Rolph and E. Shaghoulian, *$T\bar{T}$ in AdS_2 and Quantum Mechanics*, *Phys. Rev. D* **101** (2020) 026011 [[1907.04873](#)].
- [33] D.J. Gross, J. Kruthoff, A. Rolph and E. Shaghoulian, *Hamiltonian deformations in quantum mechanics, $T\bar{T}$, and the SYK model*, *Phys. Rev. D* **102** (2020) 046019 [[1912.06132](#)].
- [34] L.V. Iliesiu, J. Kruthoff, G.J. Turiaci and H. Verlinde, *JT gravity at finite cutoff*, *SciPost Phys.* **9** (2020) 023 [[2004.07242](#)].
- [35] C.V. Johnson and F. Rosso, *Solving Puzzles in Deformed JT Gravity: Phase Transitions and Non-Perturbative Effects*, *JHEP* **04** (2021) 030 [[2011.06026](#)].
- [36] F. Rosso, *$T\bar{T}$ deformation of random matrices*, *Phys. Rev. D* **103** (2021) 126017 [[2012.11714](#)].
- [37] L. Griguolo, R. Panerai, J. Papalini and D. Seminara, *Nonperturbative effects and resurgence in Jackiw-Teitelboim gravity at finite cutoff*, *Phys. Rev. D* **105** (2022) 046015 [[2106.01375](#)].

- [38] S.E. Aguilar-Gutierrez, A. Svesko and M.R. Visser, $T\bar{T}$ deformations from AdS_2 to dS_2 , *JHEP* **01** (2025) 120 [[2410.18257](#)].
- [39] S.E. Aguilar-Gutierrez, T^2 deformations in the double-scaled SYK model: Stretched horizon thermodynamics, [2410.18303](#).
- [40] S. Ebert, C. Ferko, H.-Y. Sun and Z. Sun, $T\bar{T}$ in JT Gravity and BF Gauge Theory, *SciPost Phys.* **13** (2022) 096 [[2205.07817](#)].
- [41] S. Ebert, C. Ferko, H.-Y. Sun and Z. Sun, $T\bar{T}$ deformations of supersymmetric quantum mechanics, *JHEP* **08** (2022) 121 [[2204.05897](#)].
- [42] L. Griguolo, J. Papalini, L. Russo and D. Seminara, A new perspective on dilaton gravity at finite cutoff, [2512.21774](#).
- [43] E. Witten, Multitrace operators, boundary conditions, and AdS / CFT correspondence, [hep-th/0112258](#).
- [44] A. Parvizi, M.M. Sheikh-Jabbari and V. Taghiloo, Freelance Holography, Part I: Setting Boundary Conditions Free in Gauge/Gravity Correspondence, *SciPost Phys.* **19** (2025) 043 [[2503.09371](#)].
- [45] A. Parvizi, M.M. Sheikh-Jabbari and V. Taghiloo, Freelance Holography, Part II: Moving Boundary in Gauge/Gravity Correspondence, [2503.09372](#).
- [46] E. Coleman and V. Shyam, Conformal boundary conditions from cutoff AdS_3 , *JHEP* **09** (2021) 079 [[2010.08504](#)].
- [47] K. Allameh and E. Shaghoulain, Timelike Liouville theory and AdS_3 gravity at finite cutoff, [2508.03236](#).
- [48] M.M. Sheikh-Jabbari and V. Taghiloo, AdS_3 Freelance Holography, A Detailed Analysis, [2510.10692](#).
- [49] X.-Y. Ran, F. Hao and H. Ouyang, Holography for stress-energy tensor flows, [2508.12275](#).
- [50] S. Sachdev and J. Ye, Gapless spin-fluid ground state in a random quantum heisenberg magnet, *Physical Review Letters* **70** (1993) 3339–3342.
- [51] A. Kitaev, “Hidden Correlations in the Hawking Radiation and Thermal Noise.” <https://www.youtube.com/watch?v=0Q9qN8j7EZI>, November, 2015.
- [52] A. Kitaev, “A simple model of quantum holography (part 1).” <http://online.kitp.ucsb.edu/online/entangled15/kitaev/>, April, 2015.
- [53] A. Kitaev, “A simple model of quantum holography (part 2).” <http://online.kitp.ucsb.edu/online/entangled15/kitaev2/>, April, 2015.
- [54] J.S. Cotler, G. Gur-Ari, M. Hanada, J. Polchinski, P. Saad, S.H. Shenker et al., Black Holes and Random Matrices, *JHEP* **05** (2017) 118 [[1611.04650](#)].
- [55] L. Erdős and D. Schröder, Phase Transition in the Density of States of Quantum Spin Glasses, *Math. Phys. Anal. Geom.* **17** (2014) 441 [[1407.1552](#)].
- [56] M. Berkooz, M. Isachenkov, V. Narovlansky and G. Torrents, Towards a full solution of the large N double-scaled SYK model, *JHEP* **03** (2019) 079 [[1811.02584](#)].

- [57] M. Berkooz, P. Narayan and J. Simon, *Chord diagrams, exact correlators in spin glasses and black hole bulk reconstruction*, *JHEP* **08** (2018) 192 [[1806.04380](#)].
- [58] H.W. Lin, *The bulk Hilbert space of double scaled SYK*, *JHEP* **11** (2022) 060 [[2208.07032](#)].
- [59] J. Xu, *Von Neumann Algebras in Double-Scaled SYK*, [2403.09021](#).
- [60] X. Cao and P. Gao, *Single-Sided Black Holes in Double-Scaled SYK Model and No Man's Island*, [2511.01978](#).
- [61] H.W. Lin and D. Stanford, *A symmetry algebra in double-scaled SYK*, *SciPost Phys.* **15** (2023) 234 [[2307.15725](#)].
- [62] A. Almheiri and F.K. Popov, *Holography on the quantum disk*, *JHEP* **06** (2024) 070 [[2401.05575](#)].
- [63] K. Schouten and M. Isachenkov, *The von Neumann algebraic quantum group $SU_q(1,1) \rtimes \mathbb{Z}_2$ and the DSSYK model*, [2512.10101](#).
- [64] A. Belaey, T.G. Mertens and T. Tappeiner, *Quantum group origins of edge states in double-scaled SYK*, [2503.20691](#).
- [65] M. Berkooz, M. Isachenkov, M. Isachenkov, P. Narayan and V. Narovlansky, *Quantum groups, non-commutative AdS_2 , and chords in the double-scaled SYK model*, *JHEP* **08** (2023) 076 [[2212.13668](#)].
- [66] A. Blommaert, T.G. Mertens and S. Yao, *Dynamical actions and q -representation theory for double-scaled SYK*, *JHEP* **02** (2024) 067 [[2306.00941](#)].
- [67] J. van der Heijden, E. Verlinde and J. Xu, *Quantum Symmetry and Geometry in Double-Scaled SYK*, [2511.08743](#).
- [68] E. Rabinovici, A. Sánchez-Garrido, R. Shir and J. Sonner, *A bulk manifestation of Krylov complexity*, *JHEP* **08** (2023) 213 [[2305.04355](#)].
- [69] M. Ambrosini, E. Rabinovici and J. Sonner, *Holography of K -complexity: Switchbacks and Shockwaves*, [2510.17975](#).
- [70] M. Ambrosini, E. Rabinovici, A. Sánchez-Garrido, R. Shir and J. Sonner, *Operator K -complexity in DSSYK: Krylov complexity equals bulk length*, [2412.15318](#).
- [71] M.P. Heller, J. Papalini and T. Schuhmann, *Krylov spread complexity as holographic complexity beyond JT gravity*, [2412.17785](#).
- [72] S.E. Aguilar-Gutierrez, *Building the holographic dictionary of the DSSYK from chords, complexity \mathcal{E} wormholes with matter*, *JHEP* **10** (2025) 221 [[2505.22716](#)].
- [73] S.E. Aguilar-Gutierrez and J. Xu, *Geometry of Chord Intertwiner, Multiple Shocks and Switchback in Double-Scaled SYK*, *JHEP* **02** (2026) 246 [[2506.19013](#)].
- [74] S.E. Aguilar-Gutierrez, *Symmetry sectors in chord space and relational holography in the DSSYK. Lessons from branes, wormholes, and de Sitter space*, *JHEP* **10** (2025) 044 [[2506.21447](#)].
- [75] V. Balasubramanian, J.M. Magan, P. Nandi and Q. Wu, *Spread complexity and the saturation of wormhole size*, [2412.02038](#).

- [76] S. Forste, Y. Kruse and S. Natu, *Grand Canonical vs Canonical Krylov Complexity in Double-Scaled Complex SYK Model*, [2512.07715](#).
- [77] S.E. Aguilar-Gutierrez, *Evolution With(out) Time: Relational Holography & BPS Complexity Growth in $\mathcal{N} = 2$ Double-Scaled SYK*, *JHEP* **02** (2026) 229 [[2510.11777](#)].
- [78] B. Bhattacharjee, P. Nandy and T. Pathak, *Krylov complexity in large q and double-scaled SYK model*, *JHEP* **08** (2023) 099 [[2210.02474](#)].
- [79] P. Nandy, *Tridiagonal Hamiltonians modeling the density of states of the Double-Scaled SYK model*, [2410.07847](#).
- [80] T. Anegawa and R. Watanabe, *Krylov complexity of fermion chain in double-scaled SYK and power spectrum perspective*, [2407.13293](#).
- [81] S.E. Aguilar-Gutierrez, *Towards complexity in de Sitter space from the double-scaled Sachdev-Ye-Kitaev model*, *JHEP* **10** (2024) 107 [[2403.13186](#)].
- [82] M.P. Heller, F. Ori, J. Papalini, T. Schuhmann and M.-T. Wang, *De Sitter holographic complexity from Krylov complexity in DSSYK*, [2510.13986](#).
- [83] Y. Fu, H.-S. Jeong, K.-Y. Kim and J.F. Pedraza, *Toward Krylov-based holography in double-scaled SYK*, [2510.22658](#).
- [84] S.E. Aguilar-Gutierrez, R.N. Das, J. Erdmenger and Z.-Y. Xian, *Probing the Chaos to Integrability Transition in Double-Scaled SYK*, [2601.09801](#).
- [85] J. Xu, *On Chord Dynamics and Complexity Growth in Double-Scaled SYK*, [2411.04251](#).
- [86] D.E. Parker, X. Cao, A. Avdoshkin, T. Scaffidi and E. Altman, *A Universal Operator Growth Hypothesis*, *Phys. Rev. X* **9** (2019) 041017 [[1812.08657](#)].
- [87] V. Balasubramanian, P. Caputa, J.M. Magan and Q. Wu, *Quantum chaos and the complexity of spread of states*, *Phys. Rev. D* **106** (2022) 046007 [[2202.06957](#)].
- [88] P. Nandy, A.S. Matsoukas-Roubeas, P. Martínez-Azcona, A. Dymarsky and A. del Campo, *Quantum dynamics in Krylov space: Methods and applications*, *Phys. Rept.* **1125-1128** (2025) 1 [[2405.09628](#)].
- [89] S. Baiguera, V. Balasubramanian, P. Caputa, S. Chapman, J. Haferkamp, M.P. Heller et al., *Quantum complexity in gravity, quantum field theory, and quantum information science*, [2503.10753](#).
- [90] E. Rabinovici, A. Sánchez-Garrido, R. Shir and J. Sonner, *Krylov Complexity*, [2507.06286](#).
- [91] J. Boruch, H.W. Lin and C. Yan, *Exploring supersymmetric wormholes in $\mathcal{N} = 2$ SYK with chords*, *JHEP* **12** (2023) 151 [[2308.16283](#)].
- [92] A. Blommaert, T.G. Mertens and J. Papalini, *The dilaton gravity hologram of double-scaled SYK*, *JHEP* **06** (2025) 050 [[2404.03535](#)].
- [93] M. Berkooz, N. Brukner, S.F. Ross and M. Watanabe, *Going beyond ER=EPR in the SYK model*, *JHEP* **08** (2022) 051 [[2202.11381](#)].
- [94] A. Blommaert, A. Levine, T.G. Mertens, J. Papalini and K. Parmentier, *Wormholes, branes and finite matrices in sine dilaton gravity*, *JHEP* **09** (2025) 123 [[2501.17091](#)].

- [95] H. Verlinde, *Double-scaled SYK, chords and de Sitter gravity*, *JHEP* **03** (2025) 076 [[2402.00635](#)].
- [96] H. Verlinde and M. Zhang, *SYK Correlators from 2D Liouville-de Sitter Gravity*, [2402.02584](#).
- [97] L. Susskind, *Computational Complexity and Black Hole Horizons*, *Fortsch. Phys.* **64** (2016) 24 [[1403.5695](#)].
- [98] H. Tang, *Entanglement entropy in type II₁ von Neumann algebra: examples in Double-Scaled SYK*, [2404.02449](#).
- [99] S.E. Aguilar-Gutierrez, *Cosmological Entanglement Entropy from the von Neumann Algebra of Double-Scaled SYK & Its Connection with Krylov Complexity*, [2511.03779](#).
- [100] S. Ryu and T. Takayanagi, *Holographic derivation of entanglement entropy from AdS/CFT*, *Phys. Rev. Lett.* **96** (2006) 181602 [[hep-th/0603001](#)].
- [101] S. Ryu and T. Takayanagi, *Aspects of Holographic Entanglement Entropy*, *JHEP* **08** (2006) 045 [[hep-th/0605073](#)].
- [102] T. Nishioka, S. Ryu and T. Takayanagi, *Holographic Entanglement Entropy: An Overview*, *J. Phys. A* **42** (2009) 504008 [[0905.0932](#)].
- [103] M. Rangamani and T. Takayanagi, *Holographic Entanglement Entropy*, vol. 931, Springer (2017), [10.1007/978-3-319-52573-0](#), [[1609.01287](#)].
- [104] B. Chen, *Holographic Entanglement Entropy: A Topical Review*, *Commun. Theor. Phys.* **71** (2019) 837.
- [105] D. Harlow, *Jerusalem Lectures on Black Holes and Quantum Information*, *Rev. Mod. Phys.* **88** (2016) 015002 [[1409.1231](#)].
- [106] V.E. Hubeny, M. Rangamani and T. Takayanagi, *A Covariant holographic entanglement entropy proposal*, *JHEP* **07** (2007) 062 [[0705.0016](#)].
- [107] T. Faulkner, A. Lewkowycz and J. Maldacena, *Quantum corrections to holographic entanglement entropy*, *JHEP* **11** (2013) 074 [[1307.2892](#)].
- [108] N. Engelhardt and A.C. Wall, *Quantum Extremal Surfaces: Holographic Entanglement Entropy beyond the Classical Regime*, *JHEP* **01** (2015) 073 [[1408.3203](#)].
- [109] A. Blommaert, A. Levine, T.G. Mertens, J. Papalini and K. Parmentier, *An entropic puzzle in periodic dilaton gravity and DSSYK*, *JHEP* **07** (2025) 093 [[2411.16922](#)].
- [110] A. Blommaert and A. Levine, *Sphere amplitudes and observing the universe's size*, [2505.24633](#).
- [111] L. Bossi, L. Griguolo, J. Papalini, L. Russo and D. Seminara, *Sine-dilaton gravity vs double-scaled SYK: exploring one-loop quantum corrections*, [2411.15957](#).
- [112] A. Blommaert, D. Tietto and H. Verlinde, *SYK collective field theory as complex Liouville gravity*, [2509.18462](#).
- [113] C. Cui and M. Rozali, *Splitting and gluing in sine-dilaton gravity: matter correlators and the wormhole Hilbert space*, [2509.01680](#).
- [114] M. Arundine, *The DSSYK Model: Charge and Holography*, other thesis, Università di Pisa, 12, 2025, [[2512.21366](#)].

- [115] V. Narovlansky and H. Verlinde, *Double-scaled SYK and de Sitter Holography*, [2310.16994](#).
- [116] V. Narovlansky, *Towards a microscopic description of de Sitter dynamics*, [2506.02109](#).
- [117] D. Tietto and H. Verlinde, *A microscopic model of de Sitter spacetime with an observer*, [2502.03869](#).
- [118] L. Susskind, *De Sitter Space, Double-Scaled SYK, and the Separation of Scales in the Semiclassical Limit*, [2209.09999](#).
- [119] L. Susskind, *De Sitter Space has no Chords. Almost Everything is Confined.*, *JHAP* **3** (2023) 1 [[2303.00792](#)].
- [120] H. Lin and L. Susskind, *Infinite Temperature's Not So Hot*, [2206.01083](#).
- [121] A.A. Rahman, *dS JT Gravity and Double-Scaled SYK*, [2209.09997](#).
- [122] A.A. Rahman and L. Susskind, *Comments on a Paper by Narovlansky and Verlinde*, [2312.04097](#).
- [123] A.A. Rahman and L. Susskind, *p-Chords, Wee-Chords, and de Sitter Space*, [2407.12988](#).
- [124] A.A. Rahman and L. Susskind, *Infinite Temperature is Not So Infinite: The Many Temperatures of de Sitter Space*, [2401.08555](#).
- [125] Y. Sekino and L. Susskind, *Double-Scaled SYK, QCD, and the Flat Space Limit of de Sitter Space*, [2501.09423](#).
- [126] S. Miyashita, Y. Sekino and L. Susskind, *DSSYK at Infinite Temperature: The Flat-Space Limit and the 't Hooft Model*, [2506.18054](#).
- [127] A. Herderschee and J. Kudler-Flam, *Stringy algebras, stretched horizons, and quantum-connected wormholes*, [2510.01556](#).
- [128] A. Milekhin and J. Xu, *Revisiting Brownian SYK and its possible relations to de Sitter*, *JHEP* **10** (2024) 151 [[2312.03623](#)].
- [129] A. Milekhin and J. Xu, *On scrambling, temperature and superdiffusion in de Sitter space*, *JHEP* **07** (2025) 272 [[2403.13915](#)].
- [130] K. Okuyama, *de Sitter JT gravity from double-scaled SYK*, *JHEP* **08** (2025) 181 [[2505.08116](#)].
- [131] H. Yuan, X.-H. Ge and K.-Y. Kim, *Pole skipping in two-dimensional de Sitter spacetime and double-scaled SYK model*, *Phys. Rev. D* **112** (2025) 026022 [[2408.12330](#)].
- [132] E. Gubankova, S. Sachdev and G. Tarnopolsky, *Scaling limits of complex Sachdev-Ye-Kitaev models and holographic geometry*, [2512.05294](#).
- [133] Y. Ahn, S. Grozdanov, H.-S. Jeong and J.F. Pedraza, *Cosmological pole-skipping, shock waves and quantum chaotic dynamics of de Sitter horizons*, [2508.15589](#).
- [134] S. Collier, L. Eberhardt, B. Mühlmann and V.A. Rodriguez, *Complex Liouville String*, *Phys. Rev. Lett.* **134** (2025) 251602 [[2409.17246](#)].
- [135] S. Collier, L. Eberhardt, B. Mühlmann and V.A. Rodriguez, *The complex Liouville string: The worldsheet*, *SciPost Phys.* **19** (2025) 033 [[2409.18759](#)].
- [136] S. Collier, L. Eberhardt, B. Mühlmann and V.A. Rodriguez, *The complex Liouville string: The matrix integral*, *SciPost Phys.* **18** (2025) 154 [[2410.07345](#)].

- [137] S. Collier, L. Eberhardt, B. Mühlmann and V.A. Rodriguez, *The complex Liouville string: Worldsheet boundaries and non-perturbative effects*, *SciPost Phys.* **19** (2025) 034 [[2410.09179](#)].
- [138] S. Collier, L. Eberhardt and B. Mühlmann, *A microscopic realization of dS_3* , *SciPost Phys.* **18** (2025) 131 [[2501.01486](#)].
- [139] S. Collier, L. Eberhardt and B. Mühlmann, *The complex Liouville string: the gravitational path integral*, [2501.10265](#).
- [140] D.A. Roberts, D. Stanford and A. Streicher, *Operator growth in the SYK model*, *JHEP* **06** (2018) 122 [[1802.02633](#)].
- [141] R.C. Tolman, *On the extension of thermodynamics to general relativity*, *Proceedings of the National Academy of Sciences* **14** (1928) 268.
- [142] R.C. Tolman, *Thermodynamics and relativity*, *Science* **77** (1933) 291.
- [143] R. Tolman and P. Ehrenfest, *Temperature Equilibrium in a Static Gravitational Field*, *Phys. Rev.* **36** (1930) 1791.
- [144] J. Maldacena, S.H. Shenker and D. Stanford, *A bound on chaos*, *JHEP* **08** (2016) 106 [[1503.01409](#)].
- [145] E. Jørstad, R.C. Myers and S.-M. Ruan, *Holographic complexity in dS_{d+1}* , *JHEP* **05** (2022) 119 [[2202.10684](#)].
- [146] R. Jackiw, *Lower dimensional gravity*, *Nuclear Physics B* **252** (1985) 343.
- [147] C. Teitelboim, *Gravitation and hamiltonian structure in two spacetime dimensions*, *Physics Letters B* **126** (1983) 41.
- [148] S. Ali Ahmad, A. Almheiri and S. Lin, *$T\bar{T}$ and the black hole interior*, [2503.19854](#).
- [149] E. Silverstein and G. Torroba, *Timelike-bounded dS_4 holography from a solvable sector of the T^2 deformation*, [2409.08709](#).
- [150] J.-C. Chang, Y. He, Y.-X. Liu and Y. Sun, *Toward a Unified de Sitter Holography: A Composite $T\bar{T}$ and $T\bar{T} + \Lambda_2$ Flow*, [2511.16098](#).
- [151] V. Gorbenko, E. Silverstein and G. Torroba, *dS/dS and $T\bar{T}$* , *JHEP* **03** (2019) 085 [[1811.07965](#)].
- [152] V. Shyam, *$T\bar{T} + \Lambda_2$ deformed CFT on the stretched dS_3 horizon*, *JHEP* **04** (2022) 052 [[2106.10227](#)].
- [153] E. Coleman, E.A. Mazenc, V. Shyam, E. Silverstein, R.M. Soni, G. Torroba et al., *De Sitter microstates from $T\bar{T} + \Lambda_2$ and the Hawking-Page transition*, *JHEP* **07** (2022) 140 [[2110.14670](#)].
- [154] E. Silverstein, *Black hole to cosmic horizon microstates in string/M theory: timelike boundaries and internal averaging*, [2212.00588](#).
- [155] G. Batra, G.B. De Luca, E. Silverstein, G. Torroba and S. Yang, *Bulk-local dS_3 holography: the Matter with $T\bar{T} + \Lambda_2$* , [2403.01040](#).
- [156] D. Anninos, D.A. Galante and C. Maneerat, *Cosmological observatories*, *Class. Quant. Grav.* **41** (2024) 165009 [[2402.04305](#)].

- [157] S. Chapman, D.A. Galante and E.D. Kramer, *Holographic complexity and de Sitter space*, *JHEP* **02** (2022) 198 [[2110.05522](#)].
- [158] D. Galante, *Geodesics, complexity and holography in (A)dS₂*, *PoS CORFU2021* (2022) 359.
- [159] R. Auzzi, G. Nardelli, G.P. Ungureanu and N. Zenoni, *Volume complexity of dS bubbles*, *Phys. Rev. D* **108** (2023) 026006 [[2302.03584](#)].
- [160] T. Anegawa, N. Iizuka, S.K. Sake and N. Zenoni, *Is action complexity better for de Sitter space in Jackiw-Teitelboim gravity?*, *JHEP* **06** (2023) 213 [[2303.05025](#)].
- [161] T. Anegawa and N. Iizuka, *Shock waves and delay of hyperfast growth in de Sitter complexity*, *JHEP* **08** (2023) 115 [[2304.14620](#)].
- [162] S. Baiguera, R. Berman, S. Chapman and R.C. Myers, *The cosmological switchback effect*, *JHEP* **07** (2023) 162 [[2304.15008](#)].
- [163] S.E. Aguilar-Gutierrez, M.P. Heller and S. Van der Schueren, *Complexity equals anything can grow forever in de Sitter space*, *Phys. Rev. D* **110** (2024) 066009 [[2305.11280](#)].
- [164] S.E. Aguilar-Gutierrez, A.K. Patra and J.F. Pedraza, *Entangled universes in dS wedge holography*, *JHEP* **10** (2023) 156 [[2308.05666](#)].
- [165] S.E. Aguilar-Gutierrez, *C=Anything and the switchback effect in Schwarzschild-de Sitter space*, *JHEP* **03** (2024) 062 [[2309.05848](#)].
- [166] S.E. Aguilar-Gutierrez, S. Baiguera and N. Zenoni, *Holographic complexity of the extended Schwarzschild-de Sitter space*, [2402.01357](#).
- [167] L. Susskind, *Black Holes Hint towards De Sitter Matrix Theory*, *Universe* **9** (2023) 368 [[2109.01322](#)].
- [168] E. Shaghoulian, *The central dogma and cosmological horizons*, *JHEP* **01** (2022) 132 [[2110.13210](#)].
- [169] E. Shaghoulian and L. Susskind, *Entanglement in De Sitter space*, *JHEP* **08** (2022) 198 [[2201.03603](#)].
- [170] V. Franken, H. Partouche, F. Rondeau and N. Toumbas, *Bridging the static patches: de Sitter holography and entanglement*, *JHEP* **08** (2023) 074 [[2305.12861](#)].
- [171] V. Franken, *de Sitter Connectivity from Holographic Entanglement*, in *23rd Hellenic School and Workshops on Elementary Particle Physics and Gravity*, 3, 2024 [[2403.14889](#)].
- [172] D. Anninos and E. Harris, *Interpolating geometries and the stretched dS₂ horizon*, *JHEP* **11** (2022) 166 [[2209.06144](#)].
- [173] R. Arnowitt and S. Deser, *Quantum Theory of Gravitation: General Formulation and Linearized Theory*, *Phys. Rev.* **113** (1959) 745.
- [174] R.L. Arnowitt, S. Deser and C.W. Misner, *Canonical variables for general relativity*, *Phys. Rev.* **117** (1960) 1595.
- [175] R.L. Arnowitt, S. Deser and C.W. Misner, *Gravitational-electromagnetic coupling and the classical self-energy problem*, *Phys. Rev.* **120** (1960) 313.
- [176] R. Arnowitt, S. Deser and C.W. Misner, *Interior Schwarzschild solutions and interpretation of source terms*, *Phys. Rev.* **120** (1960) 321.

- [177] R. Arnowitt, S. Deser and C.W. Misner, *Energy and the Criteria for Radiation in General Relativity*, *Phys. Rev.* **118** (1960) 1100.
- [178] R.L. Arnowitt, S. Deser and C.W. Misner, *Coordinate invariance and energy expressions in general relativity*, *Phys. Rev.* **122** (1961) 997.
- [179] R.L. Arnowitt, S. Deser and C.W. Misner, *Wave zone in general relativity*, *Phys. Rev.* **121** (1961) 1556.
- [180] G. Araujo-Regado, R. Khan and A.C. Wall, *Cauchy slice holography: a new AdS/CFT dictionary*, *JHEP* **03** (2023) 026 [[2204.00591](#)].
- [181] G. Araujo-Regado, *Holographic Cosmology on Closed Slices in 2+1 Dimensions*, [2212.03219](#).
- [182] R.M. Soni and A.C. Wall, *A New Covariant Entropy Bound from Cauchy Slice Holography*, [2407.16769](#).
- [183] G. Araujo-Regado, A. Thavanesan and A.C. Wall, *Holographic Cosmology at Finite Time*, [2511.04511](#).
- [184] A. Almheiri, A. Goel and X.-Y. Hu, *Quantum gravity of the Heisenberg algebra*, *JHEP* **08** (2024) 098 [[2403.18333](#)].
- [185] C. Zhang and W. Cai, *$T\bar{T}$ deformation on non-Hermitian two coupled SYK model*, [2312.03433](#).
- [186] J.A. Wheeler, *SUPERSPACE AND THE NATURE OF QUANTUM GEOMETRODYNAMICS*, *Adv. Ser. Astrophys. Cosmol.* **3** (1987) 27.
- [187] B.S. DeWitt, *Quantum Theory of Gravity. 1. The Canonical Theory*, *Phys. Rev.* **160** (1967) 1113.
- [188] J.D. Brown and J.W. York, Jr., *Quasilocal energy and conserved charges derived from the gravitational action*, *Phys. Rev. D* **47** (1993) 1407 [[gr-qc/9209012](#)].
- [189] D. Grumiller and R. McNees, *Thermodynamics of black holes in two (and higher) dimensions*, *JHEP* **04** (2007) 074 [[hep-th/0703230](#)].
- [190] J. Kruthoff and O. Parrikar, *On the flow of states under $T\bar{T}$* , [2006.03054](#).
- [191] A. Goel, V. Narovlansky and H. Verlinde, *Semiclassical geometry in double-scaled SYK*, *JHEP* **11** (2023) 093 [[2301.05732](#)].
- [192] A. Svesko, E. Verheijden, E.P. Verlinde and M.R. Visser, *Quasi-local energy and microcanonical entropy in two-dimensional nearly de Sitter gravity*, *JHEP* **08** (2022) 075 [[2203.00700](#)].
- [193] J.L.F. Barbon and E. Rabinovici, *Remarks on the thermodynamic stability of $T\bar{T}$ deformations*, *J. Phys. A* **53** (2020) 424001 [[2004.10138](#)].
- [194] J. Maldacena and D. Stanford, *Remarks on the Sachdev-Ye-Kitaev model*, *Phys. Rev. D* **94** (2016) 106002 [[1604.07818](#)].
- [195] G. Parisi, *D-dimensional arrays of josephson junctions, spin glasses and q-deformed harmonic oscillators*, *Journal of Physics A: Mathematical and General* **27** (1994) 7555–7568.
- [196] M. Berkooz, N. Brukner, Y. Jia and O. Mamroud, *From Chaos to Integrability in Double Scaled SYK*, [2403.01950](#).

- [197] M. Berkooz, N. Brukner, Y. Jia and O. Mamroud, *A Path Integral for Chord Diagrams and Chaotic-Integrable Transitions in Double Scaled SYK*, [2403.05980](#).
- [198] P. Gao, H. Lin and C. Peng, *D-commuting SYK model: building quantum chaos from integrable blocks*, [2411.12806](#).
- [199] M. Berkooz and O. Mamroud, *A cordial introduction to double scaled SYK*, *Rept. Prog. Phys.* **88** (2025) 036001 [[2407.09396](#)].
- [200] J. Erdmenger, S.-K. Jian and Z.-Y. Xian, *Universal chaotic dynamics from Krylov space*, *JHEP* **08** (2023) 176 [[2303.12151](#)].
- [201] P. Caputa, J.M. Magan, D. Patramanis and E. Tonni, *Krylov complexity of modular Hamiltonian evolution*, *Phys. Rev. D* **109** (2024) 086004 [[2306.14732](#)].
- [202] M. Ismail, *Classical and quantum orthogonal polynomials in one variable*, vol. 13, Cambridge university press (2005).
- [203] D. Stanford and L. Susskind, *Complexity and Shock Wave Geometries*, *Phys. Rev. D* **90** (2014) 126007 [[1406.2678](#)].
- [204] L. Susskind and Y. Zhao, *Switchbacks and the Bridge to Nowhere*, [1408.2823](#).
- [205] A. Faraji Astaneh, *Quantum Complexity of $T\bar{T}$ -deformation and Its Implications*, [2408.06055](#).
- [206] P. Kraus, J. Liu and D. Marolf, *Cutoff AdS_3 versus the $T\bar{T}$ deformation*, *JHEP* **07** (2018) 027 [[1801.02714](#)].
- [207] D. Basu, A. Chandra and Q. Wen, *Butterfly effect and $T\bar{T}$ -deformation*, [2505.14331](#).
- [208] S.H. Shenker and D. Stanford, *Multiple Shocks*, *JHEP* **12** (2014) 046 [[1312.3296](#)].
- [209] E. Witten, *Gravity and the crossed product*, *JHEP* **10** (2022) 008 [[2112.12828](#)].
- [210] V. Chandrasekaran, R. Longo, G. Penington and E. Witten, *An algebra of observables for de Sitter space*, *JHEP* **02** (2023) 082 [[2206.10780](#)].
- [211] V. Chandrasekaran, G. Penington and E. Witten, *Large N algebras and generalized entropy*, *JHEP* **04** (2023) 009 [[2209.10454](#)].
- [212] K. Jensen, J. Sorce and A.J. Speranza, *Generalized entropy for general subregions in quantum gravity*, *JHEP* **12** (2023) 020 [[2306.01837](#)].
- [213] J. Kudler-Flam, S. Leutheusser and G. Satishchandran, *Generalized black hole entropy is von Neumann entropy*, *Phys. Rev. D* **111** (2025) 025013 [[2309.15897](#)].
- [214] E. Witten, *APS Medal for Exceptional Achievement in Research: Invited article on entanglement properties of quantum field theory*, *Rev. Mod. Phys.* **90** (2018) 045003 [[1803.04993](#)].
- [215] J. Sorce, *Notes on the type classification of von Neumann algebras*, *Rev. Math. Phys.* **36** (2024) 2430002 [[2302.01958](#)].
- [216] H. Casini and M. Huerta, *Lectures on entanglement in quantum field theory*, *PoS TASI2021* (2023) 002 [[2201.13310](#)].
- [217] H. Liu, *Lectures on entanglement, von Neumann algebras, and emergence of spacetime*, in *Theoretical Advanced Study Institute in Elementary Particle Physics 2023: Aspects of Symmetry*, 10, 2025 [[2510.07017](#)].

- [218] I.E. Segal, *Irreducible representations of operator algebras*, *Bulletin of the American Mathematical Society* **53** (1947) 73.
- [219] I. Gelfand and M. Neumark, *On the imbedding of normed rings into the ring of operators in hilbert space*, *Mathematical collection* **12** (1943) 197.
- [220] G. Penington and E. Witten, *Algebras and States in JT Gravity*, [2301.07257](#).
- [221] A. Goel, H.T. Lam, G.J. Turiaci and H. Verlinde, *Expanding the Black Hole Interior: Partially Entangled Thermal States in SYK*, *JHEP* **02** (2019) 156 [[1807.03916](#)].
- [222] G. Wentzel, *Eine verallgemeinerung der quantenbedingungen für die zwecke der wellenmechanik*, *Zeitschrift für Physik* **38** (1926) 518.
- [223] H.A. Kramers, *Wellenmechanik und halbzahlige quantisierung*, *Zeitschrift für Physik* **39** (1926) 828.
- [224] L. Brillouin, *La mécanique ondulatoire de schrödinger; une méthode générale de résolution par approximations successives*, *CR Acad. Sci* **183** (1926) 24.
- [225] A. Strominger, *The dS / CFT correspondence*, *JHEP* **10** (2001) 034 [[hep-th/0106113](#)].
- [226] E. Witten, *Quantum gravity in de Sitter space*, in *Strings 2001: International Conference*, 6, 2001 [[hep-th/0106109](#)].
- [227] M. Spradlin, A. Strominger and A. Volovich, *Les Houches lectures on de Sitter space*, in *Les Houches Summer School: Session 76: Euro Summer School on Unity of Fundamental Physics: Gravity, Gauge Theory and Strings*, pp. 423–453, 10, 2001 [[hep-th/0110007](#)].
- [228] R. Bousso, A. Maloney and A. Strominger, *Conformal vacua and entropy in de Sitter space*, *Phys. Rev. D* **65** (2002) 104039 [[hep-th/0112218](#)].
- [229] J.M. Maldacena, *Non-Gaussian features of primordial fluctuations in single field inflationary models*, *JHEP* **05** (2003) 013 [[astro-ph/0210603](#)].
- [230] M.A. Vasiliev, *Higher spin gauge theories: Star product and AdS space*, [hep-th/9910096](#).
- [231] M.A. Vasiliev, *Consistent equation for interacting gauge fields of all spins in (3+1)-dimensions*, *Phys. Lett. B* **243** (1990) 378.
- [232] D. Anninos, T. Hartman and A. Strominger, *Higher Spin Realization of the dS/CFT Correspondence*, *Class. Quant. Grav.* **34** (2017) 015009 [[1108.5735](#)].
- [233] G.S. Ng and A. Strominger, *State/Operator Correspondence in Higher-Spin dS/CFT*, *Class. Quant. Grav.* **30** (2013) 104002 [[1204.1057](#)].
- [234] D. Anninos, F. Denef and D. Harlow, *Wave function of Vasiliev’s universe: A few slices thereof*, *Phys. Rev. D* **88** (2013) 084049 [[1207.5517](#)].
- [235] Y. Hikida, T. Nishioka, T. Takayanagi and Y. Taki, *Holography in de Sitter Space via Chern-Simons Gauge Theory*, *Phys. Rev. Lett.* **129** (2022) 041601 [[2110.03197](#)].
- [236] Y. Hikida, T. Nishioka, T. Takayanagi and Y. Taki, *CFT duals of three-dimensional de Sitter gravity*, *JHEP* **05** (2022) 129 [[2203.02852](#)].
- [237] H.-Y. Chen and Y. Hikida, *Three-Dimensional de Sitter Holography and Bulk Correlators at Late Time*, *Phys. Rev. Lett.* **129** (2022) 061601 [[2204.04871](#)].

- [238] H.-Y. Chen, S. Chen and Y. Hikida, *Late-time correlation functions in dS_3/CFT_2 correspondence*, *JHEP* **02** (2023) 038 [[2210.01415](#)].
- [239] J.B. Hartle, S.W. Hawking and T. Hertog, *Quantum Probabilities for Inflation from Holography*, *JCAP* **01** (2014) 015 [[1207.6653](#)].
- [240] T. Hertog and J. Hartle, *Holographic No-Boundary Measure*, *JHEP* **05** (2012) 095 [[1111.6090](#)].
- [241] N. Bobev, T. Hertog, J. Hong, J. Karlsson and V. Reys, *Microscopics of de Sitter Entropy from Precision Holography*, *Phys. Rev. X* **13** (2023) 041056 [[2211.05907](#)].
- [242] D. Anninos and D.M. Hofman, *Infrared Realization of dS_2 in AdS_2* , *Class. Quant. Grav.* **35** (2018) 085003 [[1703.04622](#)].
- [243] D. Anninos, D.A. Galante and D.M. Hofman, *De Sitter horizons & holographic liquids*, *JHEP* **07** (2019) 038 [[1811.08153](#)].
- [244] D. Anninos and D.A. Galante, *Constructing AdS_2 flow geometries*, *JHEP* **02** (2021) 045 [[2011.01944](#)].
- [245] D. Anninos, D.A. Galante and B. Mühlmann, *Finite features of quantum de Sitter space*, *Class. Quant. Grav.* **40** (2023) 025009 [[2206.14146](#)].
- [246] S.E. Aguilar-Gutierrez, E. Bahiru and R. Espíndola, *The centaur-algebra of observables*, *JHEP* **03** (2024) 008 [[2307.04233](#)].
- [247] D. Anninos, D.A. Galante and S.U. Sheorey, *Renormalisation group flows of deformed SYK models*, *JHEP* **11** (2023) 197 [[2212.04944](#)].
- [248] S. Chapman, S. Demulder, D.A. Galante, S.U. Sheorey and O. Shoval, *Krylov complexity and chaos in deformed SYK models*, [2407.09604](#).
- [249] D.A. Galante, *Modave lectures on de Sitter space & holography*, *PoS Modave2022* (2023) 003 [[2306.10141](#)].
- [250] A. Strominger, *Inflation and the dS / CFT correspondence*, *JHEP* **11** (2001) 049 [[hep-th/0110087](#)].
- [251] V. Balasubramanian, J. de Boer and D. Minic, *Mass, entropy and holography in asymptotically de Sitter spaces*, *Phys. Rev. D* **65** (2002) 123508 [[hep-th/0110108](#)].
- [252] G.W. Gibbons and S.W. Hawking, *Action Integrals and Partition Functions in Quantum Gravity*, *Phys. Rev. D* **15** (1977) 2752.
- [253] G.W. Gibbons and S.W. Hawking, *Cosmological Event Horizons, Thermodynamics, and Particle Creation*, *Phys. Rev. D* **15** (1977) 2738.
- [254] M.M. Faruk, E. Morvan and J.P. van der Schaar, *Static sphere observers and geodesics in Schwarzschild-de Sitter spacetime*, *JCAP* **05** (2024) 118 [[2312.06878](#)].
- [255] K. Doi, J. Harper, A. Mollabashi, T. Takayanagi and Y. Taki, *Pseudoentropy in dS/CFT and Timelike Entanglement Entropy*, *Phys. Rev. Lett.* **130** (2023) 031601 [[2210.09457](#)].
- [256] S. Baiguera and R. Berman, *The Cosmological Switchback Effect II*, *JHEP* **08** (2024) 086 [[2406.04397](#)].

- [257] A. Chattopadhyay, V. Malvimat and A. Mitra, *Krylov complexity of deformed conformal field theories*, *JHEP* **08** (2024) 053 [[2405.03630](#)].
- [258] P. Cooper, S. Dubovsky and A. Mohsen, *Ultraviolet complete Lorentz-invariant theory with superluminal signal propagation*, *Phys. Rev. D* **89** (2014) 084044 [[1312.2021](#)].
- [259] A. Bhattacharyya, S. Ghosh, S. Pal and A. Vinod, *Wormholes in finite cutoff JT gravity: A study of baby universes and (Krylov) complexity*, [2502.13208](#).
- [260] H. Adami, M.M. Sheikh-Jabbari and V. Taghiloo, *Gravity Is Induced By Renormalization Group Flow*, [2508.09633](#).
- [261] Y.-Z. Li, Y. Xie and S. He, *Emergent classical gravity as stress-tensor deformed field theories*, [2508.15461](#).
- [262] M.T. Anderson, *On boundary value problems for einstein metrics*, *Geometry & Topology* **12** (2008) 2009–2045.
- [263] E. Witten, *A note on boundary conditions in Euclidean gravity*, *Rev. Math. Phys.* **33** (2021) 2140004 [[1805.11559](#)].
- [264] Z. An and M.T. Anderson, *The initial boundary value problem and quasi-local Hamiltonians in General Relativity*, [2103.15673](#).
- [265] D. Anninos, D.A. Galante and C. Maneerat, *Gravitational observatories*, *JHEP* **12** (2023) 024 [[2310.08648](#)].
- [266] G. Batra, *Timelike boundaries in de Sitter JT gravity and the Gao-Wald theorem*, [2407.08913](#).
- [267] B. Banihashemi, E. Shaghoulian and S. Shashi, *Flat space gravity at finite cutoff*, [2409.07643](#).
- [268] D.A. Galante, C. Maneerat and A. Svesko, *Conformal boundaries near extremal black holes*, [2504.14003](#).
- [269] B. Banihashemi, E. Shaghoulian and S. Shashi, *Thermal effective actions from conformal boundary conditions in gravity*, [2503.17471](#).
- [270] D.A. Galante, R.C. Myers and T. Zikopoulos, *Conformal Boundary Conditions and Higher Curvature Gravity*, [2512.10930](#).
- [271] D. Anninos, D.A. Galante, S. Georgescu, C. Maneerat and A. Svesko, *The Stretched Horizon Limit*, [2512.16738](#).
- [272] X. Liu, J.E. Santos and T. Wiseman, *New Well-Posed boundary conditions for semi-classical Euclidean gravity*, *JHEP* **06** (2024) 044 [[2402.04308](#)].
- [273] T. Ishii, S. Okumura, J.-I. Sakamoto and K. Yoshida, *Gravitational perturbations as $T\bar{T}$ -deformations in 2D dilaton gravity systems*, *Nucl. Phys. B* **951** (2020) 114901 [[1906.03865](#)].
- [274] S. Okumura and K. Yoshida, *$T\bar{T}$ -deformation and Liouville gravity*, *Nucl. Phys. B* **957** (2020) 115083 [[2003.14148](#)].
- [275] A. Lewkowycz and J. Maldacena, *Generalized gravitational entropy*, *JHEP* **08** (2013) 090 [[1304.4926](#)].
- [276] J. Lin, *Entanglement entropy in Jackiw-Teitelboim Gravity*, [1807.06575](#).
- [277] J. Lin, *Ryu-Takayanagi Area as an Entanglement Edge Term*, [1704.07763](#).

- [278] A. Blommaert, T.G. Mertens and H. Verschelde, *Fine Structure of Jackiw-Teitelboim Quantum Gravity*, *JHEP* **09** (2019) 066 [[1812.00918](#)].
- [279] J. Lin, *Entanglement entropy in Jackiw-Teitelboim gravity with matter*, [2107.11872](#).
- [280] D.L. Jafferis and D.K. Kolchmeyer, *Entanglement Entropy in Jackiw-Teitelboim Gravity*, [1911.10663](#).
- [281] T.G. Mertens, J. Simón and G. Wong, *A proposal for 3d quantum gravity and its bulk factorization*, *JHEP* **06** (2023) 134 [[2210.14196](#)].
- [282] A. Belaey, T.G. Mertens and J. Papalini, *Probing the singularity at the holographic screen via q-holography*, [2507.13873](#).
- [283] A. Blommaert, T.G. Mertens and S. Yao, *The q-Schwarzian and Liouville gravity*, [2312.00871](#).
- [284] T.G. Mertens and G.J. Turiaci, *Liouville quantum gravity – holography, JT and matrices*, *JHEP* **01** (2021) 073 [[2006.07072](#)].
- [285] Y. Fan and T.G. Mertens, *From quantum groups to Liouville and dilaton quantum gravity*, *JHEP* **05** (2022) 092 [[2109.07770](#)].
- [286] H. Kyono, S. Okumura and K. Yoshida, *Comments on 2D dilaton gravity system with a hyperbolic dilaton potential*, *Nucl. Phys. B* **923** (2017) 126 [[1704.07410](#)].
- [287] K. Suzuki and T. Takayanagi, *JT gravity limit of Liouville CFT and matrix model*, *JHEP* **11** (2021) 137 [[2108.12096](#)].
- [288] A. Goel, L.V. Iliesiu, J. Kruthoff and Z. Yang, *Classifying boundary conditions in JT gravity: from energy-branes to α -branes*, *JHEP* **04** (2021) 069 [[2010.12592](#)].
- [289] S. Collier, L. Eberhardt, B. Muehlmann and V.A. Rodriguez, *The Virasoro minimal string*, *SciPost Phys.* **16** (2024) 057 [[2309.10846](#)].
- [290] J. De Vuyst, S. Eccles, P.A. Hoehn and J. Kirklin, *Gravitational entropy is observer-dependent*, [2405.00114](#).
- [291] P.A. Hoehn, I. Kotecha and F.M. Mele, *Quantum Frame Relativity of Subsystems, Correlations and Thermodynamics*, [2308.09131](#).
- [292] L. Susskind, *A Paradox and its Resolution Illustrate Principles of de Sitter Holography*, [2304.00589](#).
- [293] D.N. Page and W.K. Wootters, *EVOLUTION WITHOUT EVOLUTION: DYNAMICS DESCRIBED BY STATIONARY OBSERVABLES*, *Phys. Rev. D* **27** (1983) 2885.
- [294] W.K. Wootters, *“Time” replaced by quantum correlations*, *Int. J. Theor. Phys.* **23** (1984) 701.
- [295] D.L. Jafferis, D.K. Kolchmeyer, B. Mukhametzhanov and J. Sonner, *Matrix Models for Eigenstate Thermalization*, *Phys. Rev. X* **13** (2023) 031033 [[2209.02130](#)].
- [296] D.L. Jafferis, D.K. Kolchmeyer, B. Mukhametzhanov and J. Sonner, *Jackiw-Teitelboim gravity with matter, generalized eigenstate thermalization hypothesis, and random matrices*, *Phys. Rev. D* **108** (2023) 066015 [[2209.02131](#)].
- [297] K. Okuyama, *Discrete analogue of the Weil-Petersson volume in double scaled SYK*, *JHEP* **09** (2023) 133 [[2306.15981](#)].

- [298] K. Okuyama, *Matter correlators through a wormhole in double-scaled SYK*, *JHEP* **02** (2024) 147 [[2312.00880](#)].
- [299] K. Okuyama, *Baby universe operators in double-scaled SYK*, [2408.03726](#).
- [300] M. Guica, *An integrable Lorentz-breaking deformation of two-dimensional CFTs*, *SciPost Phys.* **5** (2018) 048 [[1710.08415](#)].
- [301] S. Chakraborty and A. Mishra, *$T\bar{T}$ and $J\bar{T}$ deformations in quantum mechanics*, *JHEP* **11** (2020) 099 [[2008.01333](#)].
- [302] M. Berkooz, V. Narovlansky and H. Raj, *Complex Sachdev-Ye-Kitaev model in the double scaling limit*, *JHEP* **02** (2021) 113 [[2006.13983](#)].
- [303] R.A. Davison, W. Fu, A. Georges, Y. Gu, K. Jensen and S. Sachdev, *Thermoelectric transport in disordered metals without quasiparticles: The Sachdev-Ye-Kitaev models and holography*, *Phys. Rev. B* **95** (2017) 155131 [[1612.00849](#)].
- [304] S. Sachdev, *Bekenstein-Hawking Entropy and Strange Metals*, *Phys. Rev. X* **5** (2015) 041025 [[1506.05111](#)].
- [305] Y. Gu, A. Kitaev, S. Sachdev and G. Tarnopolsky, *Notes on the complex Sachdev-Ye-Kitaev model*, *JHEP* **02** (2020) 157 [[1910.14099](#)].
- [306] M. Berkooz, N. Brukner, V. Narovlansky and A. Raz, *The double scaled limit of Super-Symmetric SYK models*, *JHEP* **12** (2020) 110 [[2003.04405](#)].
- [307] H.W. Lin, J. Maldacena, L. Rozenberg and J. Shan, *Looking at supersymmetric black holes for a very long time*, *SciPost Phys.* **14** (2023) 128 [[2207.00408](#)].
- [308] S. Chapman, D.A. Galante, E. Harris, S.U. Sheorey and D. Vegh, *Complex geodesics in de Sitter space*, *JHEP* **03** (2023) 006 [[2212.01398](#)].
- [309] P. Caputa, J. Kruthoff and O. Parrikar, *Building Tensor Networks for Holographic States*, *JHEP* **05** (2021) 009 [[2012.05247](#)].
- [310] V. Balasubramanian, A. Kar and T. Ugajin, *Islands in de Sitter space*, *JHEP* **02** (2021) 072 [[2008.05275](#)].
- [311] A. Levine and E. Shaghoulian, *Encoding beyond cosmological horizons in de Sitter JT gravity*, *JHEP* **02** (2023) 179 [[2204.08503](#)].
- [312] S.E. Aguilar-Gutierrez, A. Chatwin-Davies, T. Hertog, N. Pinzani-Fokeeva and B. Robinson, *Islands in Multiverse Models*, *JHEP* **11** (2021) 212 [[2108.01278](#)].
- [313] K. Okuyama, *End of the world brane in double scaled SYK*, *JHEP* **08** (2023) 053 [[2305.12674](#)].
- [314] F. Deng, Z. Wang and Y. Zhou, *End of the world brane meets $T\bar{T}$* , *JHEP* **07** (2024) 036 [[2310.15031](#)].
- [315] K. Okuyama and T. Suyama, *Solvable limit of ETH matrix model for double-scaled SYK*, *JHEP* **04** (2024) 094 [[2311.02846](#)].
- [316] M. Watanabe, *A JT/KPZ correspondence*, [2511.02529](#).
- [317] P.A. Dirac, *Lectures on quantum mechanics*, Courier Corporation (2013).

- [318] M. Henneaux and C. Teitelboim, *Quantization of Gauge Systems*, Princeton University Press (8, 1994).
- [319] W. Al-Salam and T. Chihara, *Convolutions of orthonormal polynomials*, *SIAM Journal on Mathematical Analysis* **7** (1976) 16.
- [320] M. Zhang, W.-D. Tan, M. Lu, D. Bhattacharya, J. Yang and R.B. Mann, *Finite-cutoff holographic thermodynamics*, *Phys. Rev. Res.* **8** (2026) 013208 [[2507.01010](#)].